Title
Structure-Function Analysis of Apolipoprotein A-V: Insight into Plasma Triglyceride Homeostasis

Author
Mauldin, Kasuen

Publication Date
2010

Peer reviewed|Thesis/dissertation

STRUCTURE-FUNCTION ANALYSIS OF APOLIPOPROTEIN A-V: INSIGHT INTO PLASMA TRIGLYCERIDE HOMEOSTASIS

by

Kasuen Mauldin

A dissertation submitted in partial satisfaction of the

requirements for the degree of

Doctor in Philosophy

in

Molecular and Biochemical Nutrition

in the

Graduate Division

of the

University of California, Berkeley

Committee in charge:

Professor Robert O. Ryan, Co-Chair

Professor Wally Wang, Co-Chair

Professor Barry Shane

Professor Bob B. Buchanan

Spring 2010

ABSTRACT

STRUCTURE-FUNCTION ANALYSIS OF APOLIPOPROTEIN A-V:
INSIGHT INTO PLASMA TRIGLYCERIDE HOMEOSTASIS

by

Kasuen Mauldin

Doctor of Philosophy in Molecular and Biochemical Nutrition

University of California, Berkeley

Professor Robert O. Ryan, Co-Chair

Coronary heart disease is the leading cause of death in the United States, and epidemiological studies have shown that an elevated plasma triglyceride level is an independent risk factor for cardiovascular disease. In 2001, a new member of the exchangeable apolipoprotein (apo) family, apoA-V, was discovered using comparative genomics. Studies with transgenic mice over-expressing human apoA-V and apoA-V knock-out mice have shown that there exists a negative correlation between apoA-V levels and plasma triglyceride concentrations. Such findings have also been observed in humans, where single nucleotide polymorphisms within the *APOA5* gene have been associated with hypertriglyceridemia. These physiological findings suggest that apoA-V plays a major role in the regulation of triglyceride metabolism, and elucidating the mechanism by which apoA-V functions could yield therapeutic effects.

Several features of apoA-V, including an extremely low plasma concentration, a lack of correlation with cholesterol levels despite its association with high density lipoprotein, and its insolubility at neutral pH in the absence of lipid, are unlike other exchangeable apolipoproteins. Findings indicate apoA-V is comprised of two independently folded structural domains, with the amino-terminal domain forming an amphipathic α-helix bundle in the absence of lipid. In the presence of lipid, the helix bundle motif is postulated to unfurl, exposing hydrophobic residues for lipid interaction. The carboxy-terminal region plays a key function in apoA-V lipid binding, consistent with its known association with plasma lipoproteins.

I dedicate this dissertation to the women in my family:
Grandma, Mom, Kawai and Annika,*
because they have always inspired, motivated, and supported me in everything I have done.

*While Annika has recently become my number one source of inspiration and motivation in life, her support remains to be seen. In fact, she can barely support her own head at the moment since she is only 4 months old.

ACKNOWLEDGEMENTS

I would like to thank my mom for her unconditional love and unselfish actions that have allowed me to finish my graduate work on time. She has graciously devoted her time and energy to taking care of Annika and me these past four months.

I would also like to thank Bob for the opportunity to work on this project, for his mentorship and support, and for his friendship. While I may be done with my studies on apoA-V in his lab, I will continue to seek his guidance in my future endeavors.

Lastly, thank you to my wonderful husband, Clayton, for his patience and love. We have already experienced great things together with the completion of our PhDs and the birth of our daughter. I look forward to a lifetime of adventures together.

TABLE OF CONTENTS

LIST OF TABLES

LIST OF FIGURES

CHAPTER 1:
Introduction

1.1 ABBREVIATIONS

apo = apolipoprotein
TG = triacylglycerol
HDL = high density lipoprotein
VLDL = very low density lipoprotein
HSPG = heparan sulfate proteoglycan
GPIHBP1 = glycosylphosphatidylinositol high density lipoprotein binding protein 1
LPL = lipoprotein lipase
LDLR = low density lipoprotein receptor
DMPC = dimyristoylphosphatidylcholine
LDL = low density lipoprotein
SNP = single nucleotide polymorphism
HTG = hypertriglyceridemia

Structure-function studies have been instrumental in elucidating the biological functions of members of exchangeable apolipoprotein (apo) family and the mechanism by which they regulate lipid metabolism (*1*). The major human apolipoproteins, including apoA-I, apoA-IV, apoE and apoC's, serve as structural components of lipoprotein particles, modulators of lipid metabolic enzymes and proteins, ligands for cell surface receptors and/or acceptors of cellular lipid in the reverse cholesterol transport pathway (*2*). Despite the wealth of knowledge gained in nearly forty years of research on apolipoproteins, in 2001 a new member of this protein family, termed apoA-V, was independently discovered using comparative genomics (*3*) and as an mRNA that is upregulated in response to partial hepatectomy in rats (*4*). Initial efforts to understand the metabolic role of apoA-V employed transgenic mice overexpressing human apoA-V and apoA-V knockout mice. Results revealed an inverse correlation between apoA-V concentration and plasma triacylglycerol (TG) levels. Mice overexpressing human apoA-V showed a two-thirds decrease in plasma TG compared to control littermates, and conversely, mice lacking apoA-V had four times as much plasma TG as controls (*3*). Observations in humans have confirmed TG-modulating effects of apoA-V and intensive research efforts are currently underway to define the molecular basis for its effects. Describe below are aspects of apoA-V structure that provide mechanistic insight into its biological functions.

1.2 CHARACTERIZATION OF APOA-V

The gene structure of human apoA-V contains 4 exons and is located on the long arm of human chromosome 11 adjacent to the *APOA-I/APOC-III/APOA-IV* gene cluster (*3*). This genetic information predicts a protein consisting of 366 amino acids, including a 23 amino acid signal sequence. Sequence comparisons at the amino acid level indicate ~71% identity between the human and mouse proteins (*3*) and ~42% identity between human and avian apoA-V (*5*). In mammalian species apoA-V is expressed exclusively in liver and secreted into the plasma (*3*). Recently, Alborn et al. (*6*) reported the N-terminal amino acid sequence of human apoA-V in plasma to be Arg-Lys-Gly…, confirming the predicted 23 amino acid signal peptide is cleaved *in vivo* to yield a 343 amino acid mature apolipoprotein. Following immunoprecipitation from human serum and electrophoresis, apoA-V migrates mainly as a single band with a relative molecular mass of ~39,000, consistent with molecular mass calculations based on amino acid sequence (38,905). Recently, ELISA methods have been developed, permitting accurate quantitation apoA-V. Humans plasma levels reported range from 157 ng/ml (*7*) to 258 ng/ml (*8, 9*). For comparison, the plasma concentration of the major apolipoprotein component of high density lipoprotein (HDL), apoA-I, is ~1 mg/ml (*7*).

Two features of the primary sequence of human apoA-V are worth noting. First, the presence of a single cysteine at position 204 (**Figure 1-1**) suggests that apoA-V is capable of forming homo- or hetero-dimers. Whereas recombinant apoA-V can form disulfide-linked dimers *in vitro*, Alborn et al. (*6*) found that apoA-V in human serum exists as a monomer. Second is the presence of a unique tetra proline segment from residue 293-296 (**Figure 1-1**). Since the cyclic nature of proline is disruptive to protein secondary structure, the possibility exists that these consecutive Pro demarcate distinct structural regions in the apoA-V protein.

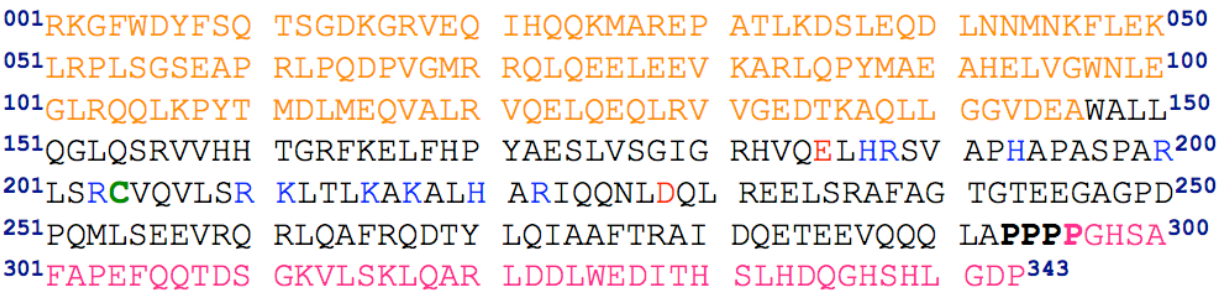

Figure 1-1. Amino acid sequence of mature human apoA-V. The sequence (single letter code) shown does not include the 23 amino acid signal peptide (*6*). Between Glu185 and Asp228 (red) there exists a cluster of residues with positive charge character (shown in blue). The only Cys at 204 is bold and in green. The four consecutive Pro between Ala292 and Gly297 are highlighted in bold font. A sequence element shown to comprise a helix bundle motif (residues 1 -146; (*10*)) is depicted in orange. The extreme C-terminal region is highlighted in pink.

Secondary structure analysis indicates apoA-V possesses characteristics typical of other exchangeable apolipoproteins, including a high content of alpha helix (*4, 11*). Consistent with this, recent far UV circular dichroism spectroscopy data on recombinant apoA-V in its lipid free state indicated ~ 50% alpha helix content. Little is known about the tertiary structure of apoA-V. Analysis that reveals sequence similarity with apolipoproteins whose structures have been determined by X-ray crystallography, including apoA-I (*12*) (44% similarity) and apoE (*13*) (40% similarity), suggest apoA-V, or some portion thereof, may adopt a helix bundle molecular architecture in the absence of lipid. While this possibility is consistent with secondary structure predictions and homology considerations, information available indicates apoA-V is found almost exclusively in association with lipoproteins (*6*), including very low density lipoprotein (VLDL), HDL, and chylomicrons (*7*). Most likely, however, apoA-V redistributes among lipoprotein particles as part of its normal metabolism in plasma, and this process may require transient existence as a lipid-free or lipid-poor protein (**Figure 1-2**). Interestingly, the lipoprotein distribution pattern of apoA-V is most similar to that of apoC-III, which is noteworthy since these proteins have opposing effects on plasma TG concentrations (*7*).

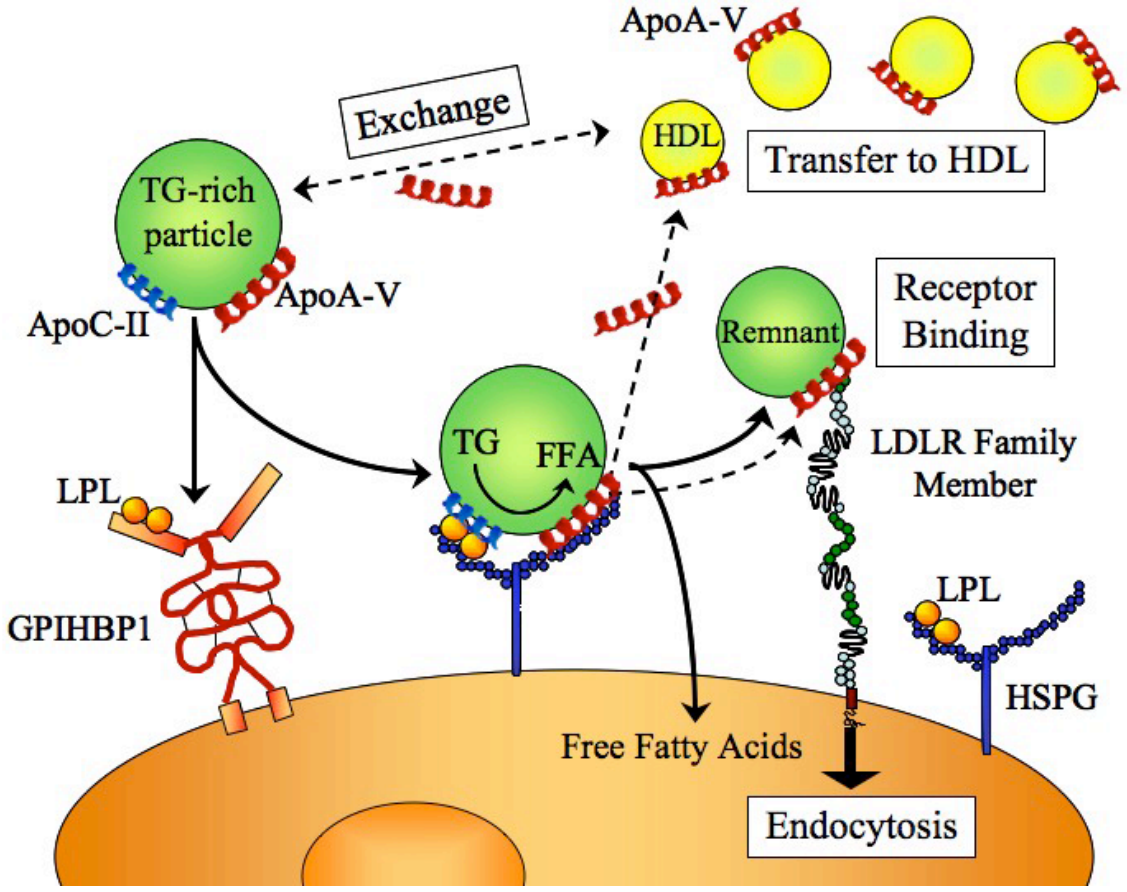

Figure 1-2. Model depicting postulated apoA-V effects on TG-rich lipoprotein metabolism. Lipoprotein-associated apoA-V interaction with HSPGs or GPIHBP1 can facilitate apoC-II activation of LPL, resulting in accelerated TG hydrolysis. Catabolism of TG-rich lipoproteins to a remnant particle may result in apoA-V dissociation/transfer to plasma HDL where it remains, poised to exchange onto nascent plasma TG-rich lipoproteins. Alternatively, apoA-V interaction with LDLR family members could facilitate remnant lipoprotein particle endocytosis. Solid arrows outline the path of lipoprotein particles; dashed arrows outline the path of apoA-V.

1.3 ACTIVATION OF LIPOPROTEIN LIPASE VIA HSPG AND GPIHBP1 BINDING

Analysis of the amino acid sequence of apoA-V revealed a stretch of 42 residues (between 186 – 227) that lacks amino acids with negatively charged side chains while containing eight with positively charged side chains (3 Lys, 5 Arg) as well as 3 His (*14*). Based on knowledge that regions of high positive charge density in other apolipoproteins (e.g. apoE) constitute heparin-binding sites, Lookene et al. (*14*) examined the heparin binding activity of apoA-V. ApoA-V•DMPC disks were shown to bind to heparin Sepharose while lipid-free apoA-V was shown to bind to heparin coated surface plasmon resonance chips. Furthermore, site directed mutagenesis of positively charged residues in this segment of the protein resulted in inhibition of heparin binding activity (*14*).

At the same time, Merkel et al. (*15*) showed that apoA-V accelerates plasma hydrolysis of TG-rich lipoproteins by facilitating interaction with heparan sulfate proteoglycan (HSPG)-bound lipoprotein lipase (LPL), but not with free LPL. In light of this observation, it has been suggested that apoA-V functions to regulate plasma TG levels via indirect activation of LPL, mediated by directing substrate lipoproteins to target cell surface HSPG to which LPL is bound (*14, 15*) (**Figure 1-2**). While this mode of regulation fits most data available, there are reports that apoA-V can stimulate LPL directly (*16, 17*). In addition, it has been found that an apoA-V variant with residues 192 – 238 deleted has lower LPL activating properties (*18*). Further studies are required to elucidate the nature of apoA-V effects on LPL / HSPGs and whether such modulation may contribute to the TG lowering effects of this apolipoprotein.

Beigneux et al. (*19*) provided further support for the concept that apoA-V can modulate plasma TG levels by promoting cell surface interactions. These authors reported that apoA-V serves as a ligand for a novel endothelial cell surface protein (**Figure 1-2**), termed glycosylphosphatidylinositol high-density lipoprotein binding protein 1 (GPIHBP1). *Gpihbp1*-deficient mice exhibited a striking accumulation of chylomicrons, even on a low-fat diet, resulting in milky plasma with TG levels as high as 5,000 mg/dL. On the basis of these results the authors concluded that GPIHBP1 plays a critical role in the lipolytic processing of chylomicrons. GPIHBP1 is located on the luminal face of the capillary endothelium, and its expression in cultured cells confers the ability to bind both LPL and chylomicrons. In studies with GPIHBP1 transfected CHO cells, specific binding to apoA-V lipid particles was observed (*19*). Taken together, these studies suggest GPIHBP1 can serve as a platform for LPL-mediated processing of chylomicrons in capillaries and that chylomicron- associated apoA-V may function as a binding partner, thereby facilitating TG hydrolysis.

1.4 RECEPTOR BINDING

Studies using apoA-V knockout mice showed that elevated plasma TG levels might be related to a lower affinity of apoA-V-deficient VLDL for the low density lipoprotein receptor (LDLR) (*20*). By extension, it may be surmised that in the absence of apoA-V, there is a decreased ability of TG-rich lipoproteins to serve as ligands for the LDLR. Although no precise consensus receptor recognition sequence has been identified for members of the LDLR family, apoE and apoB binding occurs via concentrated regions of high positive charge. The region in apoA-V with high positive charge density (residues 186 - 227) previously shown to interact with heparin has recently been implicated in binding to cell surface receptors (*21*). Surface plasmon resonance experiments showed specific binding of both lipid-free and lipid-bound apoA-V to two members of the LDLR family, LDLR-related protein (LRP) and the mosaic type-1 receptor (SorLA). In addition, pre-incubation with heparin caused a decrease in apoA-V binding to both receptors, suggesting overlap between the recognition sites for these receptors and for heparin.

Studies of apoA-V gene disrupted mice revealed that elevated plasma TG may be related to a lower affinity of apoA-V deficient VLDL for the LDL receptor (*20*). Such an effect is consistent with the concept that apoA-V itself may be a ligand for members of the LDL receptor family. It has been demonstrated that apoA-V has the ability to interact with two members of the low-density lipoprotein (LDL) receptor family, the LDL receptor-related protein (LRP) and the mosaic type-1 receptor, SorLA (*22*). The data showed specific binding of apoA-V to both receptors, raising the possibility that apoA-V facilitates endocytosis of TG-rich lipoproteins or their remnants. In addition, independent confirmation that apoA-V can serve as a ligand for members of the LDL receptor family was reported by Dichlberger et al. (*23*). These authors showed that apoA-V serves as a ligand for LDL receptor family members in the laying hen. Taken together, these studies suggest that apoA-V plays a key role in clearance of TG-rich lipoproteins *in vivo*.

1.5 APOA-V SEQUENCE POLYMORPHISMS

Single nucleotide polymorphisms (SNPs) identified in the *APOA5* gene have been linked to dyslipidemia. While most polymorphisms identified do not alter the amino acid sequence of the protein product, interesting correlations with plasma TG levels have been described. Details of apoA-V SNP analysis and correlations with TG levels may be found in two recent reviews (*24, 25*). Other polymorphisms / mutations reported that result in changes in the amino acid sequence of apoA-V include a S19W mutation (*26*) as well as two truncated variants, Q148X apoA-V and Q139X apoA-V, discussed below (*24, 27, 28*). The S19W variant, which arises from a SNP that changes a coded serine to a tryptophan in the signal peptide sequence, was predicted to interfere with secretion of the protein (*26*). Computer modeling of S19W apoA-V supports a conformational change in this region, and *in vitro* analysis using a secreted alkaline phosphatase reporter showed that the S19W mutation impaired secretion compared to the wild type signal peptide (*29*). By contrast, however, Henneman et al. (*30*) found a positive correlation between the S19W variant and plasma apoA-V levels in patients with hypertriglyceridemia (HTG), suggesting secretion efficiency is not impaired as a result of this polymorphism.

Mutations in the *APOA5* gene are associated with severe HTG in humans. Two unique mutations that result in truncated forms of the protein have been reported (*27, 28*). Interestingly, plasma from patients heterozygous for a Q139X or homozygous for a Q148X mutation displayed decreased LPL activity. Moreover, in patients heterozygous for the Q139X mutation, both truncated apoA-V and full-length apoA-V were recovered in the lipoprotein-free fraction of plasma (*28*). This finding suggests the C-terminus of apoA-V plays a role in the lipoprotein binding property of apoA-V and indicates the mutant form exerts a dominant negative effect on both the lipoprotein binding property and TG lowering effect of full length apoA-V.

Another interesting mutation in the *APOA5* gene is the c.553G>T SNP, which causes an amino acid substitution at residue 162 from a glycine to a cysteine (*31*). The carriers of the T allele had TG levels twice as high as normolipidemic patients, while TT homozygous subjects had extremely elevated plasma TG. This HTG can be attributed to decrease LPL activity (*31*). Since apoA-V has only one naturally occurring cysteine residue at position 204 (**Figure 1-1**)., this mutation resulting in an additional cysteine at position 162 could lead to intramolecular disulfide bonding, thus disrupting the conformation of the positively-charged region responsible for HSPG binding.

1.6 INSIGHT INTO MECHANISM OF ACTION

Although studies using animal models show a strong inverse correlation between apoA-V and plasma TG levels, paradoxical mysteries surrounding this protein have yet to be explained. For example, the plasma concentration of apoA-V is so low (*7*) that its effects on plasma TG levels would seem to require a mechanism distinct from the classical roles of apolipoproteins. If apoA-V is mainly associated with HDL (*4*), then why does it strongly influence plasma TG and not cholesterol levels? Another issue is the curious absence of a strong inverse correlation between apoA-V concentration and plasma TG levels in humans. Indeed, recent observations suggest a positive correlation between apoA-V and plasma TG levels in human subjects (*9, 30, 32-36*). The apparent discrepancy between animal and human findings could be due to the fact that methodic laboratory experiments in mice and rats are more straightforward, with controlled diets and conditions. In humans, however, determinants of plasma TG concentration are likely multifactorial and more complex. Patients in these studies suffered from severe HTG, Type 2 diabetes, and/or other conditions that may have obscured a correlation between apoA-V and TG concentration.

To date three mechanisms of apoA-V action have been proposed: (1) inhibitory effects on VLDL production and/or secretion, (2) stimulation of LPL-mediated TG hydrolysis, and (3) acceleration of hepatic uptake of TG-rich lipoproteins and their remnants. Adenovirus-mediated overexpression studies in mice have shown that apoA-V lowers plasma TG levels by reducing hepatic VLDL-TG production rate due to impaired lipidation of nascent VLDL without affecting the number of particles secreted (*17*). In addition, apoA-V overexpression enhances lypolysis of TG-rich lipoproteins through stimulation of LPL activity (*17*). This work supports both an intracellular mode of action, wherein apoA-V modulates TG-rich lipoprotein biogenesis and/or secretion (*11*), and a role for apoA-V in the stimulation of LPL-mediated VLDL-TG hydrolysis.

In apoA-V knockout mice, Grosskopf et al. (*20*) found that HTG was a result of decreased lipolysis of TG-rich lipoproteins and decreased removal of remnants. While the decreased lipolysis observed in apoA-V knockout mice was attributed to lower LPL activity, the decreased removal of remnants was due to VLDL particles from these mice being poor substrates for LPL and the LDL receptor (*20*). In addition, severe HTG in patients heterozygous for the Q139X truncation mutation manifest a LPL defect leading to lipolysis impairment (*28*). These data support a role for apoA-V in modulation of LPL activity and also provides evidence for apoA-V function in lipoprotein clearance from plasma.

A possible unifying concept centers around the ability of apoA-V to bind to cell surface HSPGs (**Figure 1-2**). For example, interaction of apoA-V-containing VLDL with HSPG essentially targets TG-rich lipoproteins to the site of LPL activity. This, in turn, would promote interaction of the apoC-II component of VLDL with HSPG-bound LPL, thereby activating this lipolytic enzyme. As the TG-rich lipoprotein substrate is converted to a remnant particle (e.g. VLDL → intermediate density lipoprotein), one possible fate for apoA-V is exchange/transfer onto HDL (*15*), where it resides until VLDL levels rise again. This hypothesis is appealing because recycling apoA-V could partially compensate for its low circulating concentrations. In addition, such a mechanism could explain why apoA-V is primarily associated with HDL while having a major influence on TG levels. An alternate fate for apoA-V following TG-lipolysis is

facilitation of remnant clearance via endocytic receptors (*21*). Thus, it is conceivable that a "secretion-capture (*37*)" -like process may be involved in the TG-lowering effect of apoA-V (*14*).

The metabolic role of apoA-V is incompletely understood. From a structural perspective, future goals include elucidating the precise nature of the apparent two domain structure of apoA-V. Conceivably, an N-terminal helix bundle may be connected to a less stable, lipid surface seeking C-terminal domain, as seen in apoE (*38*) and apoA-I (*12*). Further structural analyses of wild type and mutated apoA-V variants will certainly provide insight into the structural organization of this protein that manifests potent metabolic effects. As for discrepancies between observations in mice and humans, this aspect requires further investigation. As suggested by Henneman et al. (*30*) it may be that species-specific modifiers are involved. In addition, there are likely to be other factors in the human subjects studied that affect plasma TG levels and/or apoA-V concentrations. Another possibility is that instead of apoA-V driving plasma TG levels, it may be that in fact, plasma TG levels drive apoA-V levels. Under certain conditions HTG may cause apoA-V levels to increase in an attempt to drive down plasma TG concentrations. ApoA-V's effect on plasma TG levels, whether positively or negatively correlated, most likely requires the concerted effort of other TG-modulating players. Given the low concentration of apoA-V in plasma, one possibility is that, unlike conventional apolipoproteins, it exerts hormone-like effects that modulate TG levels. The significance of this research effort relates to the strong association between HTG and cardiovascular disease. By understanding the mechanism whereby apoA-V modulates plasma TG levels it may be possible to design new therapeutic strategies to prevent or treat heart disease and related conditions.

1.7 REFERENCES

1. Mahley, R. W., Innerarity, T. L., Rall, S. C., Jr., and Weisgraber, K. H. (1984) Plasma lipoproteins: apolipoprotein structure and function, *J Lipid Res 25*, 1277-1294.
2. Saito, H., Lund-Katz, S., and Phillips, M. C. (2004) Contributions of domain structure and lipid interaction to the functionality of exchangeable human apolipoproteins, *Prog Lipid Res 43*, 350-380.
3. Pennacchio, L. A., Olivier, M., Hubacek, J. A., Cohen, J. C., Cox, D. R., Fruchart, J. C., Krauss, R. M., and Rubin, E. M. (2001) An apolipoprotein influencing triglycerides in humans and mice revealed by comparative sequencing, *Science 294*, 169-173.
4. van der Vliet, H. N., Sammels, M. G., Leegwater, A. C., Levels, J. H., Reitsma, P. H., Boers, W., and Chamuleau, R. A. (2001) Apolipoprotein A-V: a novel apolipoprotein associated with an early phase of liver regeneration, *J Biol Chem 276*, 44512-44520.
5. Pennacchio, L. A., and Rubin, E. M. (2003) Apolipoprotein A5, a newly identified gene that affects plasma triglyceride levels in humans and mice, *Arterioscler Thromb Vasc Biol 23*, 529-534.
6. Alborn, W. E., Johnson, M. G., Prince, M. J., and Konrad, R. J. (2006) Definitive N-terminal protein sequence and further characterization of the novel apolipoprotein A5 in human serum, *Clin Chem 52*, 514-517.
7. O'Brien, P. J., Alborn, W. E., Sloan, J. H., Ulmer, M., Boodhoo, A., Knierman, M. D., Schultze, A. E., and Konrad, R. J. (2005) The novel apolipoprotein A5 is present in human serum, is associated with VLDL, HDL, and chylomicrons, and circulates at very low concentrations compared with other apolipoproteins, *Clin Chem 51*, 351-359.
8. Ishihara, M., Kujiraoka, T., Iwasaki, T., Nagano, M., Takano, M., Ishii, J., Tsuji, M., Ide, H., Miller, I. P., Miller, N. E., and Hattori, H. (2005) A sandwich enzyme-linked immunosorbent assay for human plasma apolipoprotein A-V concentration, *J Lipid Res 46*, 2015-2022.
9. Schaap, F. G., Nierman, M. C., Berbee, J. F., Hattori, H., Talmud, P. J., Vaessen, S. F., Rensen, P. C., Chamuleau, R. A., Kuivenhoven, J. A., and Groen, A. K. (2006) Evidence for a complex relationship between apoA-V and apoC-III in patients with severe hypertriglyceridemia, *J Lipid Res 47*, 2333-2339.
10. Wong, K., Beckstead, J. A., Lee, D., Weers, P. M., Guigard, E., Kay, C. M., and Ryan, R. O. (2008) The N-terminus of apolipoprotein A-V adopts a helix bundle molecular architecture, *Biochemistry 47*, 8768-8774.
11. Weinberg, R. B., Cook, V. R., Beckstead, J. A., Martin, D. D., Gallagher, J. W., Shelness, G. S., and Ryan, R. O. (2003) Structure and interfacial properties of human apolipoprotein A-V, *J Biol Chem 278*, 34438-34444.
12. Ajees, A. A., Anantharamaiah, G. M., Mishra, V. K., Hussain, M. M., and Murthy, H. M. (2006) Crystal structure of human apolipoprotein A-I: insights into its protective effect against cardiovascular diseases, *Proc Natl Acad Sci U S A 103*, 2126-2131.
13. Wilson, C., Wardell, M. R., Weisgraber, K. H., Mahley, R. W., and Agard, D. A. (1991) Three-dimensional structure of the LDL receptor-binding domain of human apolipoprotein E, *Science 252*, 1817-1822.

14. Lookene, A., Beckstead, J. A., Nilsson, S., Olivecrona, G., and Ryan, R. O. (2005) Apolipoprotein A-V-heparin interactions: implications for plasma lipoprotein metabolism, *J Biol Chem 280*, 25383-25387.
15. Merkel, M., Loeffler, B., Kluger, M., Fabig, N., Geppert, G., Pennacchio, L. A., Laatsch, A., and Heeren, J. (2005) Apolipoprotein AV accelerates plasma hydrolysis of triglyceride-rich lipoproteins by interaction with proteoglycan-bound lipoprotein lipase, *J Biol Chem 280*, 21553-21560.
16. Fruchart-Najib, J., Bauge, E., Niculescu, L. S., Pham, T., Thomas, B., Rommens, C., Majd, Z., Brewer, B., Pennacchio, L. A., and Fruchart, J. C. (2004) Mechanism of triglyceride lowering in mice expressing human apolipoprotein A5, *Biochem Biophys Res Commun 319*, 397-404.
17. Schaap, F. G., Rensen, P. C., Voshol, P. J., Vrins, C., van der Vliet, H. N., Chamuleau, R. A., Havekes, L. M., Groen, A. K., and van Dijk, K. W. (2004) ApoAV reduces plasma triglycerides by inhibiting very low density lipoprotein-triglyceride (VLDL-TG) production and stimulating lipoprotein lipase-mediated VLDL-TG hydrolysis, *J Biol Chem 279*, 27941-27947.
18. Sun, G., Bi, N., Li, G., Zhu, X., Zeng, W., Wu, G., Xue, H., and Chen, B. (2006) Identification of lipid binding and lipoprotein lipase activation domains of human apoAV, *Chem Phys Lipids 143*, 22-28.
19. Beigneux, A. P., Davies, B. S., Gin, P., Weinstein, M. M., Farber, E., Qiao, X., Peale, F., Bunting, S., Walzem, R. L., Wong, J. S., Blaner, W. S., Ding, Z. M., Melford, K., Wongsiriroj, N., Shu, X., de Sauvage, F., Ryan, R. O., Fong, L. G., Bensadoun, A., and Young, S. G. (2007) Glycosylphosphatidylinositol-anchored high-density lipoprotein-binding protein 1 plays a critical role in the lipolytic processing of chylomicrons, *Cell Metab 5*, 279-291.
20. Grosskopf, I., Baroukh, N., Lee, S. J., Kamari, Y., Harats, D., Rubin, E. M., Pennacchio, L. A., and Cooper, A. D. (2005) Apolipoprotein A-V deficiency results in marked hypertriglyceridemia attributable to decreased lipolysis of triglyceride-rich lipoproteins and removal of their remnants, *Arterioscler Thromb Vasc Biol 25*, 2573-2579.
21. Nilsson, S. K., Lookene, A., Beckstead, J. A., Gliemann, J., Ryan, R. O., and Olivecrona, G. (2007) Apolipoprotein A-V interaction with members of the low density lipoprotein receptor gene family, *Biochemistry 46; In Press.*
22. Nilsson, S. K., Lookene, A., Beckstead, J. A., Gliemann, J., Ryan, R. O., and Olivecrona, G. (2007) Apolipoprotein A-V interaction with members of the low density lipoprotein receptor gene family, *Biochemistry 46*, 3896-3904.
23. Dichlberger, A., Cogburn, L. A., Nimpf, J., and Schneider, W. J. (2007) Avian apolipoprotein A-V binds to LDL receptor gene family members, *J Lipid Res 48*, 1451-1456.
24. Calandra, S., Oliva, C. P., Tarugi, P., and Bertolini, S. (2006) APOA5 and triglyceride metabolism, lesson from human APOA5 deficiency, *Curr Opin Lipidol 17*, 122-127.
25. Jakel, H., Nowak, M., Helleboid-Chapman, A., Fruchart-Najib, J., and Fruchart, J. C. (2006) Is apolipoprotein A5 a novel regulator of triglyceride-rich lipoproteins?, *Ann Med 38*, 2-10.
26. Pennacchio, L. A., Olivier, M., Hubacek, J. A., Krauss, R. M., Rubin, E. M., and Cohen, J. C. (2002) Two independent apolipoprotein A5 haplotypes influence human plasma triglyceride levels, *Hum Mol Genet 11*, 3031-3038.

27. Oliva, C. P., Pisciotta, L., Li Volti, G., Sambataro, M. P., Cantafora, A., Bellocchio, A., Catapano, A., Tarugi, P., Bertolini, S., and Calandra, S. (2005) Inherited apolipoprotein A-V deficiency in severe hypertriglyceridemia, *Arterioscler Thromb Vasc Biol 25*, 411-417.
28. Marcais, C., Verges, B., Charriere, S., Pruneta, V., Merlin, M., Billon, S., Perrot, L., Drai, J., Sassolas, A., Pennacchio, L. A., Fruchart-Najib, J., Fruchart, J. C., Durlach, V., and Moulin, P. (2005) Apoa5 Q139X truncation predisposes to late-onset hyperchylomicronemia due to lipoprotein lipase impairment, *J Clin Invest 115*, 2862-2869.
29. Talmud, P. J., Palmen, J., Putt, W., Lins, L., and Humphries, S. E. (2005) Determination of the functionality of common APOA5 polymorphisms, *J Biol Chem 280*, 28215-28220.
30. Henneman, P., Schaap, F. G., Havekes, L. M., Rensen, P. C., Frants, R. R., van Tol, A., Hattori, H., Smelt, A. H., and van Dijk, K. W. (2006) Plasma apoAV levels are markedly elevated in severe hypertriglyceridemia and positively correlated with the APOA5 S19W polymorphism, *Atherosclerosis*.
31. Pullinger, C. R., Aouizerat, B. E., Movsesyan, I., Durlach, V., Sijbrands, E. J., Nakajima, K., Poon, A., Dallinga-Thie, G. M., Hattori, H., Green, L. L., Kwok, P. Y., Havel, R. J., Frost, P. H., Malloy, M. J., and Kane, J. P. (2008) An apolipoprotein A-V gene SNP is associated with marked hypertriglyceridemia among Asian-American patients, *J Lipid Res 49*, 1846-1854.
32. Becker, S., Schomburg, L., Renko, K., Tolle, M., van der Giet, M., and Tietge, U. J. (2006) Altered apolipoprotein A-V expression during the acute phase response is independent of plasma triglyceride levels in mice and humans, *Biochem Biophys Res Commun 339*, 833-839.
33. Dallinga-Thie, G. M., van Tol, A., Hattori, H., van Vark-van der Zee, L. C., Jansen, H., and Sijbrands, E. J. (2006) Plasma apolipoprotein A5 and triglycerides in type 2 diabetes, *Diabetologia 49*, 1505-1511.
34. Pruneta-Deloche, V., Ponsin, G., Groisne, L., Fruchart-Najib, J., Lagarde, M., and Moulin, P. (2005) Postprandial increase of plasma apoAV concentrations in Type 2 diabetic patients, *Atherosclerosis 181*, 403-405.
35. Talmud, P. J., Cooper, J. A., Hattori, H., Miller, I. P., Miller, G. J., and Humphries, S. E. (2006) The apolipoprotein A-V genotype and plasma apolipoprotein A-V and triglyceride levels: prospective risk of type 2 diabetes. Results from the Northwick Park Heart Study II, *Diabetologia 49*, 2337-2340.
36. Vaessen, S. F., Schaap, F. G., Kuivenhoven, J. A., Groen, A. K., Hutten, B. A., Boekholdt, S. M., Hattori, H., Sandhu, M. S., Bingham, S. A., Luben, R., Palmen, J. A., Wareham, N. J., Humphries, S. E., Kastelein, J. J., Talmud, P. J., and Khaw, K. T. (2006) Apolipoprotein A-V, triglycerides and risk of coronary artery disease: the prospective Epic-Norfolk Population Study, *J Lipid Res 47*, 2064-2070.
37. Ji, Z. S., Fazio, S., Lee, Y. L., and Mahley, R. W. (1994) Secretion-capture role for apolipoprotein E in remnant lipoprotein metabolism involving cell surface heparan sulfate proteoglycans, *J Biol Chem 269*, 2764-2772.
38. Weisgraber, K. H. (1994) Apolipoprotein E: structure-function relationships, *Adv Protein Chem 45*, 249-302.

CHAPTER 2:
Probing apolipoprotein A-V structural domains

2.1 ABBREVIATIONS

apo = apolipoprotein
ANS = 8-anilino-1-napthalene-sulfonic acid
CD = circular dichroism
HTG = hypertriglyceridemia
DMPC = dimyristoylphosphatidylcholine
HSPG = heparan sulfate proteoglycan
KO = knockout
SUV = small unilamellar vesicle
TG = triacylglycerol
VLDL = very low density lipoprotein
WT = wild type.

2.2 ABSTRACT

Human apolipoprotein A-V (apoA-V) is a potent modulator of plasma triacylglycerol (TG) levels. To probe different regions of this 343 amino acid protein, 4 single Trp apoA-V variants were prepared. The variant with a Trp at position 325, distal to the tetra-proline sequence at residues 293-296, displayed an 11 nm blue shift in wavelength of maximum fluorescence emission upon lipid association. To evaluate the structural and functional role of this carboxyl-(C)-terminal segment, a truncated apoA-V, comprising amino acids 1-292, was generated. Far UV circular dichroism spectra of full-length apoA-V and apoA-V(1-292) were similar, with ~50% α-helix content. In guanidine HCl denaturation experiments, both full-length and truncated apoA-V yielded biphasic profiles consistent with the presence of two structural domains. The denaturation profile of the lower stability component, but not the higher stability component, was affected by truncation. Truncated apoA-V displayed an attenuated ability to solubilize DMPC phospholipid vesicles compared to full-length apoA-V while a peptide corresponding to the deleted C-terminal segment displayed markedly enhanced kinetics. The data support the concept that the C-terminal region is not required for apoA-V to adopt a folded protein structure yet functions to modulate apoA-V lipid binding activity and thereby, may be relevant to the mechanism whereby it influences plasma TG levels.

2.3 BACKGROUND

A new member of the exchangeable apolipoprotein family was independently discovered in 2001 by comparative genomics (*1*) and as an mRNA that is up-regulated in rat liver following partial hepatectomy (*2*). In humans, the mature protein, termed apolipoprotein (apo) A-V, is comprised of 343 amino acids (*3*). Northern blot analysis of various tissues revealed that apoA-V mRNA expression is restricted to hepatocytes (*1*). To evaluate its function Pennacchio et al. (*1*) generated transgenic mice that overexpress apoA-V as well as gene disrupted mice that lack apoA-V. The transgenic mice displayed a 3-fold lower plasma triacylglycerol (TG) level compared to control littermates. By contrast, apoA-V gene knockout (KO) mice revealed a 4-fold higher plasma TG content compared to controls. Levels of very low-density lipoprotein (VLDL) particles were increased in homozygous KO mice and decreased in transgenic mice, compared to controls. Van der Vliet et al. (*4*) confirmed the effect of apoA-V on plasma TG levels using an adenovirus construct to over-express apoA-V in mice. ApoA-V over-expressing mice displayed markedly decreased plasma TG levels that were the result of lower VLDL levels. Interestingly, changes in plasma TG concentration were directly opposite of those reported for apoC-III KO and transgenic mice (*5, 6*). Whereas apoA-V KO mice displayed a four-fold increase in plasma TG, apoC-III gene disrupted animals showed a 30% decrease. The mechanism whereby apoA-V influences plasma TG levels is unknown but may be related to an ability to influence TG-rich lipoprotein biogenesis, secretion or metabolism. Three distinct hypotheses have been proposed to explain the action of apoA-V on plasma TG levels: a) an intracellular mode of action wherein apoA-V modulates TG-rich lipoprotein biogenesis and/or secretion (*7*); b) a direct activation of lipoprotein lipase activity (*8, 9*) or c) an indirect effect on TG-rich lipoprotein metabolism or clearance from plasma (*10-12*).

Previous studies revealed that apoA-V possesses strong lipid binding activity (*7*) while a naturally occurring C-terminal truncation variant associated with hypertriglyceridemia is largely recovered in lipoprotein free fraction of plasma (*13*). Interestingly, apoA-V contains four consecutive proline residues (Pro293 - Pro296) near the C-terminus of the protein. We postulated the 51-residue segment beyond this site constitutes a discrete structural element in apoA-V that may function to modulate its lipid affinity. To test this hypothesis and to further define the structural and functional role of this region of apoA-V we have examined the spectroscopic, lipid binding, and dynamic interfacial characteristics of a series of single tryptophan mutants and a truncated variant lacking the terminal 51 amino acids as well as a peptide corresponding to the deleted C-terminal segment. Data from these studies establish that the C-terminal segment modulates the lipid binding activity of apoA-V in a manner that may directly impact its ability to lower plasma TG.

2.4 RESULTS

Tryptophan fluorescence of apoA-V

Fluorescence spectra of wild type (WT) apoA-V revealed a wavelength of maximum Trp fluorescence emission of 340 nm in buffer that shifted to 339 nm when the protein was complexed with phospholipid (**Table 2-1**). At the same time, lipid association was accompanied by a near 3-fold enhancement in emission quantum yield (excitation 295 nm). WT apoA-V contains 4 Trp, located at positions 5, 97, 147 and 325 (**Figure 2-1**). Site directed mutagenesis of Trp to Phe was performed to create a panel of single Trp apoA-V variants. Whereas fluorescence emission spectra of apoA-V variants with Trp at positions 97, 147 or 325 in buffer yielded emission maxima between 340 and 343 nm, the corresponding value for the Trp 5 variant was red shifted to 349 nm, likely owing to its location at the extreme N-terminus of the protein. In a manner similar to WT apoA-V, lipid binding had little effect on the wavelength of maximum fluorescence emission of Trp 97 or Trp 147 apoA-V variants.

Table 2-1. Fluorescence properties of apoA-V variants.[a]

ApoA-V variant	λ_{max} (nm)[b]	
	Lipid-free	DMPC-bound
WT	340	339
Trp 5	349	344
Trp 97	343	341
Trp 147	341	340
Trp 325	340	329

[a] Spectra were recorded on a Horiba Jobin Yvon FluoroMax-3 luminescence spectrometer. Emission was scanned from 300 nm to 450 nm (excitation 295 nm; slit width 2.0 nm for the excitation and emission monochromators). All spectra were recorded in 50 mM sodium citrate, pH 3.0, 150 mM NaCl.

[b] λ_{max} is the wavelength of maximum fluorescence emission. Values reported are the mean of 3 determinations. In all cases the standard deviations were $\leq$ 1 nm.

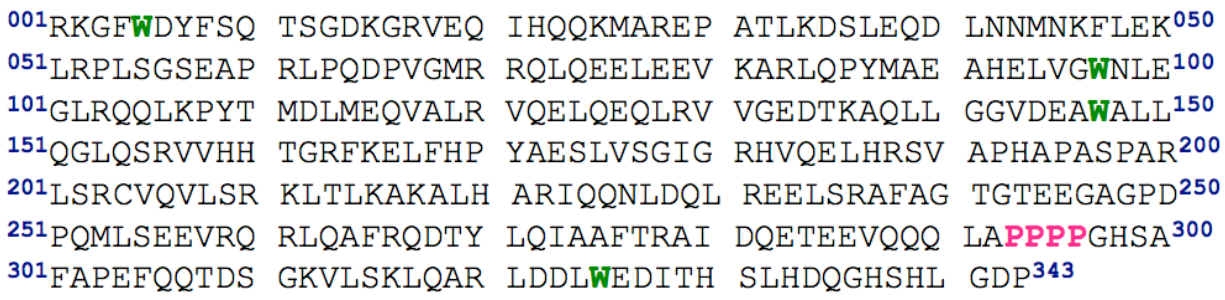

Figure 2-1. Amino acid sequence of mature human apoA-V. The Trp residues at positions 5, 97, 147, and 325 are highlighted in green and bold font. The four consecutive Pro at positions 293 – 296 are highlighted in pink and bold font.

The apoA-V variant with a Trp at position 325 underwent an 11 nm blue shift in Trp fluorescence emission maximum upon lipid association (**Figure 2-2**) suggesting this residue transitions to a more nonpolar environment upon lipid interaction. Furthermore, in contrast to WT apoA-V and the other Trp variants, Trp 325 apoA-V displayed a 25 % decrease in emission quantum yield upon lipid association.

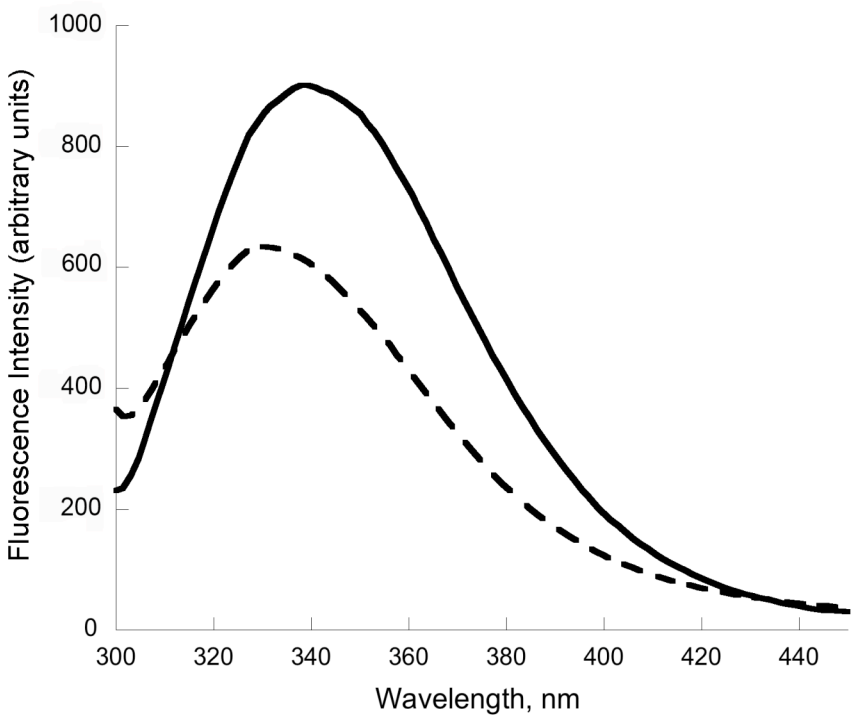

Figure 2-2. Fluorescence emission spectra of Trp 325 apoA-V. Spectra were recorded at an excitation wavelength of 295 nm (slit width 2.0 nm) at a protein concentration of in 50 mM sodium citrate, pH 3.0, 150 mM NaCl. Solid line) Trp 325 apoA-V (40 μg protein) in buffer; Dashed line) Trp 325 apoA-V-DMPC complexes (200 μg DMPC/40 μg apoA-V protein).

C-terminal truncation of apoA-V

Examination of the amino acid sequence of apoA-V revealed the presence of four consecutive proline residues at positions 293 - 296 of this 343 amino acid protein (**Figure 2-1**). Because the cyclic structure of proline imposes geometric constraints that strongly influence the secondary structure of proteins, we hypothesized that the 51 amino acid segment including and beyond this polyproline sequence constitutes a distinct structural element in apoA-V. Given that the C-terminal region of other members of the exchangeable apolipoprotein family is important in their lipid binding activity (*14*) together with the observed lipid binding induced fluorescence blue shift for the apoA-V variant with a single Trp at position 325, we evaluated the effect of deleting this segment of the protein on its structural and interfacial properties. SDS-PAGE analysis of truncated apoA-V (**Figure 2-3**) revealed a single band under reducing conditions that migrated faster than full-length apoA-V. On the other hand, under non-reducing conditions, evidence was obtained that an equivalent, albeit minor fraction of apoA-V in both samples, exists as a disulfide linked homodimer.

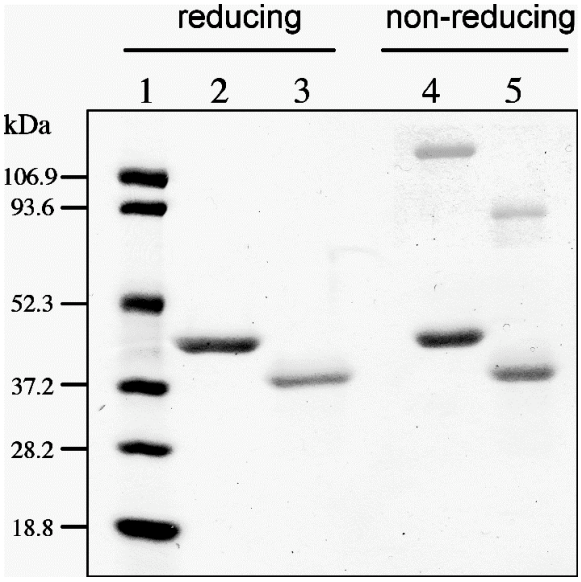

Figure 2-3. SDS-PAGE of full length and truncated apoA-V. Samples were electrophoresed on a 4 -20 % acrylamide gradient SDS slab gel under reducing or non-reducing conditions and stained with Gel Code Blue. Lane 1) protein standard, lanes 2 and 4) full-length apoA-V; lanes 3 and 5) apoA-V(1-292). [Figure generated by Jennifer A. Beckstead.]

Secondary structure characterization studies

[Data collected in collaboration with the laboratory of Dr. Paul Weers of California State University Long Beach]

Far UV CD spectroscopy of full-length apoA-V and apoA-V(1-292) yielded spectra with minima at 208 nm and 222 nm consistent with the presence of α-helix (**Figure 2-4**). Secondary structure calculations yielded an α-helix content of 50 % for both full length apoA-V and apoA-V(1-292). The similarity between these values indicates that deletion of the 51-residue segment did not disrupt the helix forming capacity of apoA-V.

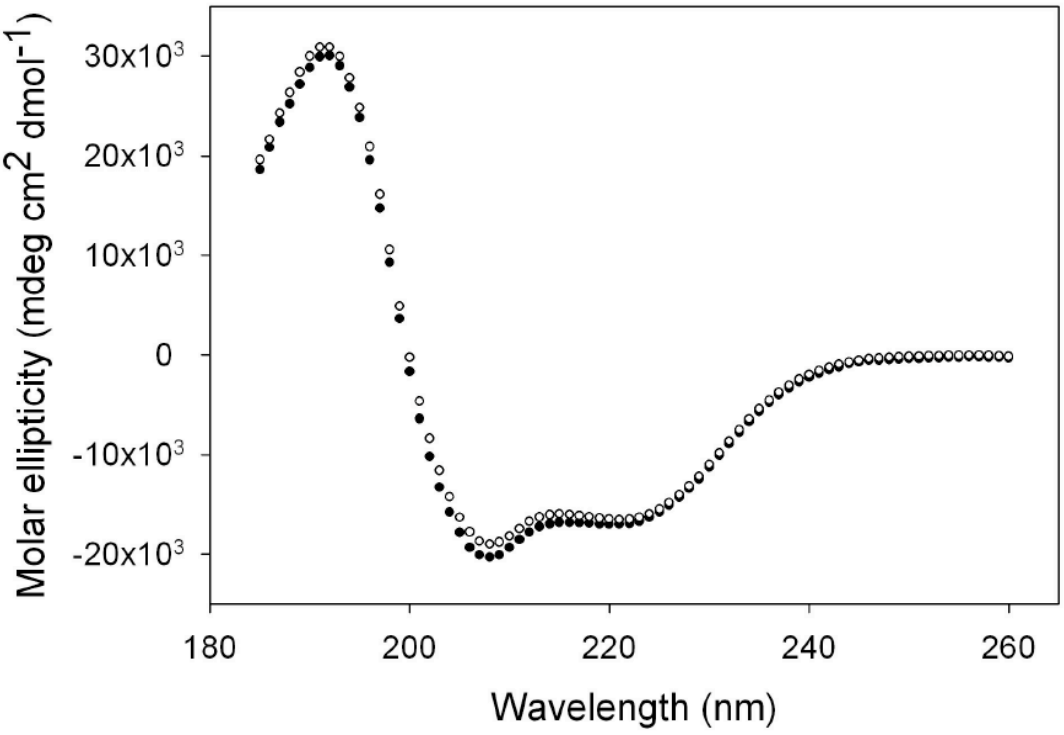

Figure 2-4. Far UV CD spectroscopy of apoA-V. Spectra were recorded at 25 °C at a protein concentration of 0.6 mg/mL in 50 mM sodium citrate, pH 3.0, 150 mM NaCl. Full-length apoA-V (filled circles); apoA-V(1-292) (open circles).

To evaluate the effect of truncation on the stability of apoA-V, guanidine HCl denaturation studies were performed (**Figure 2-5**). In contrast to the apparent two state, single transition observed with temperature-induced denaturation (14), the present results indicate the presence of independently folded structural elements in apoA-V. Full-length apoA-V gave rise to an initial transition with a midpoint at 1 M guanidine HCl and a second transition with a midpoint at ~2.6 M guanidine HCl. Interestingly, apoA-V(1-292) yielded a nearly super imposable curve for the second transition component while the first transition component was affected by the truncation. On the basis of these data it may be concluded that the present C-terminal truncation variant behaves similarly to full-length apoA-V and that the 51 residue C-terminal deletion exerts a minor influence on the unfolding behavior of apoA-V. In a separate study, the effect of Trp to Phe mutations in apoA-V on the secondary structure content of the protein was evaluated. Using the Trp 325 apoA-V variant (in which 3 of the 4 Trp residues have been mutated to Phe) as a surrogate, the far UV CD spectrum was comparable to WT apoA-V (data not shown), indicating the Trp substitution mutations did not adversely affect the secondary structure content of the protein.

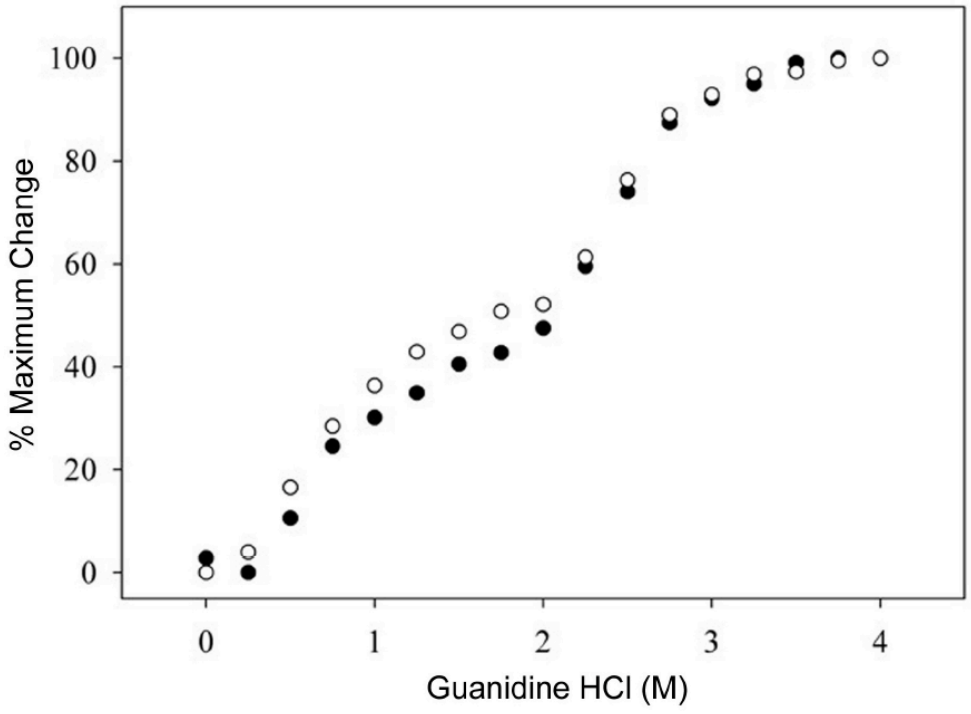

Figure 2-5. Effect of guanidine HCl on the secondary structure content of apoA-V. Indicated amounts of guanidine HCl were added to WT apoA-V and apoA-V(1-292) in buffer (50 mM sodium citrate, pH 3.0, 150 mM NaCl) and, at each concentration, the ellipticity at 222 nm was determined. Filled circles: full-length apoA-V; open circles: apoA-V(1-292).

Fluorescent dye binding

To evaluate the extent to which C-terminal truncation alters exposure of hydrophobic sites in apoA-V, the effect of full-length apoA-V and apoA-V(1-292) on the fluorescence emission intensity of ANS was examined (**Figure 2-6**). In the absence of protein, ANS has a low quantum yield with an emission wavelength maximum of 513 nm (excitation 395 nm). Introduction of full-length apoA-V induced a blue shift in ANS fluorescence emission wavelength maximum together with strong enhancement in quantum yield. By contrast, the enhancement in ANS fluorescence intensity induced by apoA-V(1-292) was lower, suggesting the deleted C-terminal segment possesses ANS binding sites and that removal of this segment did not introduce new ANS binding sites in the residual fragment. These data are similar to results seen upon C-terminal truncation of apoA-I (*14*).

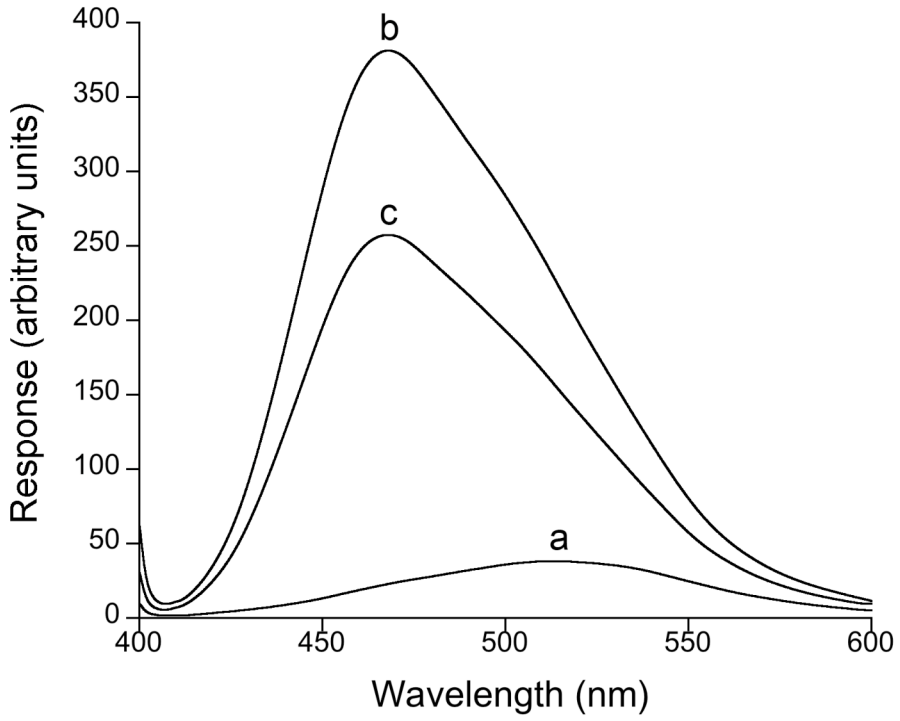

Figure 2-6. Effect of full length and truncated apoA-V on ANS fluorescence intensity. ANS (1 mM) in 50 mM sodium citrate, pH 3.0, 150 mM NaCl, was excited at 395 nm and emission monitored from 400 - 600 nm. Curve a) ANS in buffer at pH 7.0; curve b) ANS plus 20 µg full-length apoA-V; curve c) ANS plus 20 µg apoA-V(1-292).

Phospholipid vesicle solubilization studies

The effect of C-terminal truncation of apoA-V on lipid binding activity was further examined in phospholipid vesicle solubilization assays. Apolipoprotein-dependent alterations in DMPC SUV light scatter intensity (measured spectrophotometically at 325 nm) were monitored as a function of time (**Figure 2-7**). In control incubations lacking apolipoprotein, DMPC vesicle turbidity did not change. Addition of full-length apoA-V to DMPC SUVs induced a rapid time dependent reduction in turbidity. The initial rate constant (k) was 1.5 x 10^{-2} s^{-1}, assuming first order kinetics, and the reaction was near completion after ~ 300 s. In contrast, the initial rate constant was nearly 2-fold lower for apoA-V(1-292) (k = 7.4 x 10^{-3} s^{-1}). Increasing the protein concentration resulted in faster transformation rates, and a lower final sample turbidity. Nevertheless, apoA-V (1-292) turbidity remained at a higher level at all time points compared to full-length apoA-V, which displayed an ~2-fold higher solution clearance rate (results not shown). Thus, consistent with the observed decrease in ANS accessible sites upon C-terminal truncation, this variant also displays a lower lipid binding activity than full-length apoA-V.

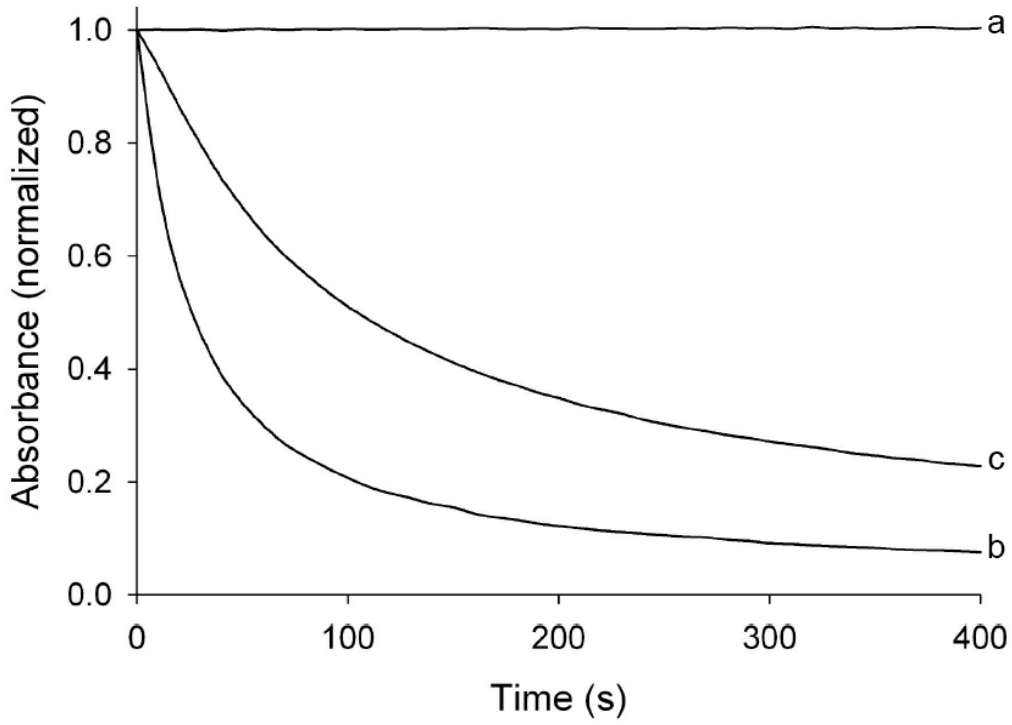

Figure 2-7. Effect of apolipoproteins or peptide on DMPC vesicle solubilization. Bilayer vesicles of DMPC (250 µg phospholipid) were incubated in buffer at 24 °C in 50 mM sodium citrate, pH 3.0, 150 mM NaCl. Sample light scatter intensity was measured spectrophotometrically at 325 nm as a function of time. Curve a) DMPC vesicles in buffer; curve b) DMPC vesicles plus 20 µg full-length apoA-V; curve c) DMPC vesicles plus 20 µg apoA-V(1-292) and curve d) 20 µg apoA-V(295-343).

Initial studies of the C-terminal peptide

Based on the finding that deletion of the C-terminal 51 amino acids in apoA-V altered its lipid binding properties, studies were performed to determine the intrinsic lipid binding activity of the deleted segment. A peptide corresponding to apoA-V amino acid residues 295 -343 was synthesized and isolated by reversed phase HPLC. This peptide contains a single Trp residue that corresponds to Trp 325 in full-length apoA-V (see **Table 2-1**). In buffer this Trp displayed a wavelength of maximum fluorescence emission (excitation 295 nm) of 354 nm. Association with DMPC, however, induced a 16 nm blue shift to 338 nm, indicating association of the peptide with the lipid surface. When peptide-DMPC complexes were subject to non-denaturing native gradient PAGE, a single population of lipid particles was present with a Stoke's diameter in the range of 20 nm. Far UV CD spectroscopy of the C-terminal peptide in buffer revealed random structure while association with DMPC induced α-helix secondary structure. Comparison of the phospholipid vesicle solubilization properties of the C-terminal peptide with full-length apoA-V and apoA-V(1-292) (**Figure 2-7**) revealed the peptide is highly effective. Under these conditions DMPC vesicle solubilization was complete by 20 seconds, too rapid to define an accurate rate constant. Nevertheless, these data are consistent with strong lipid binding activity for this segment of the protein.

2.5 DISCUSSION

The molecular basis for the profound plasma TG lowering effect of apoA-V has yet to be elucidated. An area of active investigation relates to the finding that apoA-V is a heparin binding protein (*11*) whose ability to enhance lipoprotein lipase activity is dependent upon interaction with heparan sulfate proteoglycans (HSPG) (*12*). Despite its very low concentration in plasma (*15, 16*), apoA-V associated with circulating VLDL may promote interaction with HSPG moieties at the surface of capillary endothelial cells. Since lipoprotein lipase is also bound to HSPG, apoA-V-dependent VLDL-HSPG interactions would be anticipated to facilitate interaction between lipoprotein lipase and its activator, apoC-II. The observation that apoA-V is found on both VLDL and HDL lipoprotein fractions in plasma suggests the possibility that following lipolysis, or under conditions of low plasma TG, apoA-V migrates to HDL where it exists, poised to associate with newly secreted VLDL. This lipoprotein redistribution concept is also consistent with the known poor solubility of apoA-V in the absence of lipid (*17*) as well as the strong lipid binding properties of the protein (*7*). Recently, naturally occurring truncated mutants of apoA-V were identified in humans that are associated with hypertriglyceridemia (*13, 18*). Interestingly the presence of a Q139X apoA-V mutant allele exerted a dominant negative effect on full-length apoA-V, resulting in recovery of both proteins in the lipoprotein deficient fraction of plasma (*13*). Thus, it may be considered that lipoprotein association is important for manifestation of the TG lowering effects of apoA-V.

Examination of the amino acid sequence of apoA-V revealed the presence of an unusual tetra-proline sequence (residues 293-296) that we hypothesized could demarcate an independently folded structural domain that conceivably participates in the lipid binding activity of this protein. Evidence that this region of the protein associates with lipid was obtained from characterization of single tryptophan apoA-V variants. ApoA-V containing a single Trp at position 325 displayed a blue shift in fluorescence emission maximum upon lipid interaction, consistent with a transition from a relatively solvent exposed to a more hydrophobic environment. When considered together with the four consecutive Pro residues in the C-terminus, we targeted this region of the protein for truncation. Whereas apoA-V(1-292) was very similar to full-length apoA-V in terms of global secondary structure content, it possessed a decreased number of solvent exposed hydrophobic sites and a decreased ability to solubilize bilayer vesicles of DMPC. In DMPC solubilization assays the apolipoprotein must not only bind to the phospholipid surface but also induce reorganization of the vesicles into smaller discoidal lipid-protein complexes (*19*). This requires apolipoprotein penetration, bilayer disruption and a conformational change in the protein. If truncation affected any of these steps, the result would be manifest as a slower solubilization rate. Taken together the data suggest that the C-terminus of apoA-V functions in the lipid binding activity of this protein. In this manner, the C-terminus of apoA-V appears to resemble other members of the exchangeable apolipoprotein family (*14, 20*). Confirmation of the role of the C-terminal segment of apoA-V in lipid binding activity of this protein was obtained using an isolated peptide corresponding to this region. ApoA-V(295-343) induced formation of a discrete population of reconstituted HDL and showed markedly enhanced phospholipid solubilization kinetics.

By analogy, the C-terminus of human apoA-I is recognized as the major lipid binding element in this protein (*21*). Removal of C-terminal residues 193 - 243 from apoA-I induces a decrease in lipid binding activity together with a loss of ANS binding sites. Recent X-ray crystallography evidence (*22*) suggests the C-terminus of apoA-I exists as a distinct structural entity while the main body of the protein adopts a four helix bundle molecular architecture with the C-terminus organized as two solvent exposed helical segments. By the same token, the C-terminal domain of apoE comprises ~83 residues and is the major lipid binding segment in this protein (*23*). In a manner similar to apoA-I, the N-terminus of apoE is organized as a four helix bundle.

While further work is required to elucidate the precise domain structure in apoA-V, the present data indicate the existence of two independently folded structural elements, one of relatively high stability and a second of lower stability. Interestingly, the guanidine HCl denaturation profile observed in the present study is similar to that reported for apoE (*24*). The observation that C-terminal truncation affected the guanidine HCl induced unfolding of only the lower stability component of the curve suggests that, in a manner similar to apoE, the N-terminal region corresponds to the more stable structural entity. In contrast, a previous study employing temperature-induced denaturation of apoA-V revealed a single transition midpoint (*17*). It is worth mentioning that temperature-induced denaturation of apoE also revealed a single transition profile (*25*) while guanidine HCl denaturation studies revealed a two domain structure (*24*). This is interesting because the method used to unfold a protein gives insight into its structural interactions. For instance, comparing temperature and guanidine HCl denaturation studies, it has been shown that the former assesses the overall stability of a protein while the latter assesses mainly the contributions of hydrophobic interactions on protein stability. This is due to the fact that guanidine HCl (a salt) can ionize in aqueous solution, masking the electrostatic interactions of the protein of interest (*26*). Taking into account the denaturation methods used and the data obtained from each, it can be concluded that the increased stability of the N-terminal region of apoA-V compared to the C-terminal region is due to hydrophobic or nonionic interactions. Whether the N-terminal region of the protein adopts a helix bundle conformation similar to that seen for the N-terminus of apoE (*27*), apoA-I (*22*) or apolipophorin III (*28, 29*), remains to be determined. Studies are currently in progress to define the boundaries of the apparently distinct structural elements present in apoA-V and to determine the mechanism of its plasma TG modulation activity.

2.6 MATERIALS AND METHODS

Apolipoproteins

Recombinant human apoA-V was prepared as described by Beckstead et al. (*17*). Site directed mutagenesis was performed using the QuickChange II XL kit from Stratagene (La Jolla, CA) according to the manufacturers instructions. All mutations were verified by DNA sequencing. A 48 amino acid peptide corresponding to apoA-V residues 295- 343 was prepared by solid phase peptide synthesis, isolated by reversed phase HPLC and characterized by mass spectrometry on an Applied Biosystems Voyager System 1054. The observed mass (5,319.7) was in good agreement with the expected molecular mass based on the amino acid sequence (5,318.8).

Analytical procedures

Protein concentrations were determined using the bicinchoninic acid assay (Pierce Chemical Co.) using bovine serum albumin as standard. C-terminal peptide concentrations were determined spectrophotometrically at 280 nm using an extinction coefficient = 5500 M^{-1} cm^{-1}. SDS-PAGE was performed on 4 - 20 % acrylamide slab gels run at a constant 30 mA for 1.*5* h. Gels were stained with Gel Code Blue (Pierce Chemical Co.).

Far UV circular dichroism spectroscopy

Far UV CD measurements were performed on a Jasco 810 spectropolarimeter. Scans were repeated five times to obtain the average value using a 0.02 cm path length and a protein concentration of 0.6 mg/mL. Protein was dissolved in 50 mM sodium citrate, pH 3.0, 150 mM NaCl. For guanidine HCl denaturation experiments, apoA-V samples (0.2 mg/mL) were incubated overnight at a given denaturant concentration in order to attain equilibrium, and ellipticity was measured at 222 nm (0.1 cm path length). Ellipticity values were converted into molar ellipticity (millidegrees cm^2 $decimole^{-1}$) using a mean residue weight value of 113.4 for full length apoA-V and 114.3 for apoA-V(1-292). Protein secondary structure content was calculated using the self-consisted method with Dicroprot version 2.6 (*30*).

Fluorescence spectroscopy

Fluorescence spectra were obtained on a Horiba Jobin Yvon FluoroMax-3 luminescence spectrometer. Protein (40 µg/ml) was dissolved in 50 mM sodium citrate, pH 3.0, 150 mM NaCl. Dimyristoylphosphatidylcholine (DMPC) bound apoA-V samples were prepared at a 5:1 DMPC:apoA-V ratio (w/w). Samples were excited at 295 nm and emission collected from 300 to 450 nm (slit width 2.0 nm). Spectra of 8-anilino-1-napthalene sulfonic acid (ANS) solutions (250 mM) were obtained in buffer alone and in the presence of apoA-V at 50 mg/mL on a Perkin Elmer LS50B luminescence spectrometer. Samples were excited at 395 nm with emission

monitored from 400 - 600 nm (3.0 nm slit width). Since ANS fluorescence in buffer is negligible (*31*), spectra were recorded in the presence of a minimum 100-fold excess of ANS with respect to protein (mol/mol).

DMPC solubilization studies.

Small unilamellar vesicles (SUV) of DMPC were prepared by extrusion through a 200 nm filter as described by Weers et al. (*32*). Protein and lipid vesicles were prepared in 50 mM sodium citrate, pH 3.0, 150 mM NaCl. DMPC (250 μg) was incubated in the absence or presence of 100 μg apolipoprotein, maintaining the sample temperature at 24 °C with a Peltier controlled cell holder. The change in sample light scatter intensity was measured with a Shimadzu spectrophotometer at 325 nm.

2.7 REFERENCES

1. Pennacchio, L. A., Olivier, M., Hubacek, J. A., Cohen, J. C., Cox, D. R., Fruchart, J. C., Krauss, R. M., and Rubin, E. M. (2001) An apolipoprotein influencing triglycerides in humans and mice revealed by comparative sequencing, *Science 294*, 169-173.
2. van der Vliet, H. N., Sammels, M. G., Leegwater, A. C., Levels, J. H., Reitsma, P. H., Boers, W., and Chamuleau, R. A. (2001) Apolipoprotein A-V: a novel apolipoprotein associated with an early phase of liver regeneration, *J Biol Chem 276*, 44512-44520.
3. Alborn, W. E., Johnson, M. G., Prince, M. J., and Konrad, R. J. (2006) Definitive N-terminal protein sequence and further characterization of the novel apolipoprotein A5 in human serum, *Clin Chem 52*, 514-517.
4. van der Vliet, H. N., Schaap, F. G., Levels, J. H., Ottenhoff, R., Looije, N., Wesseling, J. G., Groen, A. K., and Chamuleau, R. A. (2002) Adenoviral overexpression of apolipoprotein A-V reduces serum levels of triglycerides and cholesterol in mice, *Biochem Biophys Res Commun 295*, 1156-1159.
5. Ito, Y., Azrolan, N., O'Connell, A., Walsh, A., and Breslow, J. L. (1990) Hypertriglyceridemia as a result of human apo CIII gene expression in transgenic mice, *Science 249*, 790-793.
6. Maeda, N., Li, H., Lee, D., Oliver, P., Quarfordt, S. H., and Osada, J. (1994) Targeted disruption of the apolipoprotein C-III gene in mice results in hypotriglyceridemia and protection from postprandial hypertriglyceridemia, *J Biol Chem 269*, 23610-23616.
7. Weinberg, R. B., Cook, V. R., Beckstead, J. A., Martin, D. D., Gallagher, J. W., Shelness, G. S., and Ryan, R. O. (2003) Structure and interfacial properties of human apolipoprotein A-V, *J Biol Chem 278*, 34438-34444.
8. Schaap, F. G., Rensen, P. C., Voshol, P. J., Vrins, C., van der Vliet, H. N., Chamuleau, R. A., Havekes, L. M., Groen, A. K., and van Dijk, K. W. (2004) ApoAV reduces plasma triglycerides by inhibiting very low density lipoprotein-triglyceride (VLDL-TG) production and stimulating lipoprotein lipase-mediated VLDL-TG hydrolysis, *J Biol Chem 279*, 27941-27947.
9. Fruchart-Najib, J., Bauge, E., Niculescu, L. S., Pham, T., Thomas, B., Rommens, C., Majd, Z., Brewer, B., Pennacchio, L. A., and Fruchart, J. C. (2004) Mechanism of triglyceride lowering in mice expressing human apolipoprotein A5, *Biochem Biophys Res Commun 319*, 397-404.
10. Grosskopf, I., Baroukh, N., Lee, S. J., Kamari, Y., Harats, D., Rubin, E. M., Pennacchio, L. A., and Cooper, A. D. (2005) Apolipoprotein A-V deficiency results in marked hypertriglyceridemia attributable to decreased lipolysis of triglyceride-rich lipoproteins and removal of their remnants, *Arterioscler Thromb Vasc Biol 25*, 2573-2579.
11. Lookene, A., Beckstead, J. A., Nilsson, S., Olivecrona, G., and Ryan, R. O. (2005) Apolipoprotein A-V-heparin interactions: implications for plasma lipoprotein metabolism, *J Biol Chem 280*, 25383-25387.
12. Merkel, M., Loeffler, B., Kluger, M., Fabig, N., Geppert, G., Pennacchio, L. A., Laatsch, A., and Heeren, J. (2005) Apolipoprotein AV accelerates plasma hydrolysis of triglyceride-rich lipoproteins by interaction with proteoglycan-bound lipoprotein lipase, *J Biol Chem 280*, 21553-21560.

13. Marcais, C., Verges, B., Charriere, S., Pruneta, V., Merlin, M., Billon, S., Perrot, L., Drai, J., Sassolas, A., Pennacchio, L. A., Fruchart-Najib, J., Fruchart, J. C., Durlach, V., and Moulin, P. (2005) Apoa5 Q139X truncation predisposes to late-onset hyperchylomicronemia due to lipoprotein lipase impairment, *J Clin Invest 115*, 2862-2869.
14. Saito, H., Lund-Katz, S., and Phillips, M. C. (2004) Contributions of domain structure and lipid interaction to the functionality of exchangeable human apolipoproteins, *Prog Lipid Res 43*, 350-380.
15. Ishihara, M., Kujiraoka, T., Iwasaki, T., Nagano, M., Takano, M., Ishii, J., Tsuji, M., Ide, H., Miller, I. P., Miller, N. E., and Hattori, H. (2005) A sandwich enzyme-linked immunosorbent assay for human plasma apolipoprotein A-V concentration, *J Lipid Res 46*, 2015-2022.
16. O'Brien, P. J., Alborn, W. E., Sloan, J. H., Ulmer, M., Boodhoo, A., Knierman, M. D., Schultze, A. E., and Konrad, R. J. (2005) The novel apolipoprotein A5 is present in human serum, is associated with VLDL, HDL, and chylomicrons, and circulates at very low concentrations compared with other apolipoproteins, *Clin Chem 51*, 351-359.
17. Beckstead, J. A., Oda, M. N., Martin, D. D., Forte, T. M., Bielicki, J. K., Berger, T., Luty, R., Kay, C. M., and Ryan, R. O. (2003) Structure-function studies of human apolipoprotein A-V: a regulator of plasma lipid homeostasis, *Biochemistry 42*, 9416-9423.
18. Oliva, C. P., Pisciotta, L., Li Volti, G., Sambataro, M. P., Cantafora, A., Bellocchio, A., Catapano, A., Tarugi, P., Bertolini, S., and Calandra, S. (2005) Inherited apolipoprotein A-V deficiency in severe hypertriglyceridemia, *Arterioscler Thromb Vasc Biol 25*, 411-417.
19. Weers, P. M., Van Der Horst, D. J., and Ryan, R. O. (2000) Interaction of locust apolipophorin III with lipoproteins and phospholipid vesicles: effect of glycosylation, *J Lipid Res 41*, 416-423.
20. Saito, H., Dhanasekaran, P., Nguyen, D., Holvoet, P., Lund-Katz, S., and Phillips, M. C. (2003) Domain structure and lipid interaction in human apolipoproteins A-I and E, a general model, *J Biol Chem 278*, 23227-23232.
21. Ji, Y., and Jonas, A. (1995) Properties of an N-terminal proteolytic fragment of apolipoprotein AI in solution and in reconstituted high density lipoproteins, *J Biol Chem 270*, 11290-11297.
22. Ajees, A. A., Anantharamaiah, G. M., Mishra, V. K., Hussain, M. M., and Murthy, H. M. (2006) Crystal structure of human apolipoprotein A-I: insights into its protective effect against cardiovascular diseases, *Proc Natl Acad Sci U S A 103*, 2126-2131.
23. Westerlund, J. A., and Weisgraber, K. H. (1993) Discrete carboxyl-terminal segments of apolipoprotein E mediate lipoprotein association and protein oligomerization, *J Biol Chem 268*, 15745-15750.
24. Wetterau, J. R., Aggerbeck, L. P., Rall, S. C., Jr., and Weisgraber, K. H. (1988) Human apolipoprotein E3 in aqueous solution. I. Evidence for two structural domains, *J Biol Chem 263*, 6240-6248.
25. Morrow, J. A., Segall, M. L., Lund-Katz, S., Phillips, M. C., Knapp, M., Rupp, B., and Weisgraber, K. H. (2000) Differences in stability among the human apolipoprotein E isoforms determined by the amino-terminal domain, *Biochemistry 39*, 11657-11666.

26. Monera, O. D., Kay, C. M., and Hodges, R. S. (1994) Protein denaturation with guanidine hydrochloride or urea provides a different estimate of stability depending on the contributions of electrostatic interactions, *Protein Sci 3*, 1984-1991.
27. Wilson, C., Wardell, M. R., Weisgraber, K. H., Mahley, R. W., and Agard, D. A. (1991) Three-dimensional structure of the LDL receptor-binding domain of human apolipoprotein E, *Science 252*, 1817-1822.
28. Breiter, D. R., Kanost, M. R., Benning, M. M., Wesenberg, G., Law, J. H., Wells, M. A., Rayment, I., and Holden, H. M. (1991) Molecular structure of an apolipoprotein determined at 2.5-A resolution, *Biochemistry 30*, 603-608.
29. Wang, J., Sykes, B. D., and Ryan, R. O. (2002) Structural basis for the conformational adaptability of apolipophorin III, a helix-bundle exchangeable apolipoprotein, *Proc Natl Acad Sci U S A 99*, 1188-1193.
30. Sreerama, N., and Woody, R. W. (1993) A self-consistent method for the analysis of protein secondary structure from circular dichroism, *Anal Biochem 209*, 32-44.
31. Stryer, L. (1965) The interaction of a naphthalene dye with apomyoglobin and apohemoglobin. A fluorescent probe of non-polar binding sites, *J Mol Biol 13*, 482-495.
32. Weers, P. M., Narayanaswami, V., and Ryan, R. O. (2001) Modulation of the lipid binding properties of the N-terminal domain of human apolipoprotein E3, *Eur J Biochem 268*, 3728-3735.

CHAPTER 3:
Characterization of apolipoprotein A-V lipid-free amino-terminal structural domain

3.1 ABBREVIATIONS

apo = apolipoprotein
HTG = hypertriglyceridemia
TG = triglyceride
HDL = high density lipoprotein
VLDL = very low density lipoprotein
CFE = carbon filled Epon
CD = circular dichroism
ANS = 8-anilino-1-naphthalene sulfonic acid
SDS = sodium dodecyl sulfate
PAGE = polyacrylamide gel electrophoresis
NT = amino terminal

3.2 ABSTRACT

Previous studies of recombinant full-length human apolipoprotein A-V (apoA-V) provided evidence for the presence of two independently folded structural domains. Computer-assisted sequence analysis and limited proteolysis studies identified an N-terminal fragment as a candidate for one of the domains. C-terminal truncation variants in this size range, apoA-V(1-146) and apoA-V(1-169), were expressed in *E. coli* and isolated. Unlike full-length apoA-V or apoA-V(1-169), apoA-V(1-146) was soluble in neutral pH buffer in the absence of lipid. Sedimentation equilibrium analysis yielded a weight average molecular weight = 18,811, indicating apoA-V(1-146) exists as a monomer in solution. Guanidine HCl denaturation experiments at pH 3.0 yielded a one-step native to unfolded transition that corresponds directly with the more stable component of the two-stage denaturation profile displayed by full-length apoA-V. On the other hand, denaturation experiments conducted at pH 7.0 revealed a less stable structure. In a manner similar to known helix bundle apolipoproteins, apoA-V(1-146) induced a relatively small enhancement in 8-anilino-1-naphthalene sulfonic acid fluorescence intensity. Quenching studies with single Trp apoA-V(1-146) variants revealed that a unique site predicted to reside on the nonpolar face of an amphipathic α-helix was protected from quenching by KI. Taken together, the data suggest the N-terminal 146 residues of human apoA-V adopts a helix bundle molecular architecture in the absence of lipid and, thus, likely exists as an independently folded structural domain within the context of the intact protein.

3.3 BACKGROUND

Hypertriglyceridemia (HTG) is strongly and positively correlated with susceptibility to atherosclerosis (*1*). Furthermore, HTG is a risk factor for development of the metabolic syndrome and the accompanying insulin resistance, hypertension, obesity and inflammation. Based on this, there is considerable interest in understanding factors that regulate plasma triglyceride (TG) levels. The discovery of a new apolipoprotein in 2001, termed apolipoprotein (apo) A-V, has sparked an intensive research effort (*2, 3*). The impact of apoA-V on plasma TG levels is vividly illustrated by the seminal report of Pennacchio et al. (*4*). Using genetically modified mice, these authors showed that plasma TG concentrations in human *APOA5* transgenic mice were 3-fold lower than control littermates. At the same time, apoA-V gene disrupted mice displayed a four-fold increase in plasma TG.

Human apoA-V is synthesized in the liver as a 366 amino acid pre-protein. Following cleavage of a 23 amino acid signal peptide, mature apoA-V, consisting of 343 residues, can be detected in plasma (*5*). Comparative sequence analysis indicates apoA-V is a member of the class of exchangeable apolipoproteins and predicts a hydrophobic protein with a significant amount of α-helical secondary structure (*6*). This prediction has been confirmed by far UV circular dichroism spectroscopy analysis (*7*). A distinguishing feature of recombinant lipid-free apoA-V is poor solubility in neutral pH buffer (*8*). Characterization studies of lipid-free apoA-V revealed strong lipid binding activity (*6*). Consistent with this, apoA-V is found exclusively associated with lipoproteins in the plasma compartment. In mice apoA-V is predominantly associated with HDL (*9*) while in humans it is found in the VLDL and HDL fractions (*10*). Evidence suggests that apoA-V can exchange between VLDL and HDL, possibly as a function of plasma lipoprotein homeostasis (*9*).

In 2005 Marçais et al. reported the presence of a mutant form of apoA-V in a family with HTG (*11*). The mutation introduces a premature stop codon, resulting in a truncated apoA-V variant that is recovered in the lipoprotein-deficient fraction of plasma. These data suggest the C-terminal portion of apoA-V is a determinant of its lipoprotein binding ability. Subsequent studies revealed the C-terminus contributes to the lipid binding activity of apoA-V (*7*). It was reported that deletion of the C-terminal 51 amino acids from apoA-V resulted in a variant protein that displayed lower lipid binding activity yet still possessed two independently folded structural domains. In the present study we sought to define the boundary between these domains and to characterize the N-terminal domain in isolation. The results obtained reveal that lipid-free apoA-V(1-146) adopts a relatively stable, monomeric, asymmetric tertiary fold that is consistent with an amphipathic α-helix bundle.

3.4 RESULTS

Limited proteolysis of full-length apoA-V

Based on similarities with other members of the exchangeable apolipoprotein family (*12, 13*), we hypothesized that the N-terminus of apoA-V may exist in solution as an independently folded, amphipathic α-helix bundle. In the case of another two-domain apolipoprotein, apoE, limited proteolysis yielded two major fragments (*14, 15*) that were shown to exist as independently folded structural domains (*16, 17*). Due to the insolubility of lipid free full-length apoA-V at neutral pH, proteolytic digestion experiments were conducted at pH 3.0 using pepsin. Isolated recombinant apoA-V was incubated with pepsin (1000:1 w/w) as a function of time, followed by SDS-PAGE analysis of the digestion products (**Figure 3-1**). The data showed that, as intact apoA-V was rapidly degraded, two prominent fragments, one of ~22 kDa and the other ~18 kDa, were generated. At longer time points, or higher protease concentrations, complete degradation of apoA-V occurred (data not shown). Based on the apparent protection of the 18 kDa and 22 kDa fragments from limited proteolysis, these fragments were subjected to further characterization. Electro spray ionization mass spectrometry analysis yielded molecular mass values of 18,721.2 and 22,198.9. N-terminal sequencing of the cleavage products revealed the first seven to ten amino acid residues of the 18 kDa band corresponded to V-S-G-I-G-R-H-V-Q-E-L while that for the 22 kDa band was M-H-H-H-H-H-H. Since recombinant apoA-V employed in the proteolysis studies possessed an N-terminal His-Tag extension, we conclude that the larger cleavage product corresponds to the N-terminal portion of apoA-V (residues 1 – 175). The identity of the smaller 18 kDa band corresponds to apoA-V residues 176 – 343, presumably encompassing the C-terminal structural domain of apoA-V.

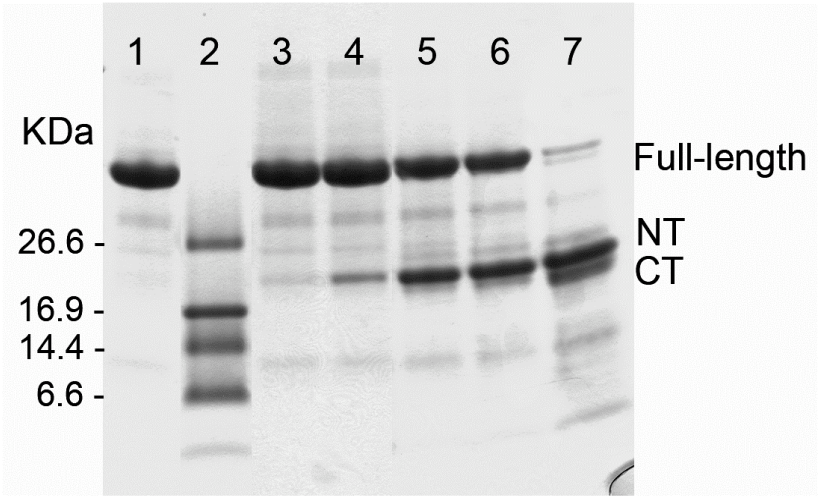

Figure 3-1. SDS PAGE analysis of pepsin limited proteolysis of apoA-V full length. Proteins were electrophoresed on a 10 – 20 % acrylamide SDS slab gel and stained with Gel Code Blue reagent. Lane 1, untreated apoA-V full length; lane 2, molecular mass markers; lane 3, pepsin treated apoA-V full length 0 min; lane 4, pepsin treated 5 min; lane 5, pepsin treated 30 min; lane 6, pepsin treated 60 min; lane 7, pepsin treated 120 min. NT = N-terminal fragment, CT = C-terminal fragment.

In silico analysis of apoA-V N-terminal domain

Evaluation of the N-terminal sequence of apoA-V (residues 1 – 175) by the Coils program (*18*) predicts that residues Ala31–Arg52, Val67–Gln85 and Asp112–Asp134 adopt α-helix secondary structure. Given that a hallmark feature of the class of exchangeable apolipoproteins is the presence of amphipathic α-helices approximately 22 amino acids in length, we sought to assess if these predicted helices would display amphipathic character (i.e. possess distinct nonpolar and polar faces with positively charged amino acids located at the interface between the polar and nonpolar faces, while negatively charged residues reside at the apex of the polar face (*19*)). An Edmundson wheel (*20*) projection of the sequence from Gly68 to Gln85 reveals these characteristic features (**Figure 3-2**) consistent with earlier hydropathy analysis (*6*). Furthermore, similar to other members of the class of exchangeable apolipoproteins, two of the three α-helix segments predicted by the Coils program are punctuated by proline residues (**Figure 3-3**).

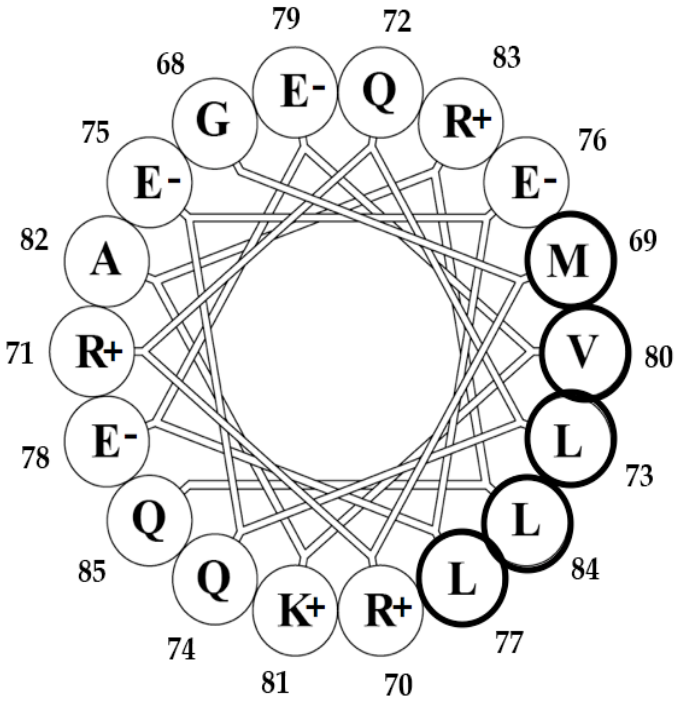

Figure 3-2. Helical wheel diagram for a predicted helix in apoA-V(1-146). The amino acid residues depicted are numbered with hydrophobic residues circled in bold and charged residues indicated.

RKGFWDYFSQ TSGDKGRVEQ IHQQKMAREP ATLKDSLEQD LNNMNKFLEK

LRPLSGSEAP RLPQDPVGMR RQLQEELEEV KARLQPYMAE AHELVGWNLE

GLRQQLKPYT MDLMEQVALR VQELQEQLRV VGEDTKAQLL GGVDEA

Figure 3-3. Amino acid sequence of apoA-V(1-146). Residues postulated to adopt alpha helix secondary structure, as predicted by Coils program analysis, are underlined. Proline residues are depicted in bold.

Isolation and characterization of apoA-V(1-146)

In an effort to study the N-terminal fragment of apoA-V in greater detail, two truncation variants, apoA-V(1-169) and apoA-V(1-146), were expressed in *E. coli*, isolated and characterized (**Figure 3-4**). ApoA-V(1-292) was previously characterized and found to possess two structural domains (*7*). Unlike full-length apoA-V, apoA-V(1-292) or apoA-V(1-169), apoA-V(1-146) was soluble in aqueous buffer at neutral pH. Furthermore, limited proteolysis experiments with apoA-V(1-146) revealed resistance to further degradation. Given the favorable solubility properties of this variant and the apparent similarity of this truncated apoA-V variant to one of the protease resistant fragments generated upon pepsin treatment of full-length apoA-V, characterization studies of apoA-V(1-146) were performed.

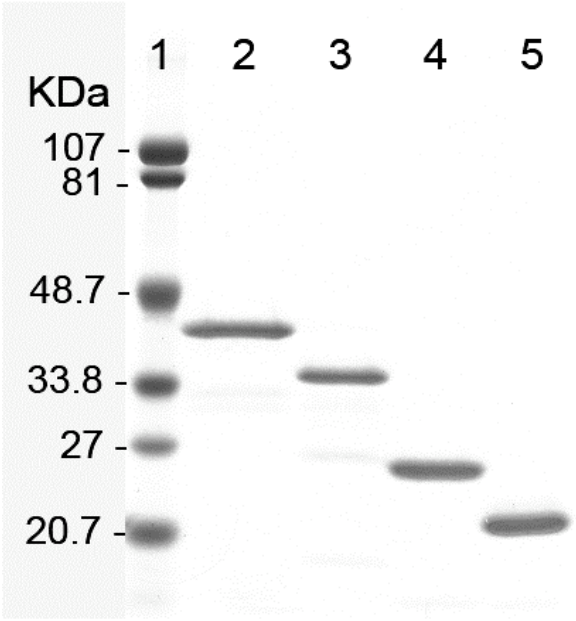

Figure 3-4. SDS-PAGE analysis of isolated apoA-V truncation variants. Lane 1, molecular mass markers; lane 2, apoA-V full length; lane 3, apoA-V(1-292); lane 4, apoA-V(1-169); lane 5, apoA-V(1-146). [Figure generated by Jennifer A. Beckstead.]

Hydrodynamic properties

[Data collected in collaboration with the laboratory of Dr. Cyril M. Kay at the University of Alberta]

The hydrodynamic properties of apoA-V(1-146) were investigated by sedimentation equilibrium analyses performed at pH 7.0 (**Table 3-1**). The initial centrifugation speed was set at 22,000 rpm and equilibrium was reached after 18 h. Data were collected at 22,000, 24,000 and 26,000 rpm. The apparent average molecular weight of apoA-V(1-146) was 18,811 Da, a value that corresponds well with the calculated molecular weight of this protein (18,795 Da). This data indicates that, unlike full-length apoA-V (*8*), apoA-V(1-146) exists in solution as a monomer. To evaluate the shape of apoA-V(1-146) in solution, sedimentation velocity experiments were conducted. Using the Svedberg software, the data were fit to a single species model yielding a sedimentation coefficient ~1.8. The program Sednterp was then used to calculate an axial ratio value. Using a prolate model and a hydration expansion of 17.1%, an axial ratio (a/b) = 7 was obtained.

Table 3-1. Result summary of sedimentation velocity runs on apoA-V (1-146)

Sample Concentration (mg/mL)	**$S_{20,w}$**	**$S^0_{20,w}$**	**Axial Ratio**
0.55	1.868	1.877	6.385
0.24	1.756	1.760	7.883

CD spectroscopy and stability studies

Far UV CD spectroscopy of apoA-V(1-146) at pH 7.4 yielded a spectrum with minima at 208 nm and 222 nm. Deconvolution of the spectra yielded 40.4 % alpha helix secondary structure content, consistent with predictions from Coils program analysis. To assess the stability properties of apoA-V(1-146) in solution, the effect of guanidine-HCl concentration on ellipticity values at 222 nm were determined (**Figure 3-5**). At pH 3.0 (pH at which comparisons with data on full-length apoA-V can be made), as the concentration of denaturant increased form 0 M to 4 M, apoA-V(1-146) unfolded in a single transition, with a midpoint at 2.0 M guanidine HCl. At pH 7.4, although apoA-V (1-146) still undergoes a one-step native ⇨ unfolded transition, the transition midpoint is shifted to 0.9 M guanidine-HCl, a value similar to that reported for apoA-I (*21*).

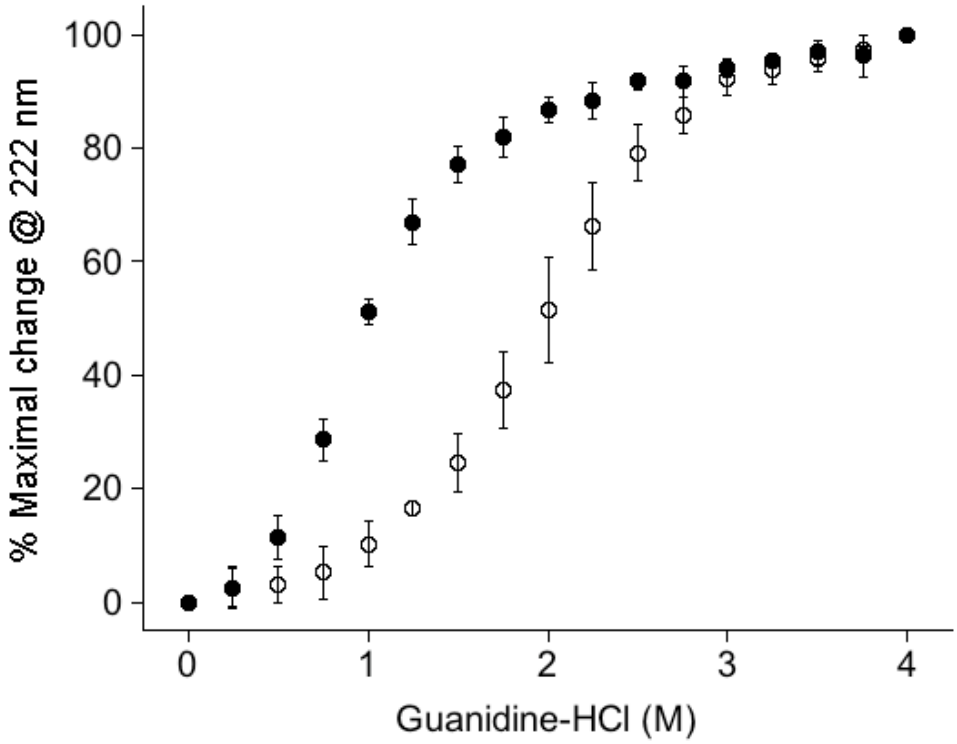

Figure 3-5. Guanidine-HCl denaturation of apoA-V (1-146). The molar ellipticity of protein was measured at 222 nm at a concentration of 0.2 mg/mL in 50 mM citrate, 150 mM NaCl, pH 3.0 (open circles) or 20 mM phosphate buffer, pH 7.4 (closed circles), at various concentrations of guanidine-HCl (± SD, n = 4).

Fluorescent dye binding

ANS, a hydrophobic fluorescent dye, binds to exposed hydrophobic surfaces in proteins (*22*). In the absence of protein, ANS has a very low quantum yield with an emission wavelength maximum of ~520 nm (excitation 395 nm). Albumin, a serum lipid transport protein known to possess exposed hydrophobic lipid binding sites, induced a significant enhancement in ANS fluorescence intensity as well as a blue shift in the wavelength of maximum fluorescence emission at pH 7.4 (**Figure 3-6**). By contrast, known helix-bundle apolipoproteins, including apoE3 NT (*23*) and apolipophorin III (*24*) had a lesser effect on ANS fluorescence intensity. In a similar manner, apoA-V(1-146) induced a relatively small enhancement in ANS fluorescence intensity, consistent with sequestration of hydrophobic sites in this protein from the aqueous milieu.

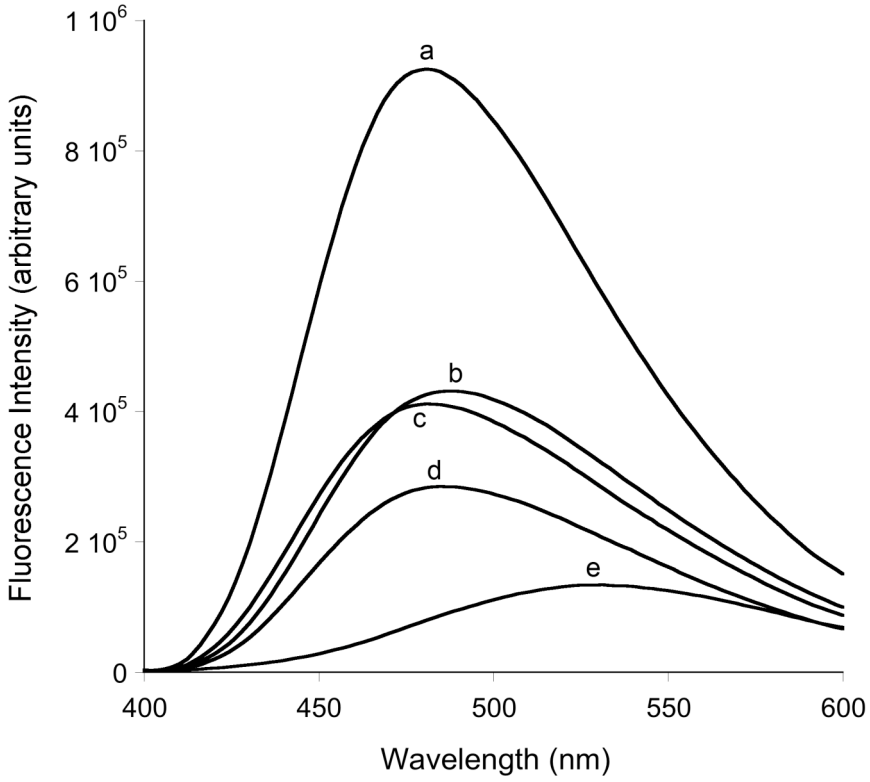

Figure 3-6. Effect of proteins on ANS fluorescence. (a) Albumin, (b) apoA-V(1-146), (c) apoLp III, (d) apoE3 NT, and (e) ANS in buffer.

Tryptophan fluorescence emission of apoA-V(1-146) variants

ApoA-V(1-146) has two naturally occurring Trp, located at positions 5 and 97. Fluorescence emission (excitation 295 nm) spectra of wild type apoA-V(1-146) gave rise to a λ_{max} = 350 nm (**Table 3-2**). To determine the individual contribution of the two Trp residues in this protein, single Trp variant apoA-V(1-146) were generated. To test the hypothesis that apoA-V(1-146) adopts a helix bundle conformation in solution, a single Trp was also introduced into Trp-null apoA-V(1-146) by replacing Leu73 with Trp. Based on predictions this sequence position should reside on the nonpolar face of an amphipathic α-helix (see **Figure 3-2**). At neutral pH, the λ_{max} of each of the three single Trp variants was 349 nm. In contrast, when Trp fluorescence emission was monitored at pH 3.0, both the Trp@73 and Trp@97 variants show a blue shift in λ_{max} to 338 nm and 341 nm, respectively (**Table 3-2**).

Table 3-2. Fluorescence properties of apoA-V(1-146) single Trp variants.[a]

ApoA-V (1-146) variant	pH 7.4 λ_{max} (nm)[b]	pH 3.0 λ_{max} (nm)[b]
"WT"	350	347
Trp 5	349	348
Trp 97	349	341
Trp 73	349	338

[a] Spectra were recorded on a Horiba Jobin Yvon FluoroMax-4 luminescence spectrometer. Emission was scanned from 300 nm to 450 nm (excitation 295 nm; slit width 2.0 nm for the excitation and emission monochromators). All spectra were recorded in either 20 mM sodium phosphate, pH 7.4, 150 mM NaCl or 50 mM sodium citrate, pH 3.0, 150 mM NaCl.

[b] λ_{max} is the wavelength of maximum fluorescence emission. Values reported are the mean of 3 determinations. In all cases the standard deviations were ≤ 1 nm.

Fluorescence quenching

To obtain additional information about the local environments of Trp5, Trp97 and Trp73 in single Trp apoA-V(1-146) variants, fluorescence quenching studies were performed with potassium iodide (KI) as the quenching agent. Stern-Volmer plots for each single Trp variant were linear (**Figure 3-7**), and K_{SV} constants were obtained from the slope of the plots. The values obtained were 3.2 M^{-1} for the W@5 variant, 2.2 M^{-1} for the W@97 variant and 1.8 M^{-1} for the W@73 variant.

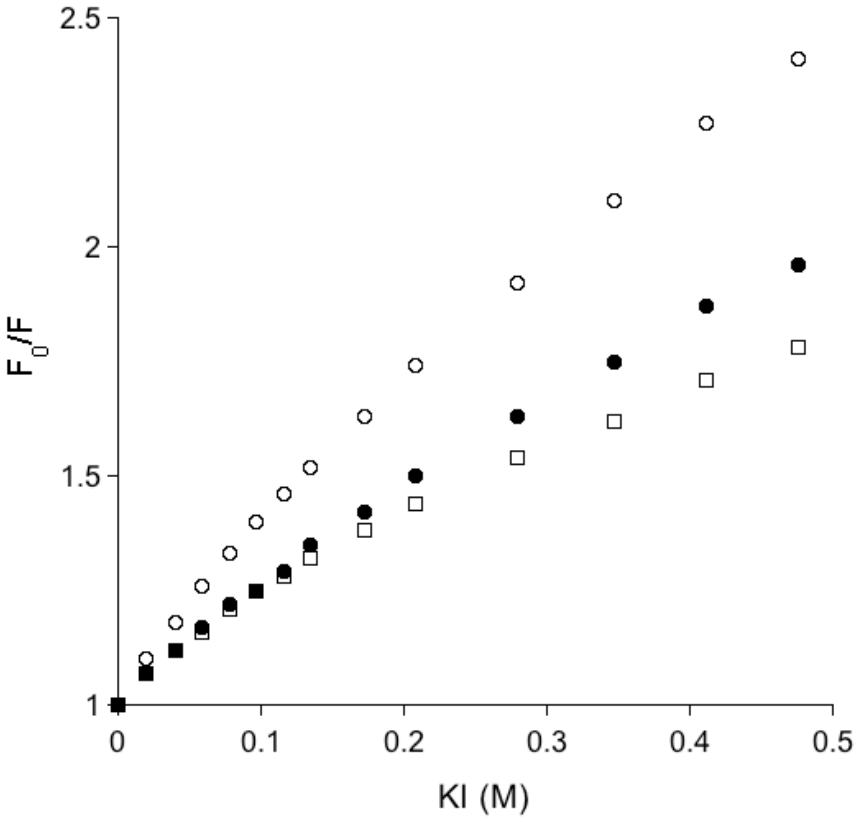

Figure 3-7. Trp fluorescence quenching of apoA-V(1-146) by KI at pH 7.4. Stern-Volmer plots of apoA-V(1-146) W@5 (open circles), apoA-V(1-146) W@97 (closed circles), and apoA-V(1-146) W@73 (open squares).

3.5 DISCUSSION

The amphipathic α-helix bundle is a common structural motif among exchangeable apolipoproteins in their lipid-free state. X-ray crystallography studies of apoE NT domain (*23*), apolipophorin III (*25*) as well as apoA-I (*13*) reveal elongated up-and-down bundles of 4 or 5 amphipathic α-helices. In every case the helices orient such that their hydrophobic faces are directed toward the bundle interior. At the same time, hydrophilic moieties are directed to the solvent, conferring aqueous solubility to these proteins (*26*). In the present study, the data are consistent with the presence of at least 3 distinct α-helices in apoA-V(1-146) (**Figure 3-8**). Whereas the 3-helix bundle motif exists among helix bundle proteins in general (*27-29*), no 3-helix bundle motifs have been reported for apolipoproteins. Evidence for the presence of only 3 helix segments in apoA-V(1-146) is based upon predictions from Coils program analysis. However, caution must be exercised in this case since a similar analysis of human apoE3 N-terminal domain primary structure predicts residues 1 – 183 also possesses 3 distinct helix segments. Whereas Coils analysis faithfully predicts the boundaries for 3 out of the 4 helices known (on the basis of X-ray crystallography (*23*)) to exist in apoE-NT, helix 1 was not identified by this program. Based on this, it is conceivable that apoA-V(1-146) may possess a fourth helix segment that was simply not predicted by Coils program analysis. Given the location of the three identified helix segments, a fourth helix, if present, could be located at the extreme N-terminus of this truncated apoA-V or between proline residues 86 and 108, consistent with fluorescence quenching data of Trp97. In fact, apoA-V(1-146) could conceivably contain five amphipathic helices, as has been shown with apolipophorin III (*24, 25*). The actual tertiary organization of apoA-V NT domain will require detailed high-resolution structure data from NMR spectroscopy and/or X-ray crystallography.

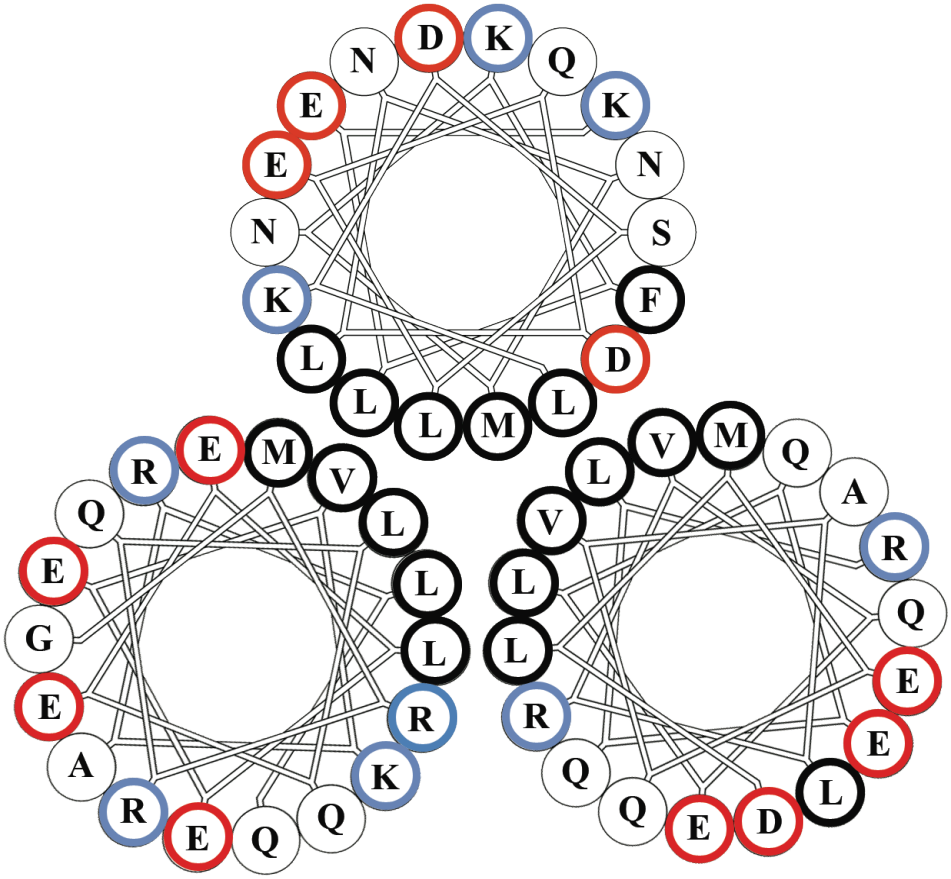

Figure 3-8. Model depicting postulated apoA-V(1-146) amphipathic helix bundle motif in the absence of lipid. Hydrophobic residues (bold) are oriented toward the center of the hydrophobic core while positively-charged (blue) and negatively-charged (red) residues are exposed to the aqueous environment.

On the basis of structural studies and other evidence, hypotheses have been proposed to explain the lipid surface seeking behavior of helix bundle apolipoproteins. Thus, whereas hydrophobic helix-helix interactions contribute to stabilization of the bundle conformation, these interactions are replaced by helix-lipid interactions in a lipid-associated state. Such a transition, however, requires that the bundle undergo conformational "opening" to expose hydrophobic lipid binding sites in the protein interior (*12, 13, 30*). Several lines of evidence are consistent with this hypothesis and, in the case of apoE-NT domain, this transition plays a key role in manifestation of its low density lipoprotein receptor recognition properties (*31*). Given the evidence that apoA-V(1-146) adopts a helix bundle motif, it is likely that a similar transition occurs upon lipid association with this protein.

In certain helix bundle apolipoproteins, the helix bundle motif constitutes the sole structural element of the protein (*24, 25*). In other cases, however, the helix bundle motif exists as a domain in the context of a larger protein. Thus, for example, apoE exists as a two domain protein comprised of an N-terminal helix bundle and a C-terminal lipid binding domain (*12*). Likewise, the N-terminus of apoA-I adopts a helix bundle that is connected to a short C-terminal segment with high lipid binding affinity (*13*). Given the relatively large size of apoA-V and the results of guanidine HCl denaturation studies (*7*), it is evident that two independently folded structural domains are present. Furthermore, recent studies with another C-terminal truncation variant, apoA-V(1-292), provided evidence that the N-terminus comprises the more stable component of the two structural elements in apoA-V (*7*). In the case of apoE, the N-terminal 165 amino acids adopt a 4-helix bundle conformation (*32*). From denaturation data, primary sequence analysis, and limited proteolysis, it may be concluded that the N-terminus of apoA-V adopts a similar molecular architecture in the absence of lipid. Indeed, several lines of evidence indicate that the N-terminal 146 amino acids of apoA-V exist as a helix bundle. Evidence supporting this interpretation includes the solubility properties of apoA-V(1-146). Whereas full length apoA-V and truncation variants longer than 146 residues are insoluble in neutral pH buffer, this is not the case for apoA-V(1-146). In general, it is envisioned that solubility is conferred to helix bundle apolipoproteins because of their ability to sequester hydrophobic lipid binding sites in the bundle interior. Because of this, isolated helix bundle apolipoproteins often exist in solution in a monomeric state (*17*). In the case of apoA-V(1-146), sedimentation equilibrium experiments provide evidence that the protein exists in solution as a monomer and, consistent with other helix bundle apolipoproteins, sedimentation velocity experiments yielded an axial ratio value that is consistent with a highly asymmetric structure. Similar values have been reported for helix bundle apolipoproteins (*33*) and these findings are supported by high-resolution structure data (*13, 23-25*).

An ability of helix bundle apolipoproteins to sequester their hydrophobic lipid binding sites in the bundle interior is generally manifest by a lower ability to enhance the fluorescence signal of ANS relative to proteins known to have exposed hydrophobic sites (*34*). ApoA-V(1-146) behaved similarly to apolipophorin III and apoE3-NT, suggesting it too adopts a helix bundle structure. Based on Coils analysis, the Trp at position 5 is predicted to be solvent exposed. Fluorescence quenching studies with KI at pH 7.4 show Trp5 is more susceptible to quenching, consistent with its location at the extreme N-terminus of the protein. On the other hand Trp73 is anticipated to reside on the hydrophobic face of an amphipathic α-helix based on Coils and Edmundson wheel analyses. The λ_{max} of Trp73 at 338 nm (at pH 3.0) suggests it

resides in a more nonpolar environment under these conditions. KI quenching studies with apoA-V(1-146) Trp@73 reveals the Trp at this position is relatively protected from this quencher, lending additional evidence for its proposed location within a helix bundle. KI quenching shows Trp97 to be more protected from the quencher than Trp5 but not more than Trp73. Thus it is conceivable that the region encompassing Trp97 adopts amphipathic α-helix secondary structure. While Trp73 was the least susceptible to fluorescence quenching, it was not completely inaccessible, which along with the Trp fluorescence emission results and the denaturation studies at pH 7.4, imply that apoA-V NT at neutral pH may adopt a "loosely" folded helix bundle under physiological conditions. Given the greater propensity of molten globule like conformations in apolipoproteins to associate with lipid surfaces (*35*), this property may be relevant to the function of this structural element in apoA-V, possibly in concert with the C-terminal region of intact apoA-V.

At present it is unknown if the NT domain of apoA-V alone is capable of manifesting biological effects seen with full-length apoA-V. Based on results of studies of a mutant/truncated form of apoA-V in human subjects that is associated with severe HTG (*11*), this segment of the protein alone may not be sufficient to manifest the biological effects seen with apoA-V in genetically engineered mice. Indeed, previous studies have suggested that residues in the region of 186 – 242 in apoA-V are responsible for the heparin binding ability of apoA-V (*36*) as well as its function as a ligand for members of the low density lipoprotein receptor family (*37*) or the recently identified glycosylphosphatidyl inositol high density lipoprotein binding protein 1 (*38*). Adenovirus mediated gene transfer of apoA-V(1-146) into apoA-V gene disrupted mice will permit this question to be addressed.

3.6 MATERIALS AND METHODS

Site-directed mutagenesis and overexpression of recombinant proteins

Recombinant human apoA-V and C-terminal truncation variants were produced in *E. coli* and isolated as described (*8*). ApoE-NT was prepared as described by Fisher at al. (*39*) and apolipophorin III was prepared according to Ryan et al. (*40*). Site-directed mutagenesis was performed with the QuikChange II XL Site-Directed Mutagenesis Kit (Stratagene). Primers were designed to introduce a premature stop codon or to substitute Trp5 with Phe, Trp97 with Phe or substitute Leu73 of Trp null apoA-V(1-146) with Trp. In all cases, introduction of the desired mutations was verified by DNA sequencing.

Limited Proteolysis

Aliquots of full-length apoA-V (0.1 mg/ml) in 50 mM sodium citrate, pH 3.0, 150 mM NaCl, were incubated with 0.1 µg/ml porcine gastric pepsin (Sigma) at 22 °C for up to 2 h. The reaction was stopped by addition of SDS-PAGE sample treatment buffer and the fragmentation pattern assessed by SDS gel electrophoresis on a Tricine, 10 – 20 % acrylamide slab run at a constant 125 V for 1.5 h and stained with Gel Code Blue (Pierce Chemical Co.). Where indicated separated protein fragments were electrophoretically transferred to a PVDF membrane and then subjected to N-terminal sequencing analysis (University of California, Davis, Molecular Structure Facility).

Analytical procedures

Protein concentrations were determined with the bicinchoninic acid assay (Pierce Chemical Co.) using bovine serum albumin as standard.

Analytical Ultracentrifugation

Sedimentation equilibrium experiments were conducted at 20 °C in a Beckman XL-I analytical ultracentrifuge using interference optics, as described by Laue and Stafford (*41*). Aliquots (110 µL) of the sample solution were loaded into six sector CFE sample cells, allowing three concentrations to be run simultaneously. Runs were performed at three different speeds and each speed was maintained until there was no significant difference in $r^2/2$ versus absorbance scans taken 2 h apart to ensure that equilibrium was achieved. Sedimentation equilibrium data were evaluated using the NONLIN program, which employs the nonlinear least squares curve-fitting algorithm described by Johnson et al. (*42*). The protein's partial specific volume and the solvent density were estimated using the Sednterp program (*43*). Sedimentation velocity experiments were run at 40,000 rpm and 20 °C using absorbance optics. Runs were performed at loading concentration of 0.55 mg/mL and 0.24 mg/mL, respectively. Up to 260 scans were performed during the run. A sedimentation coefficient value was obtained by analyzing 10 sets

of data selected between the 160th and 205th scan using the Svedberg software. From the amino acid composition, a hydration value of 0.44 was obtained, assuming that all charged groups are exposed.

Circular dichroism spectroscopy

Circular dichroism (CD) measurements were performed on an AVIV 410 spectrophotometer or a Jasco 810 spectropolarimeter. Far UV CD scans were obtained between 185 and 260 nm in 20 mM sodium phosphate, pH 7.4 using a protein concentration of 0.5 mg/mL determined by the absorbance at 280 nm. The α-helical content was calculated with the self consistent method using Dicroprot version 2.6 (*44*). For guanidine-HCl denaturation studies, protein samples were dissolved in 50 mM citrate, pH 3.0 or 20 mM sodium phosphate, pH 7.4. ApoA-V samples (0.2 mg/mL) were incubated overnight at a given denaturant concentration in order to attain equilibrium, and ellipticity was measured at 222 nm.

Fluorescence spectroscopy

Fluorescence spectra were obtained on a Horiba Jobin Yvon FluoroMax-4 luminescence spectrometer. Protein (100 μg/ml) was dissolved in either 50 mM citrate, pH 3.0, 150 mM NaCl, or 20 mM sodium phosphate, pH 7.4, 150 mM NaCl. Samples were excited at 295 nm and emission collected from 300 to 450 nm (slit width 2.0 nm). Spectra of 8-anilino-1-naphthalene sulfonic acid (ANS) solutions (250 mM) were obtained in pH 7.4 buffer alone and in the presence of specified proteins at 50 μg/mL. Samples were excited at 395 nm with emission monitored from 400 - 600 nm (2.0 nm slit width). Since ANS fluorescence in buffer is negligible (*22*), spectra were recorded in the presence of a minimum 100-fold excess of ANS with respect to protein (mol/mol). For KI quenching studies protein samples were excited at 295 nm and emission monitored at their λ_{max}. The solution of KI contained 1 mM sodium thiosulfate to prevent formation of free iodine and all readings were corrected for dilution. The data were analyzed using the Stern-Volmer equation: $F_0/F = 1 + K_{SV}[Q]$, where F_0 and F represent the emission intensity maximum in the absence and presence of quencher, respectively. The collisional quenching constant (K_{SV}) was determined from the initial slope of plots of F_0/F versus [Q].

3.7 REFERENCES

1. Yuan, G., Al-Shali, K. Z., and Hegele, R. A. (2007) Hypertriglyceridemia: its etiology, effects and treatment, *Cmaj 176*, 1113-1120.
2. Jakel, H., Nowak, M., Helleboid-Chapman, A., Fruchart-Najib, J., and Fruchart, J. C. (2006) Is apolipoprotein A5 a novel regulator of triglyceride-rich lipoproteins?, *Ann Med 38*, 2-10.
3. Wong, K., and Ryan, R. O. (2007) Characterization of apolipoprotein A-V structure and mode of plasma triacylglycerol regulation, *Curr Opin Lipidol 18*, 319-324.
4. Pennacchio, L. A., Olivier, M., Hubacek, J. A., Cohen, J. C., Cox, D. R., Fruchart, J. C., Krauss, R. M., and Rubin, E. M. (2001) An apolipoprotein influencing triglycerides in humans and mice revealed by comparative sequencing, *Science 294*, 169-173.
5. Alborn, W. E., Johnson, M. G., Prince, M. J., and Konrad, R. J. (2006) Definitive N-terminal protein sequence and further characterization of the novel apolipoprotein A5 in human serum, *Clin Chem 52*, 514-517.
6. Weinberg, R. B., Cook, V. R., Beckstead, J. A., Martin, D. D., Gallagher, J. W., Shelness, G. S., and Ryan, R. O. (2003) Structure and interfacial properties of human apolipoprotein A-V, *J Biol Chem 278*, 34438-34444.
7. Beckstead, J. A., Wong, K., Gupta, V., Wan, C. P., Cook, V. R., Weinberg, R. B., Weers, P. M., and Ryan, R. O. (2007) The C terminus of apolipoprotein A-V modulates lipid-binding activity, *J Biol Chem 282*, 15484-15489.
8. Beckstead, J. A., Oda, M. N., Martin, D. D., Forte, T. M., Bielicki, J. K., Berger, T., Luty, R., Kay, C. M., and Ryan, R. O. (2003) Structure-function studies of human apolipoprotein A-V: a regulator of plasma lipid homeostasis, *Biochemistry 42*, 9416-9423.
9. Nelbach, L., Shu, X., Konrad, R. J., Ryan, R. O., and Forte, T. M. (2008) Effect of apolipoprotein A-V on plasma triglyceride, lipoprotein size, and composition in genetically engineered mice, *J Lipid Res 49*, 572-580.
10. O'Brien, P. J., Alborn, W. E., Sloan, J. H., Ulmer, M., Boodhoo, A., Knierman, M. D., Schultze, A. E., and Konrad, R. J. (2005) The novel apolipoprotein A5 is present in human serum, is associated with VLDL, HDL, and chylomicrons, and circulates at very low concentrations compared with other apolipoproteins, *Clin Chem 51*, 351-359.
11. Marcais, C., Verges, B., Charriere, S., Pruneta, V., Merlin, M., Billon, S., Perrot, L., Drai, J., Sassolas, A., Pennacchio, L. A., Fruchart-Najib, J., Fruchart, J. C., Durlach, V., and Moulin, P. (2005) Apoa5 Q139X truncation predisposes to late-onset hyperchylomicronemia due to lipoprotein lipase impairment, *J Clin Invest 115*, 2862-2869.
12. Weisgraber, K. H. (1994) Apolipoprotein E: structure-function relationships, *Adv Protein Chem 45*, 249-302.
13. Ajees, A. A., Anantharamaiah, G. M., Mishra, V. K., Hussain, M. M., and Murthy, H. M. (2006) Crystal structure of human apolipoprotein A-I: insights into its protective effect against cardiovascular diseases, *Proc Natl Acad Sci U S A 103*, 2126-2131.
14. Bradley, W. A., Gilliam, E. B., Gotto, A. M., Jr., and Gianturco, S. H. (1982) Apolipoprotein-E degradation in human very low density lipoproteins by plasma

protease(s): chemical and biological consequences, *Biochem Biophys Res Commun 109*, 1360-1367.
15. Innerarity, T. L., Friedlander, E. J., Rall, S. C., Jr., Weisgraber, K. H., and Mahley, R. W. (1983) The receptor-binding domain of human apolipoprotein E. Binding of apolipoprotein E fragments, *J Biol Chem 258*, 12341-12347.
16. Wetterau, J. R., Aggerbeck, L. P., Rall, S. C., Jr., and Weisgraber, K. H. (1988) Human apolipoprotein E3 in aqueous solution. I. Evidence for two structural domains, *J Biol Chem 263*, 6240-6248.
17. Aggerbeck, L. P., Wetterau, J. R., Weisgraber, K. H., Wu, C. S., and Lindgren, F. T. (1988) Human apolipoprotein E3 in aqueous solution. II. Properties of the amino- and carboxyl-terminal domains, *J Biol Chem 263*, 6249-6258.
18. Lupas, A., Van Dyke, M., and Stock, J. (1991) Predicting coiled coils from protein sequences, *Science 252*, 1162-1164.
19. Segrest, J. P., Jones, M. K., De Loof, H., Brouillette, C. G., Venkatachalapathi, Y. V., and Anantharamaiah, G. M. (1992) The amphipathic helix in the exchangeable apolipoproteins: a review of secondary structure and function, *J Lipid Res 33*, 141-166.
20. Schiffer, M., and Edmundson, A. B. (1967) Use of helical wheels to represent the structures of proteins and to identify segments with helical potential, *Biophys J 7*, 121-135.
21. Reijngoud, D. J., and Phillips, M. C. (1982) Mechanism of dissociation of human apolipoprotein A-I from complexes with dimyristoylphosphatidylcholine as studied by guanidine hydrochloride denaturation, *Biochemistry 21*, 2969-2976.
22. Stryer, L. (1965) The interaction of a naphthalene dye with apomyoglobin and apohemoglobin. A fluorescent probe of non-polar binding sites, *J Mol Biol 13*, 482-495.
23. Wilson, C., Wardell, M. R., Weisgraber, K. H., Mahley, R. W., and Agard, D. A. (1991) Three-dimensional structure of the LDL receptor-binding domain of human apolipoprotein E, *Science 252*, 1817-1822.
24. Wang, J., Sykes, B. D., and Ryan, R. O. (2002) Structural basis for the conformational adaptability of apolipophorin III, a helix-bundle exchangeable apolipoprotein, *Proc Natl Acad Sci U S A 99*, 1188-1193.
25. Breiter, D. R., Kanost, M. R., Benning, M. M., Wesenberg, G., Law, J. H., Wells, M. A., Rayment, I., and Holden, H. M. (1991) Molecular structure of an apolipoprotein determined at 2.5-A resolution, *Biochemistry 30*, 603-608.
26. Wang, J., Narayanaswami, V., Sykes, B. D., and Ryan, R. O. (1998) Interhelical contacts are required for the helix bundle fold of apolipophorin III and its ability to interact with lipoproteins, *Protein Sci 7*, 336-341.
27. Evans, C. L., Long, J. E., Gallagher, T. R., Hirst, J. D., and Searle, M. S. (2008) Conformation and dynamics of the three-helix bundle UBA domain of p62 from experiment and simulation, *Proteins 71*, 227-240.
28. Yang, J. S., Wallin, S., and Shakhnovich, E. I. (2008) Universality and diversity of folding mechanics for three-helix bundle proteins, *Proc Natl Acad Sci U S A 105*, 895-900.
29. Worrall, L. J., and Walkinshaw, M. D. (2007) Crystal structure of the C-terminal three-helix bundle subdomain of C. elegans Hsp70, *Biochem Biophys Res Commun 357*, 105-110.

30. Narayanaswami, V., Wang, J., Schieve, D., Kay, C. M., and Ryan, R. O. (1999) A molecular trigger of lipid binding-induced opening of a helix bundle exchangeable apolipoprotein, *Proc Natl Acad Sci U S A 96*, 4366-4371.
31. Raussens, V., Fisher, C. A., Goormaghtigh, E., Ryan, R. O., and Ruysschaert, J. M. (1998) The low density lipoprotein receptor active conformation of apolipoprotein E. Helix organization in n-terminal domain-phospholipid disc particles, *J Biol Chem 273*, 25825-25830.
32. Segelke, B. W., Forstner, M., Knapp, M., Trakhanov, S. D., Parkin, S., Newhouse, Y. M., Bellamy, H. D., Weisgraber, K. H., and Rupp, B. (2000) Conformational flexibility in the apolipoprotein E amino-terminal domain structure determined from three new crystal forms: implications for lipid binding, *Protein Sci 9*, 886-897.
33. Kiss, R. S., Kay, C. M., and Ryan, R. O. (1999) Amphipathic alpha-helix bundle organization of lipid-free chicken apolipoprotein A-I, *Biochemistry 38*, 4327-4334.
34. Weers, P. M., Narayanaswami, V., and Ryan, R. O. (2001) Modulation of the lipid binding properties of the N-terminal domain of human apolipoprotein E3, *Eur J Biochem 268*, 3728-3735.
35. Soulages, J. L., and Bendavid, O. J. (1998) The lipid binding activity of the exchangeable apolipoprotein apolipophorin-III correlates with the formation of a partially folded conformation, *Biochemistry 37*, 10203-10210.
36. Lookene, A., Beckstead, J. A., Nilsson, S., Olivecrona, G., and Ryan, R. O. (2005) Apolipoprotein A-V-heparin interactions: implications for plasma lipoprotein metabolism, *J Biol Chem 280*, 25383-25387.
37. Nilsson, S. K., Lookene, A., Beckstead, J. A., Gliemann, J., Ryan, R. O., and Olivecrona, G. (2007) Apolipoprotein A-V interaction with members of the low density lipoprotein receptor gene family, *Biochemistry 46*, 3896-3904.
38. Beigneux, A. P., Davies, B. S., Gin, P., Weinstein, M. M., Farber, E., Qiao, X., Peale, F., Bunting, S., Walzem, R. L., Wong, J. S., Blaner, W. S., Ding, Z. M., Melford, K., Wongsiriroj, N., Shu, X., de Sauvage, F., Ryan, R. O., Fong, L. G., Bensadoun, A., and Young, S. G. (2007) Glycosylphosphatidylinositol-anchored high-density lipoprotein-binding protein 1 plays a critical role in the lipolytic processing of chylomicrons, *Cell Metab 5*, 279-291.
39. Fisher, C. A., Wang, J., Francis, G. A., Sykes, B. D., Kay, C. M., and Ryan, R. O. (1997) Bacterial overexpression, isotope enrichment, and NMR analysis of the N-terminal domain of human apolipoprotein E, *Biochem Cell Biol 75*, 45-53.
40. Ryan, R. O., Schieve, D., Wientzek, M., Narayanaswami, V., Oikawa, K., Kay, C. M., and Agellon, L. B. (1995) Bacterial expression and site-directed mutagenesis of a functional recombinant apolipoprotein, *J Lipid Res 36*, 1066-1072.
41. Laue, T. M., and Stafford, W. F., 3rd. (1999) Modern applications of analytical ultracentrifugation, *Annu Rev Biophys Biomol Struct 28*, 75-100.
42. Johnson, M. L., Correia, J. J., Yphantis, D. A., and Halvorson, H. R. (1981) Analysis of data from the analytical ultracentrifuge by nonlinear least-squares techniques, *Biophys J 36*, 575-588.
43. Laue, T. M., Shah, B. D., Ridgeway, T. M., and Pelletier, S. L. (1991) *Analytical Ultracentrifugation in Biochemistry and Polymer Science*, R. Soc. Chem., Cambridge, UK.

44. Sreerama, N., and Woody, R. W. (1993) A self-consistent method for the analysis of protein secondary structure from circular dichroism, *Anal Biochem 209*, 32-44.

CHAPTER 4:
Apolipoprotein A-V amino-terminal structural domain lipid interactions

4.1 ABBREVIATIONS

apo = apolipoprotein
HTG = hypertriglyceridemia
DMPC = dimyristoylphosphatidylcholine
NT = N-terminus
CT = C-terminus
rHDL = reconstituted HDL
CD = circular dichroism
ATR-FTIR = attenuated total reflectance Fourier transformed infrared spectroscopy

4.2 ABSTRACT

The N-terminal 146 residues of apolipoprotein (apo) A-V adopt a helix bundle conformation in the absence of lipid. Since similar sized truncation mutants in human subjects correlate with severe hypertriglyceridemia (HTG), the lipid binding properties of apoA-V(1-146) were studied. Upon incubation with phospholipid *in vitro,* apoA-V(1-146) forms reconstituted high density lipoproteins 15 - 17 nm in diameter. Far UV circular dichroism spectroscopy analyses of lipid bound apoA-V(1-146) yielded an α–helix secondary structure content of 60%. Fourier transformed infrared spectroscopy analysis revealed that apoA-V(1-146) α–helix segments align perpendicular with respect to particle phospholipid fatty acyl chains. Fluorescence spectroscopy of single Trp variant apoA-V(1-146) indicate lipid interaction is accompanied by a conformational change. The data are consistent with a model wherein apoA-V(1-146) α–helices circumscribe the perimeter of a disk-shaped bilayer. The ability of apoA-V(1-146) to solubilize dimyristoylphosphatidylcholine vesicles at a rate faster than full-length apoA-V suggests N- and C-terminal interactions in the full-length protein modulate its lipid binding properties. Preferential association of apoA-V(1-146) with murine plasma HDL, but not with VLDL, suggests particle size is a determinant of its lipoprotein binding specificity. It may be concluded that defective lipoprotein binding of truncated apoA-V contributes to the HTG phenotype associated with truncation mutations in human subjects.

4.3 BACKGROUND

The helix bundle motif is a common molecular architecture in proteins (1). Exchangeable apolipoproteins (apo) are known to adopt this conformation, which supports their dual existence in alternate lipid-free and lipid-bound states. Classic examples of the helix bundle structure include the N-terminal (NT) domains of apoE (2) and apoA-I (3) as well as apolipophorin III (4). In the case of apoE and apoA-I, the helix bundle motifs are present within the context of a larger protein structure. In each of these examples the bundle exists as an up-and-down series of amphipathic α–helices wherein the hydrophobic face of each helical segment orients toward the interior of the bundle. At the same time, the polar face of the amphipathic helices is directed toward the exterior of the bundle. In this way the globular structure is stabilized by hydrophobic helix-helix interactions and is conferred with water solubility through projection of polar and charged amino acid side chains toward the aqueous milieu. Upon interaction with lipid surfaces, the helix bundle is postulated to unfurl, adopting an extended open conformation that promotes interaction between the hydrophobic faces of amphipathic helices and the lipid surface. Essentially, lipid binding of helix bundle apolipoproteins substitutes helix-helix contacts in the bundle for helix-lipid contacts that stabilize the lipid bound state.

In 2001 a new apolipoprotein, termed apoA-V, was reported that profoundly affects plasma TG levels (*5, 6*). Structural studies revealed that apoA-V is a two domain protein (7) and that its N-terminal 146 residues adopt a helix bundle structure in the absence of lipid (8). Truncated apoA-V proteins in this size range have been reported in human subjects with severe hypertriglyceridemia (HTG) (*9, 10*). One of these truncation mutants, Q139X apoA-V, does not associate with VLDL or HDL in circulation (9). By contrast, full-length apoA-V is found on both these lipoprotein classes in normolipidemic subjects (11). Insofar as these individuals had no other common mutations known to cause HTG, it is likely that a lipid-binding defect in truncated apoA-V is associated with the HTG phenotype. To address this mechanistically, the lipid interaction properties of recombinant apoA-V(1-146) were investigated. Results obtained provide a molecular explanation for the correlation between naturally occurring C-terminal (CT) truncations in apoA-V and HTG.

4.4 RESULTS

Characterization of apoA-V(1-146) binding to phospholipid vesicles

Incubation of apoA-V(1-146) with a DMPC vesicle dispersion caused a decrease in solution light scattering intensity consistent with formation of lipid complexes (i.e. rHDL). Native gradient PAGE analysis revealed a discrete population of particles with a Stoke's diameter in the range of 15–17 nm (**Figure 4-1**). These complexes, which are similar in size to discoidal particles formed with full-length apoA-V (12), indicate the NT domain of apoA-V possesses intrinsic lipid binding capability.

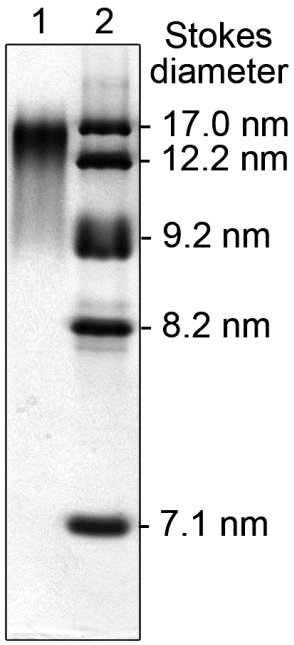

Figure 4-1. Native gradient PAGE of apoA-V(1-146)•DMPC complexes. ApoA-V(1-146)•DMPC complexes were prepared as described in Experimental Procedures and applied to a 4-20 % acryalamide gradient gel. Following electrophoresis the gel was stained with Coomassie Blue. Lane (1) apoA-V(1-146)•DMPC complexes (5 µg protein); lane (2) molecular size standards.

Far UV CD spectroscopy analysis

The effect of lipid association on the secondary structure content of apoA-V(1-146) was evaluated by far-UV CD spectroscopy (**Figure 4-2**). The spectrum of lipid-free apoA-V(1-146) (**curve a**) has minima at 208 and 222 nm, indicating the presence of α–helix secondary structure. Deconvolution of the spectrum yielded a value of 40 % α–helix. Upon interaction with DMPC, however, a significant enhancement in α–helix content was noted as seen by the increase in negative ellipticity at 208 and 222 nm (**curve b**). Deconvolution of the spectra yielded a value of 60 % α–helix structure.

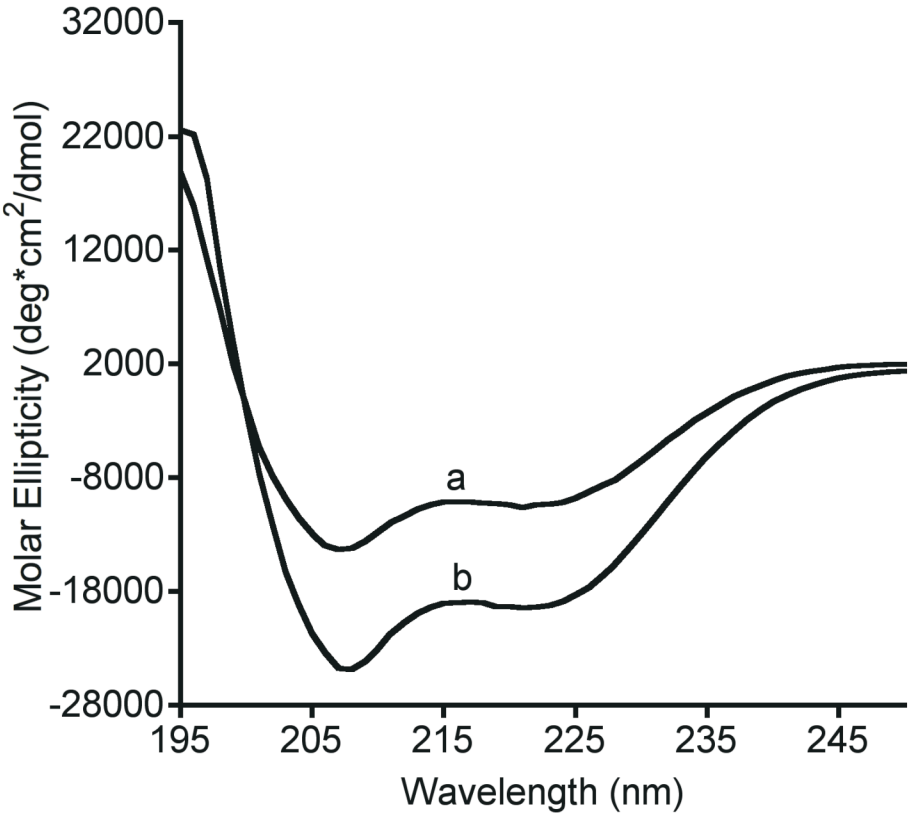

Figure 4-2. Effect of lipid interaction in the spectroscopic properties of apoA-V(1-146). Far UV circular dichroism spectra of lipid-free apoA-V(1-146) (curve a) and apoA-V(1-146)•DMPC (curve b) were collected in 10 mM sodium phosphate at a protein concentration of 0.5 mg/mL.

Orientation of α-helices in apoA-V(1-146) lipid complexes

[Data collected in collaboration with the laboratory of Dr. Vincent Raussens at Université Libre de Bruxelles]

ATR-FTIR spectra of apoA-V(1-146)•DMPC complexes were recorded with parallel and perpendicular polarized light (**Figure 4-3**). The amide I region of the spectra (1700 – 1600 cm^{-1}) was used to determine the orientation of α–helices in apoA-V(1-146) relative to DMPC hydrocarbon chains of the bilayer component of the rHDL. A dichroic spectrum was obtained by subtracting the spectrum recorded with perpendicular polarized light from the spectrum recorded with parallel polarized light. Bands corresponding to dipoles that orient parallel to the hydrocarbon chain progression observed for saturated hydrocarbon chains had a positive deviation in the dichroic spectrum. Thus, these orient parallel to the normal of the germanium (Ge) plate. ApoA-V(1-146) helix orientation was determined using the amide I band. In the dichroic spectrum, a negative deviation at ~1650 cm^{-1} is observed, indicating a parallel orientation of the associated dipole to the surface of the Ge plate and, thus, a perpendicular orientation with respect to a vector normal to the face of the disk. From the secondary structure of apoA-V(1-146) and the frequency of the negative deviation, it may be concluded that the dipole responsible for this deviation is associated with α–helices, which orient in the direction of the helical axes. Thus, the negative deviation observed indicates that the helices are primarily oriented perpendicular to the normal vector of the disk and, therefore, perpendicular to the hydrocarbon chains of the lipids.

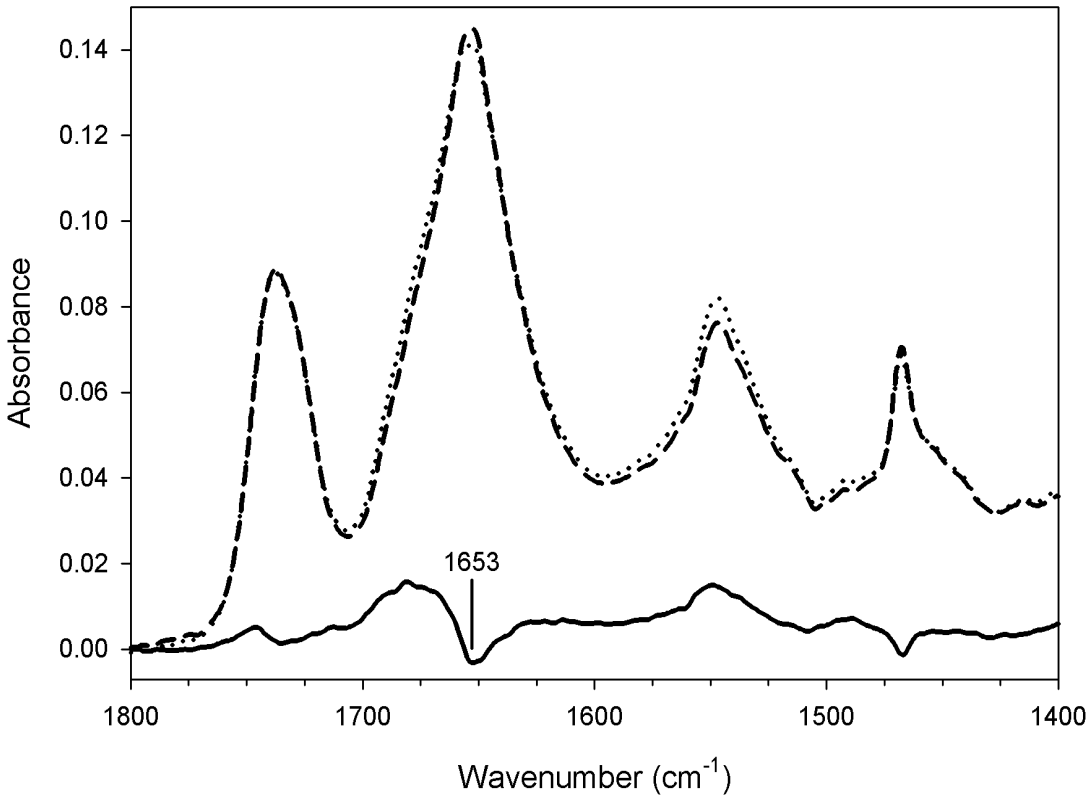

Figure 4-3. Infrared spectroscopy analysis of apoA-V(1-146)•DMPC complexes. ATR-FTIR spectra of apoA-V(1-146)•DMPC disks recorded with light polarized parallel to a normal to the surface of the internal reflection element (dotted line) and with light polarized perpendicular to the normal to the surface (dashed line). Both spectra have been rescaled based on the lipid band at 1740 cm^{-1}. The solid line represents the calculated dichroic spectrum. To improved visualization, the dichroic spectrum is shown at 2 x intensity versus the other spectra.

Quantification of secondary structure conformers present was performed on samples subjected to deuteration. The predominant secondary structure conformer present is α–helix (61%), in good agreement with the value determined by CD spectroscopy.

Trp fluorescence emission analysis

The wavelength of maximum fluorescence emission of tryptophan residues is a useful tool to monitor changes and to make inferences regarding local structure and environment. Single Trp apoA-V(1-146) variants were generated to explore the effect of lipid association on specific regions of apoA-V(1-146). All apoA-V(1-146) variants generated were characterized by far UV CD spectroscopy. No significant differences were noted, indicating the conserved substitution mutations introduced did not alter the secondary structure content of the protein. ApoaA-V possesses two naturally occurring Trp, at positions 5 and 97. Primary sequence analysis using Coils program (*13*) and Edmundson helical wheel diagrams (*14*) indicate that these Trp are located at the extreme N-terminus (Trp5) and in a loop or "linker" segment between α–helices (Trp97). When these Trp residues were mutated to generate the corresponding single Trp apoA-V(1-146) variants, fluorescence emission analysis revealed they are largely exposed to solvent in the absence of lipid and undergo relatively small blue shifts in their wavelength of maximum fluorescence emission upon interaction with DMPC (**Table 4-1**). To extend this approach, a panel of single Trp apoA-V(1-146) variants were constructed via site-directed mutagenesis. For these studies Asn45, Leu73, Val117 and Leu128 were individually mutated to Trp in the context of a Trp-null apoA-V(1-146) background. Based on sequence analysis Trp45 is predicted to reside on the polar face of an amphipathic α–helix while the Trp73, Trp117 and Trp128 are postulated to reside on the hydrophobic face of amphipathic α-helices. Trp fluorescence emission spectra of these single Trp apoA-V(1-146) variants were analyzed in lipid-free and lipid-bound states (**Table 4-1**). Whereas Trp@45 apoA-V(1-146) undergoes a 4 nm blue shift upon interaction with lipid, Trp@73 apoA-V(1-146) and Trp@128 apoA-V(1-146) underwent 11 nm shifts, consistent with their relocation to a more nonpolar environment upon lipid interaction. Compared to the other mutants, Trp@117 appears to reside in a relatively nonpolar environment in the lipid-free conformation. At the same time, this Trp undergoes a 5 nm blue shift to 335 nm upon lipid association of the protein.

Table 4-1. Fluorescence properties of apoA-V(1-146) variants.[a]

ApoA-V(1-146) single Trp variant	Predicted Trp location[b]	λ_{max} (nm)[c]	
		Lipid-free	DMPC-bound
Trp@5	Extreme N-terminus	350	345
Trp@45	Polar-face	350	346
Trp@73	Nonpolar-face	349	338
Trp@97	"Linker"	349	348
Trp@117	Nonpolar-face	340	335
Trp@128	Nonpolar-face	349	338

[a] Spectra were recorded on a Jobin Yvon FluoroMax-4 luminescence spectrometer. Emission spectra were recorded from 300 nm to 450 nm (excitation 295 nm) in 20 mM sodium phosphate, pH 7.4, 150 mM NaCl (slit width 2.0 nm for the excitation and emission monochromators) at a protein concentration of 0.5 mg/mL. In DMPC-bound samples, a DMPC:protein ratio of 5:1 was used.

[b] Based on primary sequence analysis using Coils program (*13*) and Edmundson helical wheel diagrams (*14*).

[c] λ_{max} is the wavelength of maximum fluorescence emission. Values reported are the mean of at least three independent determinations. In all cases, the standard deviation was ≤ 1 nm.

Trp fluorescence quenching studies of DMPC-bound single Trp apoA-V variants

To further evaluate the effect of lipid binding on solvent exposure of Trp residues in single Trp apoA-V(1-146) variants, KI and acrylamide quenching studies were conducted. In the lipid-bound state, Trp@5 apoA-V(1-146) and Trp@45 apoA-V(1-146) remain highly susceptible to both KI quenching and acrylamide quenching with relatively high K_{sv} constants (**Table 4-2**) while lipid-bound Trp@73 apoA-V(1-146), Trp@117 apoA-V(1-146), and Trp@128 apoA-V(1-146) gave rise to low K_{sv} constants, suggesting protection from quenchers. Trp@97 apoA-V(1-46) was more susceptible to acrylamide quenching than KI.

Table 4-2. Trp fluorescence quenching of apoA-V(1-146) variants bound to DMPC.[a]

ApoA-V(1-146) single Trp variant	Predicted Trp location[b]	K_{sv}[c]	
		KI	Acrylamide
Trp@5	Extreme N-terminus	2.7 M^{-1}	3.8 M^{-1}
Trp@45	Polar-face	2.8 M^{-1}	3.6 M^{-1}
Trp@73	Nonpolar-face	1.0 M^{-1}	2.2 M^{-1}
Trp@97	"Linker"	1.4 M^{-1}	4.1 M^{-1}
Trp@117	Nonpolar-face	1.1 M^{-1}	2.0 M^{-1}
Trp@128	Nonpolar-face	1.0 M^{-1}	2.2 M^{-1}

[a] Spectra were recorded on a Jobin Yvon FluoroMax-4 luminescence spectrometer. The average of two emission spectra were recorded from 320 nm to 355 nm (excitation 295 nm) in 20 mM sodium phosphate, pH 7.4, 150 mM NaCl (slit width 2.0 nm for the excitation and emission monochromators) at a protein concentration of 0.5 mg/mL with a DMPC:protein ratio of 5:1.

[b] Based on primary sequence analysis using Coils program (*13*) and Edmundson helical wheel diagrams (*14*).

[c] K_{sv} is the Stern-Volmer constant

Phospholipid vesicle solubilization kinetics

The data presented in Figure 4-1 illustrate that apoA-V(1-146) is capable of binding lipid to form rHDL. In an effort to characterize the relative lipid binding activity of this protein, kinetic analysis of apoA-V(1-146)-dependent solubilization of DMPC vesicles was measured. (**Figure 4-4**). In control incubations lacking apolipoprotein, DMPC vesicles remain turbid with no change in solution light scattering intensity as a function of time (**curve a**). Upon addition of full-length apoA-V, a time-dependent reduction in turbidity was observed with a calculated initial rate constant (k) of 1.3 x 10^{-2} s^{-1} (**curve b**). The isolated NT domain, apoA-V(1-146), induced faster solubilization, with an initial rate constant of 3.3 x 10^{-2} s^{-1} (**curve c**).

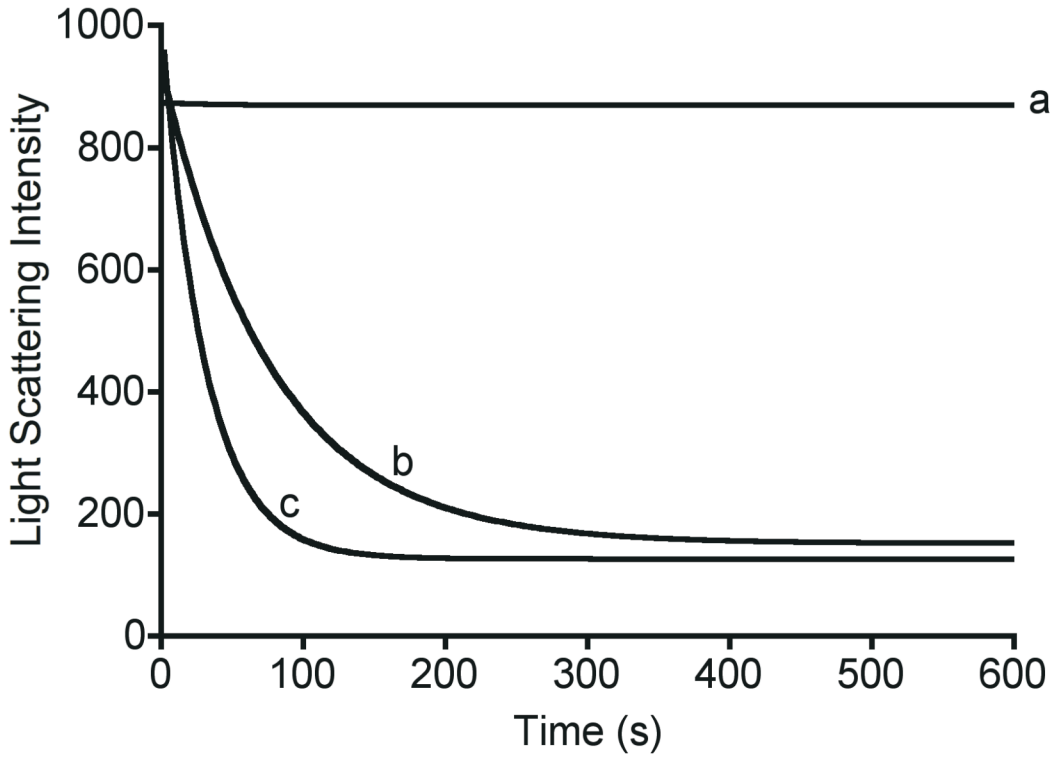

Figure 4-4. Effect of apoA-V truncation on DMPC vesicle solubilization kinetics. DMPC vesicles (500 µg) in 50 mM sodium citrate, pH 3.0, 150 mM NaCl, were incubated at 23 ºC in the absence (curve a) or presence of 100 µg full-length apoA-V (curve b) or apoA-V (1-146) (curve c). Right angle light scattering was monitored at 600 nm as a function of time.

ApoA-V(1-146) binding to phospholipase C modified LDL

When human LDL is incubated with PL-C, enzymatic conversion of LDL phosphatidylcholine to diacylglycerol induces apolipoprotein association and prevents LDL particle aggregation and subsequent sample turbidity development (*15*). Incubation of LDL with PL-C in the absence of exogenous apolipoprotein results in rapid sample turbidity development (**Figure 4-5, curve a**) whereas control incubations lacking PL-C do not develop turbidity over time (**curve e**). Although incubations with recombinant human apoA-I remained clear (**curve d**), incubations with apoE3 NT become turbid over time (**curve b**), consistent with previous results (*16*). LDL incubations with PL-C in the presence of apoA-V(1-146) showed an intermediate level of protection from sample turbidity development as a function of time (**curve c**).

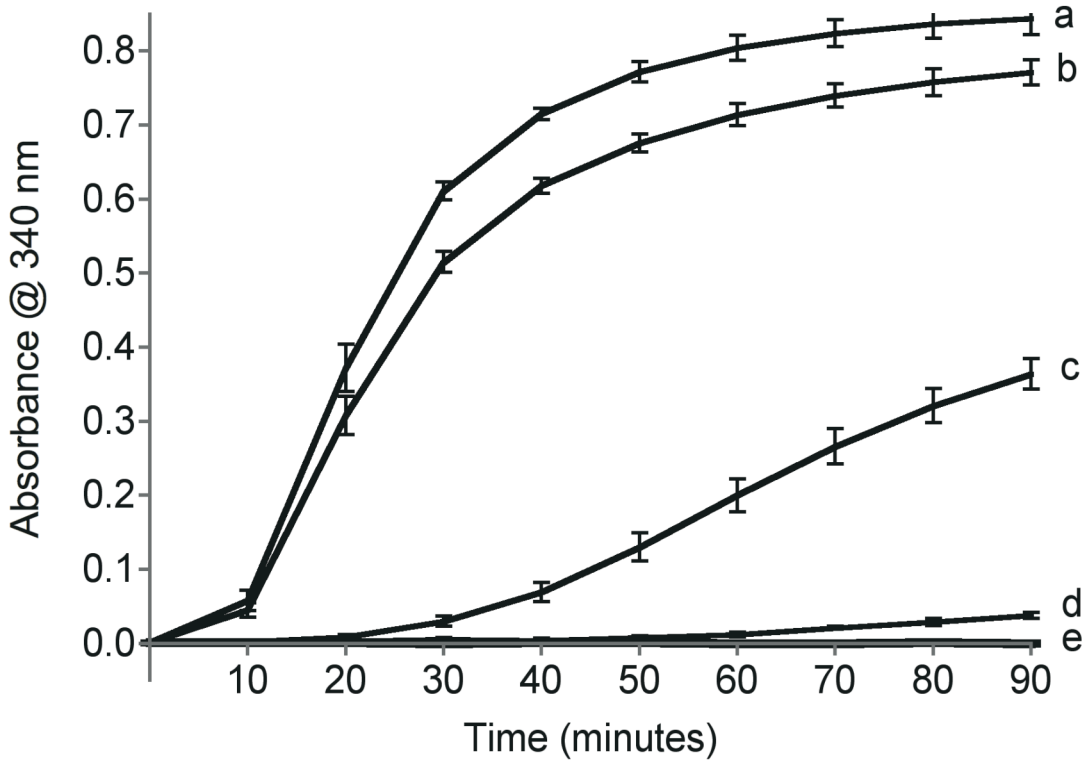

Figure 4-5. Effect of apolipoproteins on PL-C induced aggregation of human LDL. Human LDL (50 µg protein) was incubated at 37 ºC in the absence (curve e) or presence (curve a) of PL-C (0.6 Units). Other incubations contained LDL, PL-C and 50 µg apoE3 NT (curve b), apoA-V(1-146) (curve c), or apoA-I (curve d). Sample absorbance at 340 nm was measured as a function of time. Values represent mean ± standard deviation (n = 3).

ApoA-V(1-146) binding to VLDL and HDL from apoA5(-/-) mice

It was previously reported that the naturally occurring truncation variant, Q139X apoA-V, does not associate with lipoproteins *in vivo* (9). To evaluate the ability of apoA-V(1-146) to associate with VLDL and HDL *in vitro*, recombinant apoA-V(1-146) was incubated with apoA-V deficient VLDL and HDL obtained from *apoA5(-/-)* mice. Following incubation, the lipoproteins were re-isolated by ultracentrifugation and analyzed by immunoblotting (**Figure 4-6)**. The data show that, whereas full-length apoA-V associates with both VLDL and HDL, apoA-V(1-146) does not associate with VLDL. Furthermore, while nearly all of the full-length apoA-V bound to HDL, only a fraction of apoA-V(1-146) was recovered in association with HDL.

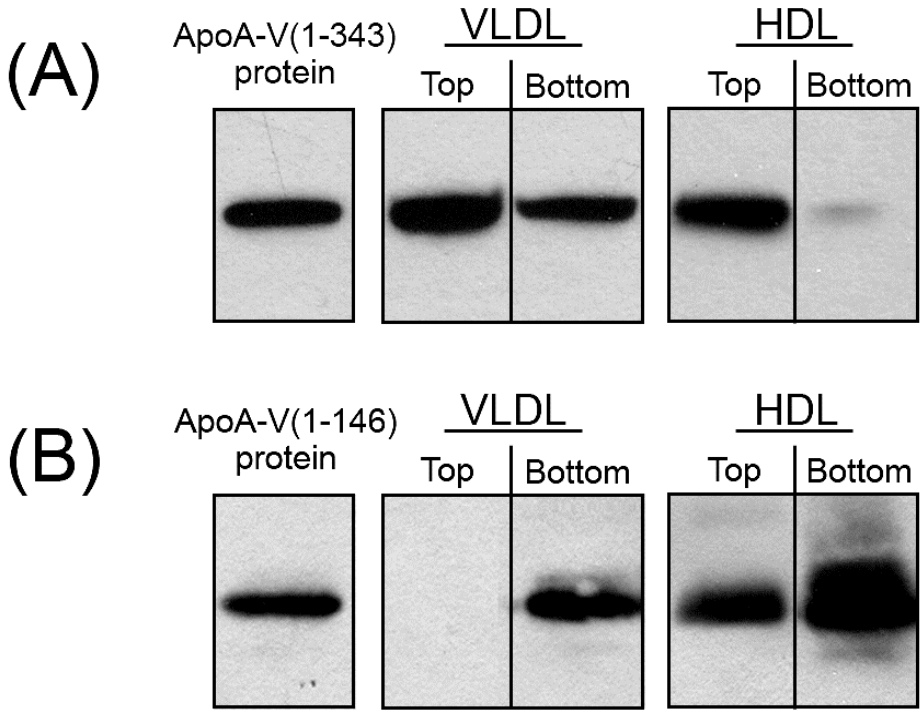

Figure 4-6. Lipoprotein binding properties of apoA-V(1-146). VLDL or HDL (0.1 mg/mL protein), isolated from plasma of *apoa5 (-/-)* mice were incubated with (A) 0.02 mg/mL full-length apoA-V(1-343) or (B) 0.01 mg/mL apoA-V(1-146) for 1 h at 22 ºC in Tris-buffered saline. Following incubation, VLDL and HDL were re-isolated by density ultracentrifugation and subjected to immunoblot analysis with goat anti-human apoA-V IgG. Results shown are representative of at least three independent experiments. On the left of each panel is a control blot with recombinant apoA-V.

4.5 DISCUSSION

Exchangeable apolipoproteins can transfer among lipoproteins in plasma and, in the process, likely exist in a lipid-poor state. The helix bundle motif is postulated to facilitate this exchange by promoting apolipoprotein solubility in both polar and nonpolar environments. The size of potential lipid substrate particles is an important factor regulating apolipoprotein transfer in the circulation (*17*). ApoA-V is an exchangeable apolipoprotein, which in humans, is found on chylomicrons, VLDL, and HDL (11). Presumably, apoA-V transfers among the different lipoprotein populations, as proposed by Nelbach *et al.* (*18*). The NT domain of apoA-V adopts a helix bundle conformation in the absence of lipid, and this may facilitate exchange between lipoprotein particles. In the present studies, we characterized the ability of the this domain to bind to particles of various lipid compositions and sizes, including DMPC vesicles, modified LDL, and HDL and VLDL from *apoa5* (-/-) mice, in an effort to gain insight into its intrinsic lipid-binding properties.

Compared to other well-studied exchangeable apolipoproteins, full-length apoA-V is unique in that it is not soluble at neutral pH in a lipid-free state (6). When bound to lipid, however, apoA-V is soluble at physiological pH. This suggests that during transfer between lipoprotein particles in circulation, apoA-V may exist in a lipid-poor, rather than lipid-free state. The ability of apoA-V(1-146) to form discoidal complexes with phospholipid in the size range of nascent HDL particles may be physiologically relevant since apoA-V exchange between lipoprotein particles in circulation may require transient existence in a lipid-core depleted particle.

Upon lipid interaction, it appears that apoA-V(1-146) undergoes a conformational change, as judged by an increase in α–helix secondary structure content and altered solvent exposure of reporter Trp residues. The increase in helix content upon lipid interaction is similar to that of other exchangeable apolipoproteins, such as apoA-I (*19*). The amphipathic helix bundle motif in the lipid-free state adopts a globular conformation wherein the hydrophobic face of its helices orient toward the center of the bundle (*20*). Upon lipid association, the protein is predicted to adopt an open conformation, where the hydrophobic faces of its amphipathic helices interacts directly with the lipid surface (*20*). Linear IR dichroism experiments of apoA-V(1–146)•DMPC disks are consistent with a model wherein the helices orient perpendicular with respect to the DMPC bilayer fatty acyl chains. This indicates that, in the lipid-bound state, apoA-V(1-146) adopts a belt-like conformation around the perimeter of the particle, as described for other exchangeable apolipoproteins (*21-26*).

The lipid-induced conformational change in apoA-V(1-146) was studied using a panel of single Trp variants. Each single Trp variant reported on a specific region within apoA-V(1-146). Certain Trp residues were predicted to reside in a linker region between amphipathic helices or on the polar face of an amphipathic helix while others were predicted to reside on the nonpolar face of amphipathic helices. In keeping with these predictions, only variants with Trp predicted to reside on the hydrophobic face of amphipathic helices showed a blue shift in wavelength of maximum fluorescence emission between alternate lipid-free and lipid-bound states. This

suggests that, when presented with a suitable lipid surface, the helix bundle opens, exposing the bundle interior.

To further characterize conformational adaptations in apoA-V(1-146), the relative exposure of various regions within the NT domain were investigated as a function of lipid binding. In Trp fluorescence quenching studies it was observed that single Trp apoA-V(1-146) variants with their Trp predicted to be on the nonpolar face of amphipathic helices gave rise to the lowest K_{sv} values, suggesting these regions of the protein maintain close contact with the lipid surface. For example, Trp97 is predicted to reside in a linker region between two amphipathic helices. Consistent with this, Trp@97 apoA-V(1-146) fluorescence emission was highly quenched by acrylamide but less so by KI. This could be due to electrostatic repulsion of KI by negatively charged residues located near Trp97.

An ability of apoA-V(1-146) to initiate contact with lipid surfaces is suggested by phospholipid vesicle solubilization studies comparing truncated and full-length apoA-V. The CT domain of apoA-V has been previously shown to avidly bind lipid (7). Interestingly, despite the absence of the CT domain, apoA-V(1-146) solubilizes DMPC at a faster rate than full-length apoA-V. This suggests that N- and C-terminal domain interactions in the intact protein modulate the lipid binding properties of apoA-V. This may be similar to interactions in apoA-I. In this apolipoprotein, the CT domain initiates lipid-binding while the NT helix bundle opens up to stabilize the lipid associated state (*27*).

While DMPC solubilization assays characterize apolipoprotein-induced phospholipid vesicle disruption and reorganization, PL-C modified LDL provides a means to assess binding to spherical lipoprotein substrates. PL-C activity generates apolipoprotein binding sites by hydrolyzing phosphatidylcholine moieties present in the surface monolayer (*15*). Conversion of phosphatidylcholine into diacylglycerol destabilizes the lipoprotein particle and promotes aggregation (*28*). Apolipoproteins protect LDL against PL-C-induced aggregation by forming a stable binding interaction with the modified particles (*15*). ApoA-V(1-146) binding to PL-C treated LDL was intermediate with respect to other apolipoproteins examined. This finding is consistent with the stability properties of these apolipoproteins. At physiological pH apoA-V(1-146) is less stable than apoE3 NT (guanidine HCl denaturation midpoint of 2.0 M *versus* 2.5 M, respectively) (*8, 29*) yet is more stable that apoA-I (1 M guanidine HCl denaturation midpoint) (*30*). Thus, it appears that intrinsic stability of helix bundle apolipoproteins in solution correlates directly with the ability to bind newly created sites on a spherical lipoprotein substrate (8).

The ability of apoA-V(1-146) to associate with physiologically relevant lipoproteins was assessed using VLDL and HDL isolated from *apoa5* knockout mice. Importantly apoA-V(1-146) failed to associate with VLDL and associated sparingly with HDL. This finding is intriguing in light of the report that, unlike full-length apoA-V, apoA-V(1-146) also fails to associate with intracellular lipid droplets (*31*). In considering the size of various lipid substrates, VLDL and lipid droplets are considerably larger than HDL or other lipid particles employed in this study. The data indicate that apoA-V(1-146) can associate with smaller lipid substrate particles to a limited degree but apparently lacks the ability to interact with larger lipid particles. One explanation could be related to the tighter packing of phospholipid molecules on the surface of larger particles due to their decreased radius of curvature, as compared to smaller particles (*32,*

33). Tighter packing of phospholipid polar head groups enveloping a lipid core could interfere with the ability of apoA-V(1-146) to access hydrophobic surfaces and initiate binding. This aspect is obviated in the case of PL-C modified LDL but not in the binding experiments with VLDL and HDL. In the latter case, differences in surface lipid composition and/or protein content could also influence binding of apoA-V(1-146). Regardless, it is apparent that, with natural lipoprotein substrates *in vitro*, apoA-V(1-146) binding is defective. Since this is not due to an intrinsic inability to bind lipid, it suggests the CT of apoA-V modulates the lipid interaction properties of the NT domain.

Naturally occurring apoA-V truncations, including Q139X (9), Q148X (10) and Q97X (*34*) have been reported in human subjects and are associated with severe hypertriglyceridemia. The distribution of apoA-V in ultracentrifugally isolated lipoprotein classes was evaluated in several carriers of the Q139X truncation mutation and demonstrated that the truncated form of the protein does not associate with plasma lipoproteins and is found only in the lipid poor d > 1.21 g/mL fraction. Because the Q139X apoA-V mutation nomenclature includes the 23 amino acid signal peptide, the mature protein is actually 116 amino acids in length. Although apoA-V(1-146) is longer than these natural mutants, binding studies with natural lipoproteins recapitulate observations in human plasma of individuals carrying these mutant forms of apoA-V.

The present findings provide a potential explanation for the HTG observed in patients with truncated apoA-V. The lack of a CT domain alters lipid binding activity such that truncated apoA-V fails to effectively bind to circulating lipoproteins, particularly TG-rich particles. Current hypotheses suggest apoA-V interactions with heparan-sulfate proteoglycans (*35, 36*) and/or glycosyl phosphatidylinositol high density lipoprotein binding protein-1 (*37*) indirectly enhances lipoprotein lipase activity to facilitate hydrolysis of VLDL associated TG. Data from Nilsson *et al.* indicate apoA-V also serves as a ligand for endocytic receptors of the LDL receptor family (*35-38*) where it is possible that apoA-V may have an important role in clearance of VLDL remnants. The putative binding site on apoA-V for lipoprotein lipase activity enhancement and cell-surface molecule interactions resides within the CT domain of the protein. The absence of this binding site most likely contributes to defective hydrolysis and clearance of TG-rich lipoproteins. In any case, association of apoA-V with TG-rich lipoproteins is presumably required for manifestation of these effects. If a CT truncated apoA-V is unable to bind larger, TG-rich lipoproteins, then the resulting apoA-V deficient particles could potentially have an increased plasma residence time, contributing to HTG. Thus, it may be that defective lipid binding arising from the lack of a CT domain precludes binding to circulating lipoproteins, thereby preventing potential TG lowering effects attributed to full-length apoA-V.

4.6 ACKNOWLEDGEMENTS

Thank you to Lisa Nelbach of Children's Hospital Oakland Research Institute for providing mouse blood and Dr. Susan Marqusee of University of California, Berkeley for access to the circular dichroism spectrometer.

4.7 MATERIALS AND METHODS

Site-directed mutagenesis and recombinant protein expression

Recombinant human apoA-V and CT truncation variants were produced in *E. coli* and isolated as described (12). ApoE3 NT was prepared as described by Fisher *et al.* (*39*). Recombinant apoA-I was prepared as described by Ryan *et al.* (*40*). Site-directed mutagenesis was performed with the QuikChange II XL Site-Directed Mutagenesis Kit (Stratagene). Primers were designed to introduce a premature stop codon or to substitute Trp5 with Phe, Trp97 with Phe or substitute Asn45, Leu73, Val117, or Leu128 of Trp null apoA-V(1-146) with Trp. In all cases, introduction of the desired mutations was verified by DNA sequencing.

Interaction of apoA-V(1-146) with phospholipid

Dimyristoylphosphatidylcholine (DMPC) bilayer vesicles were incubated with apoA-V(1-146) at a ratio of 5:1 by weight as previously described (12). The size distribution of DMPC-apoA-V(1-146) complexes was evaluated by nondenaturing gradient PAGE as described by Nichols *et al.* (*41*).

Circular dichroism spectroscopy

Circular dichroism (CD) spectroscopy measurements were performed on an AVIV 410 spectrophotometer. Far UV CD scans were obtained between 195 and 250 nm in 10 mM sodium phosphate, pH 7.4 using a protein concentration of 0.5 mg/mL determined from the absorbance at 280 nm. The α-helical content was calculated with the self-consistent method using Dicroprot version 2.6 (*42*).

Infrared spectroscopy

Attenuated total reflectance Fourier transformed infrared spectroscopy (ATR-FTIR) spectra were recorded on a Bruker IFS 55 IR spectrophotometer equipped with a reflectance accessory and a polarizer mount assembly with an aluminum wire grid on a KRS-5 element. The internal reflection element was a germanium ATR plate (50 mm×20 mm×2 mm) with an aperture angle of 45° yielding 25 internal reflections. Oriented multilayers were formed by slow evaporation of ~10 µl of apoA-V(1-146)•DMPC (1 mg/ml) on one side of the ATR plate under a gentle stream of nitrogen, yielding a semi-dry film bearing residual water molecules. The ATR plate was then sealed in a universal sample holder. Spectra were recorded at a 2 cm^{-1} nominal resolution. A total of 128 accumulations were performed to improve the signal/noise ratio. The spectrometer was constantly purged with dry air. All measurements were made at 25 °C.

Secondary structure measurements were carried out on samples following deuteration for 1 h as previously described (*43*). Briefly, Fourier self-deconvolution was applied to enhance resolution of the spectra in the amide I region. Least squares iterative curve fitting was

performed to fit different components of the amide I band revealed by the self-deconvolution to the non-deconvolved spectrum between 1700 and 1600 cm^{-1}. The proportion of various secondary-structural elements was computed as reported in (*43*).

Analytical procedures

Protein concentrations were determined with the bicinchoninic acid assay (Pierce Chemical Co.) with bovine serum albumin as standard.

Fluorescence spectroscopy

Fluorescence spectra were obtained on a Horiba Jobin Yvon FluoroMax-4 luminescence spectrometer. Protein (0.5 μg/μL) was dissolved in 20 mM sodium phosphate, pH 7.4, 150 mM NaCl. Samples were excited at 295 nm and emission collected from 300 to 450 nm (slit width 2.0 nm). For Trp fluorescence quenching studies DMPC-bound apoA-V(1-146) samples (200 μg protein in 400 μL total volume) were excited at 295 nm and emission monitored at their λ_{max} (slit width 2.0 nm). Quenching of Trp fluorescence in 20 mM sodium phosphate, pH 7.4, 150 mM NaCl by addition of either KI or acrylamide in the concentration range 0.0 – 0.6 M was measured. The solution of KI contained 1 mM sodium thiosulfate to prevent formation of free iodine and all readings were corrected for dilution. For acrylamide quenching, fluorescence intensities were corrected for the absorption of acrylamide at 295 nm.

$$I_{corr.} = 10^{(\frac{0.23[acryl]}{2})} I_{meas.}$$

where 0.23 is the molar extinction coefficient of acrylamide at 295 nm (*44*). The data were analyzed using the Stern-Volmer equation,

$$F_0/F = 1 + K_{SV}[Q]$$

where F_0 and F represent the emission intensity maximum in the absence and presence of quencher, respectively, and [Q] is quencher concentration. The collisional quenching constant (K_{SV}) was determined from the initial slope of plots of F_0/F versus [Q].

DMPC vesicle solubilization

DMPC bilayer vesicles were prepared by extrusion through a 100 nm filter as described by Weers *et al.* (*16*). Stock solutions of protein and lipid vesicles were prepared in 50 mM citrate, pH 3.0, 150 mM NaCl. 500 μg DMPC was incubated in the absence or presence of 100 μg apolipoprotein (400 μL total volume) at 23 °C in a thermostated cell holder. Sample right angle light scattering intensity was monitored on a Perkin Elmer LS50B luminescence spectrometer as a function of time, with the excitation and emission monochromaters set at 600 nm (2 nm slit width).

Low density lipoprotein (LDL) binding assay

Human LDL (Intracel) was incubated for 90 min at 37 °C in the presence or absence of *Bacillus cereus* phospholipase C (PL-C) (0.6 U per 50 μg LDL protein). Where indicated, apolipoprotein (50 μg per 50 μg LDL protein) was included in the reaction mixture. Incubations were conducted in 50 mM Tris-HCl, pH 7.5, 150 mM NaCl and 2 mM $CaCl_2$ in a total sample volume of 200 μL. Sample turbidity was measured at 340 nm on a Spectramax 340 microtiter plate reader (Sunnyvale, CA, USA) (*15*).

Incubation of apoA-V(1-146) with isolated HDL and VLDL from apoa5(-/-) mice

Blood from male apoA-V deficient mice, average age 4 months, fasted for 4 h, was collected into tubes containing K_3EDTA and kept on ice. After centrifugation at 2,000 g for 10 min at 4 °C, plasma was removed and treated with a protease inhibitor cocktail as described by Nelbach *et al.* (*18*). Plasma was pooled, stored at 4 °C and used within 2 days. Plasma VLDL and HDL were isolated by sequential ultracentrifugation as described by Lindgren *et al.* (*45*). Isolated VLDL (d<1.006 g/mL) or HDL (d 1.063–1.21 g/mL) was incubated with recombinant apoA-V(1-146) (weight ratio 10:1, lipoprotein protein : apoA-V(1-146)) for 1 h at 22 °C in Tris-buffered saline. After incubation, ultracentrifugation was performed to re-isolate VLDL (d<1.006 g/mL, top fraction) and HDL (d<1.21 g/mL, top fraction). The bottom, lipoprotein-free, fractions from each tube were also recovered. Similar studies were carried out with full-length recombinant apoA-V.

Immunoblotting

For immunoblotting, protein samples were separated on a 10 – 20 % acrylamide gradient, Tricine-SDS slab gel (Invitrogen). Proteins were electrophoretically transferred to a 0.2 μm PVDF membrane (Bio-Rad Laboratories) at a constant current of 150 mA for 3 h. Nonspecific binding sites on the membrane were blocked with 0.1 % TTBS [0.1 % Tween 20, 20 mM Tris, and 150 mM NaCl (pH 7.2)] overnight, at 4 °C with rotation. Goat anti-apoA-V IgG (12) (1:10,000 dilution in 0.1 % TTBS) was incubated with the membrane for 1 h with rotation. The mixture was washed three times in TTBS, and then HRP-conjugated donkey anti-goat secondary antibody was incubated with the membrane for 1 h. After washing, the membrane was incubated with SuperSignal West Femto Maximum Sensitivity Substrate (Pierce Chemical Co.) and exposed to CL-Xposure Film (Pierce Chemical Co.) for less than 10 s. Film was developed using a Kodak M35A X-OMAT processor.

4.8 REFERENCES

1. Kamtekar, S., and Hecht, M. H. (1995) Protein Motifs. 7. The four-helix bundle: what determines a fold?, *Faseb J 9*, 1013-1022.
2. Wilson, C., Wardell, M. R., Weisgraber, K. H., Mahley, R. W., and Agard, D. A. (1991) Three-dimensional structure of the LDL receptor-binding domain of human apolipoprotein E, *Science 252*, 1817-1822.
3. Ajees, A. A., Anantharamaiah, G. M., Mishra, V. K., Hussain, M. M., and Murthy, H. M. (2006) Crystal structure of human apolipoprotein A-I: insights into its protective effect against cardiovascular diseases, *Proc Natl Acad Sci U S A 103*, 2126-2131.
4. Breiter, D. R., Kanost, M. R., Benning, M. M., Wesenberg, G., Law, J. H., Wells, M. A., Rayment, I., and Holden, H. M. (1991) Molecular structure of an apolipoprotein determined at 2.5-A resolution, *Biochemistry 30*, 603-608.
5. Pennacchio, L. A., Olivier, M., Hubacek, J. A., Cohen, J. C., Cox, D. R., Fruchart, J. C., Krauss, R. M., and Rubin, E. M. (2001) An apolipoprotein influencing triglycerides in humans and mice revealed by comparative sequencing, *Science 294*, 169-173.
6. van der Vliet, H. N., Sammels, M. G., Leegwater, A. C., Levels, J. H., Reitsma, P. H., Boers, W., and Chamuleau, R. A. (2001) Apolipoprotein A-V: a novel apolipoprotein associated with an early phase of liver regeneration, *J Biol Chem 276*, 44512-44520.
7. Beckstead, J. A., Wong, K., Gupta, V., Wan, C. P., Cook, V. R., Weinberg, R. B., Weers, P. M., and Ryan, R. O. (2007) The C terminus of apolipoprotein A-V modulates lipid-binding activity, *J Biol Chem 282*, 15484-15489.
8. Wong, K., Beckstead, J. A., Lee, D., Weers, P. M., Guigard, E., Kay, C. M., and Ryan, R. O. (2008) The N-terminus of apolipoprotein A-V adopts a helix bundle molecular architecture, *Biochemistry 47*, 8768-8774.
9. Marcais, C., Verges, B., Charriere, S., Pruneta, V., Merlin, M., Billon, S., Perrot, L., Drai, J., Sassolas, A., Pennacchio, L. A., Fruchart-Najib, J., Fruchart, J. C., Durlach, V., and Moulin, P. (2005) Apoa5 Q139X truncation predisposes to late-onset hyperchylomicronemia due to lipoprotein lipase impairment, *J Clin Invest 115*, 2862-2869.
10. Oliva, C. P., Pisciotta, L., Li Volti, G., Sambataro, M. P., Cantafora, A., Bellocchio, A., Catapano, A., Tarugi, P., Bertolini, S., and Calandra, S. (2005) Inherited apolipoprotein A-V deficiency in severe hypertriglyceridemia, *Arterioscler Thromb Vasc Biol 25*, 411-417.
11. O'Brien, P. J., Alborn, W. E., Sloan, J. H., Ulmer, M., Boodhoo, A., Knierman, M. D., Schultze, A. E., and Konrad, R. J. (2005) The novel apolipoprotein A5 is present in human serum, is associated with VLDL, HDL, and chylomicrons, and circulates at very low concentrations compared with other apolipoproteins, *Clin Chem 51*, 351-359.
12. Beckstead, J. A., Oda, M. N., Martin, D. D., Forte, T. M., Bielicki, J. K., Berger, T., Luty, R., Kay, C. M., and Ryan, R. O. (2003) Structure-function studies of human apolipoprotein A-V: a regulator of plasma lipid homeostasis, *Biochemistry 42*, 9416-9423.
13. Lupas, A., Van Dyke, M., and Stock, J. (1991) Predicting coiled coils from protein sequences, *Science 252*, 1162-1164.

14. Schiffer, M., and Edmundson, A. B. (1967) Use of helical wheels to represent the structures of proteins and to identify segments with helical potential, *Biophys J 7*, 121-135.
15. Liu, H., Scraba, D. G., and Ryan, R. O. (1993) Prevention of phospholipase-C induced aggregation of low density lipoprotein by amphipathic apolipoproteins, *FEBS Lett 316*, 27-33.
16. Weers, P. M., Narayanaswami, V., and Ryan, R. O. (2001) Modulation of the lipid binding properties of the N-terminal domain of human apolipoprotein E3, *Eur J Biochem 268*, 3728-3735.
17. Connelly, P. W., and Kuksis, A. (1981) Effect of core composition and particle size of lipid emulsions on apolipoprotein transfer of plasma lipoproteins in vivo, *Biochim Biophys Acta 666*, 80-89.
18. Nelbach, L., Shu, X., Konrad, R. J., Ryan, R. O., and Forte, T. M. (2008) Effect of apolipoprotein A-V on plasma triglyceride, lipoprotein size, and composition in genetically engineered mice, *J Lipid Res 49*, 572-580.
19. Wald, J. H., Krul, E. S., and Jonas, A. (1990) Structure of apolipoprotein A-I in three homogeneous, reconstituted high density lipoprotein particles, *J Biol Chem 265*, 20037-20043.
20. Segrest, J. P., Jones, M. K., De Loof, H., Brouillette, C. G., Venkatachalapathi, Y. V., and Anantharamaiah, G. M. (1992) The amphipathic helix in the exchangeable apolipoproteins: a review of secondary structure and function, *J Lipid Res 33*, 141-166.
21. Raussens, V., Narayanaswami, V., Goormaghtigh, E., Ryan, R. O., and Ruysschaert, J. M. (1995) Alignment of the apolipophorin-III alpha-helices in complex with dimyristoylphosphatidylcholine. A unique spatial orientation, *J Biol Chem 270*, 12542-12547.
22. Raussens, V., Fisher, C. A., Goormaghtigh, E., Ryan, R. O., and Ruysschaert, J. M. (1998) The low density lipoprotein receptor active conformation of apolipoprotein E. Helix organization in n-terminal domain-phospholipid disc particles, *J Biol Chem 273*, 25825-25830.
23. Raussens, V., Drury, J., Forte, T. M., Choy, N., Goormaghtigh, E., Ruysschaert, J. M., and Narayanaswami, V. (2005) Orientation and mode of lipid-binding interaction of human apolipoprotein E C-terminal domain, *Biochem J 387*, 747-754.
24. Narayanaswami, V., Maiorano, J. N., Dhanasekaran, P., Ryan, R. O., Phillips, M. C., Lund-Katz, S., and Davidson, W. S. (2004) Helix orientation of the functional domains in apolipoprotein e in discoidal high density lipoprotein particles, *J Biol Chem 279*, 14273-14279.
25. Martin, D. D., Budamagunta, M. S., Ryan, R. O., Voss, J. C., and Oda, M. N. (2006) Apolipoprotein A-I assumes a "looped belt" conformation on reconstituted high density lipoprotein, *J Biol Chem 281*, 20418-20426.
26. Silva, R. A., Schneeweis, L. A., Krishnan, S. C., Zhang, X., Axelsen, P. H., and Davidson, W. S. (2007) The structure of apolipoprotein A-II in discoidal high density lipoproteins, *J Biol Chem 282*, 9713-9721.
27. Ji, Y., and Jonas, A. (1995) Properties of an N-terminal proteolytic fragment of apolipoprotein AI in solution and in reconstituted high density lipoproteins, *J Biol Chem 270*, 11290-11297.

28. Suits, A. G., Chait, A., Aviram, M., and Heinecke, J. W. (1989) Phagocytosis of aggregated lipoprotein by macrophages: low density lipoprotein receptor-dependent foam-cell formation, *Proc Natl Acad Sci U S A 86*, 2713-2717.
29. Wetterau, J. R., Aggerbeck, L. P., Rall, S. C., Jr., and Weisgraber, K. H. (1988) Human apolipoprotein E3 in aqueous solution. I. Evidence for two structural domains, *J Biol Chem 263*, 6240-6248.
30. Reijngoud, D. J., and Phillips, M. C. (1982) Mechanism of dissociation of human apolipoprotein A-I from complexes with dimyristoylphosphatidylcholine as studied by guanidine hydrochloride denaturation, *Biochemistry 21*, 2969-2976.
31. Shu, X., Ryan, R. O., and Forte, T. M. (2008) Intracellular lipid droplet targeting by apolipoprotein A-V requires the carboxyl-terminal segment, *J Lipid Res 49*, 1670-1676.
32. Tajima, S., Yokoyama, S., and Yamamoto, A. (1983) Effect of lipid particle size on association of apolipoproteins with lipid, *J Biol Chem 258*, 10073-10082.
33. Wetterau, J. R., and Jonas, A. (1982) Effect of dipalmitoylphosphatidylcholine vesicle curvature on the reaction with human apolipoprotein A-I, *J Biol Chem 257*, 10961-10966.
34. Priore Oliva, C., Tarugi, P., Calandra, S., Pisciotta, L., Bellocchio, A., Bertolini, S., Guardamagna, O., and Schaap, F. G. (2006) A novel sequence variant in APOA5 gene found in patients with severe hypertriglyceridemia, *Atherosclerosis 188*, 215-217.
35. Lookene, A., Beckstead, J. A., Nilsson, S., Olivecrona, G., and Ryan, R. O. (2005) Apolipoprotein A-V-heparin interactions: implications for plasma lipoprotein metabolism, *J Biol Chem 280*, 25383-25387.
36. Merkel, M., Loeffler, B., Kluger, M., Fabig, N., Geppert, G., Pennacchio, L. A., Laatsch, A., and Heeren, J. (2005) Apolipoprotein AV accelerates plasma hydrolysis of triglyceride-rich lipoproteins by interaction with proteoglycan-bound lipoprotein lipase, *J Biol Chem 280*, 21553-21560.
37. Beigneux, A. P., Davies, B. S., Gin, P., Weinstein, M. M., Farber, E., Qiao, X., Peale, F., Bunting, S., Walzem, R. L., Wong, J. S., Blaner, W. S., Ding, Z. M., Melford, K., Wongsiriroj, N., Shu, X., de Sauvage, F., Ryan, R. O., Fong, L. G., Bensadoun, A., and Young, S. G. (2007) Glycosylphosphatidylinositol-anchored high-density lipoprotein-binding protein 1 plays a critical role in the lipolytic processing of chylomicrons, *Cell Metab 5*, 279-291.
38. Nilsson, S. K., Lookene, A., Beckstead, J. A., Gliemann, J., Ryan, R. O., and Olivecrona, G. (2007) Apolipoprotein A-V interaction with members of the low density lipoprotein receptor gene family, *Biochemistry 46*, 3896-3904.
39. Fisher, C. A., Wang, J., Francis, G. A., Sykes, B. D., Kay, C. M., and Ryan, R. O. (1997) Bacterial overexpression, isotope enrichment, and NMR analysis of the N-terminal domain of human apolipoprotein E, *Biochem Cell Biol 75*, 45-53.
40. Ryan, R. O., Forte, T. M., and Oda, M. N. (2003) Optimized bacterial expression of human apolipoprotein A-I, *Protein Expr Purif 27*, 98-103.
41. Nichols, A. V., Krauss, R. M., and Musliner, T. A. (1986) Nondenaturing polyacrylamide gradient gel electrophoresis, *Methods Enzymol 128*, 417-431.
42. Sreerama, N., and Woody, R. W. (1993) A self-consistent method for the analysis of protein secondary structure from circular dichroism, *Anal Biochem 209*, 32-44.
43. Goormaghtigh, E., Cabiaux, V., and Ruysschaert, J. M. (1990) Secondary structure and dosage of soluble and membrane proteins by attenuated total reflection Fourier-transform infrared spectroscopy on hydrated films, *Eur J Biochem 193*, 409-420.

44. Tallmadge, D. H., Huebner, J. S., and Borkman, R. F. (1989) Acrylamide quenching of tryptophan photochemistry and photophysics, *Photochem. Photobiol. 49*, 381-386.
45. Lindgren, F. T., Jensen, L. C., and Hatch, F. T. (1972) The isolation and quantitative analysis of serum lipoproteins., in *Blood Lipids and Lipoproteins: Quantitation, Composition, and Metabolism.* (Nelson, G. J., Ed.), pp 181-274, Wiley-Interscience, New York.

CHAPTER 5:
The carboxyl-terminal segment of apolipoprotein A-V: lipid-induced conformational change

5.1 ABBREVIATIONS

apo = apolipoprotein
TG = triacylglycerol
HTG = hypertriglyceridemia
rHDL = reconstituted high density lipoprotein
DMPC = dimyristoylphosphatidylcholine
PL-C = phospholipase C
CD = circular dichroism
TFE = trifluoroethanol
HSPG = heparan sulfate proteoglycan
NMR = nuclear magnetic resonance spectroscopy
HSQC = heteronuclear single quantum correlation NMR Spectrum
NOESY = nuclear Overhauser effect NMR spectroscopy
DSS = 2,2-dimethyl-2-silapentane-5-sulfonate

5.2 ABSTRACT

Apolipoprotein (apo) A-V is a 343 residue, multi-domain protein that plays an important role in regulation of plasma triglyceride homeostasis. Primary sequence analysis revealed a unique tetra-proline sequence (Pro293 – Pro296) near the carboxyl terminus of the protein. A peptide corresponding to the 48 residue segment beyond the tetra-proline motif was generated from a recombinant apoA-V precursor wherein Pro295 was replaced by Met. Cyanogen bromide cleavage of the precursor protein, followed by negative affinity chromatography, yielded a purified peptide. Native polyacrylamide gel electrophoresis verified that apoA-V(296-343) solubilizes phospholipid vesicles, forming a relatively heterogeneous reconstituted high density lipoprotein population with Stoke's diameters > 17 nm. At the same time, apoA-V(296-343) failed to bind spherical lipoprotein substrates *in vitro*. Far UV circular dichroism spectroscopy revealed the peptide is unstructured in buffer yet adopts significant α-helical secondary structure in the presence of the lipid mimetic solvent, trifluoroethanol (TFE; 50% v/v). Heteronuclear multidemensional NMR spectroscopy experiments were conducted with uniformly ^{15}N and $^{15}N/^{13}C$ labeled peptide in 50 % TFE. Peptide backbone assignment and secondary structure prediction using TALOS+ reveals it adopts an α-helix between residues 309 – 334. In TFE, apoA-V(296-343) adopts an extended amphipathic α-helix, consistent with a role in lipoprotein binding as a component of full-length apoA-V. This is the first high-resolution structure of a portion of apoA-V.

5.3 BACKGROUND

Apolipoprotein (apo) A-V was discovered in 2001 in a comparative genomics study (*1*) and as an mRNA up-regulated during rat liver regeneration (*2*). Subsequent research has shown that apoA-V serves as a potent modulator of plasma triacylglycerol (TG) homeostasis. Mature apoA-V is a non-glycosylated protein comprised of 343 amino acids. An interesting feature of apoA-V is the presence of four consecutive Pro near the carboxyl (C)-terminus (Pro293 – Pro296). Whereas the 47 residue segment C-terminal to the tetra-proline sequence was postulated to comprise an independent structural domain in apoA-V, guanidine HCl denaturation studies showed this segment is actually part of a larger C-terminal domain (*3*). A recombinant C-terminal truncated apoA-V, missing the region beyond residue 292, displayed defective lipid binding activity compared to full-length apoA-V. Furthermore, in the absence of a C-terminal domain, the N-terminal domain of apoA-V (residues 1-146) loses its capacity to bind larger lipoprotein substrates, such as very low density lipoprotein (*4*). When taken together with observations that naturally occurring C-terminal truncated apoA-V mutants in humans are associated with severe hypertriglyceridemia (HTG) (*5, 6*), it is conceivable that residues 296-343 of apoA-V are required for proper functioning of this protein. In the present study, we have designed a protocol for expression and purification of recombinant of apoA-V(296-343). Structure-function analyses reveal unique lipid-binding properties of apoA-V(296-343) while heteronuclear multidimensional NMR studies provide evidence that, although apoA-V(296-343) is unstructured in buffer alone, it adopts α-helix secondary structure in a lipid mimetic environment.

5.4 RESULTS

Isolation of purified apoA-V(296-343) peptide

Due to the size of the peptide under investigation (48 amino acids) and a desire to generate isotopically enriched apoA-V(296-343), a protocol was established to generate recombinant peptide from a larger, apoA-V(148-343) precursor. Site directed mutagenesis was performed to replace the sole Met in this fragment with Ile, while a second mutagenesis introduced Met in place of Pro295. As predicted, CNBr cleavage of the resulting variant apoA-V(148-343) yielded two major fragments. Negative affinity chromatography was performed to isolate the peptide from unreacted precursor protein and the apoA-V(148-295) CNBr reaction product (**Figure 5-1**). One liter of culture media yielded ~2 mg of high-purity peptide.

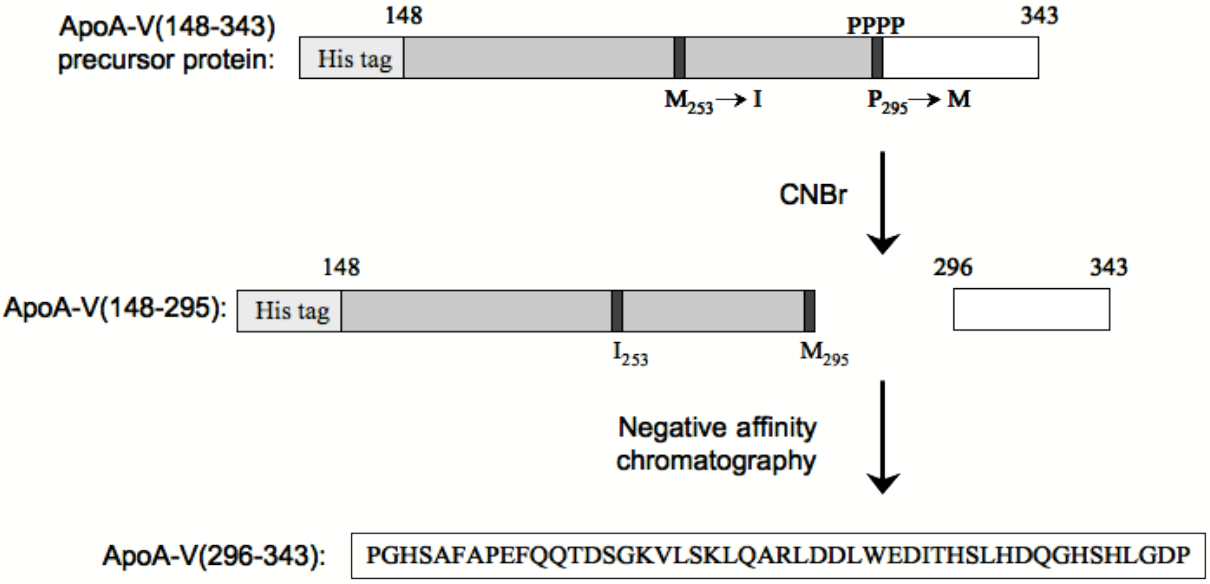

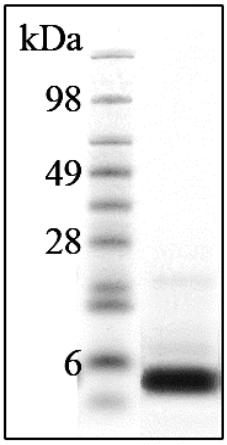

Figure 5-1. Flow chart of apoA-V(296-343) production method and SDS PAGE of peptide purity.

ApoA-V(296-343) reconstituted high density lipoproteins

Incubation of apoA-V(296-343) with bilayer vesicles of DMPC induced rapid clearing of solution turbidity, indicative of rHDL formation. Native PAGE analysis revealed a relatively heterogeneous population of particles with a Stoke's diameters > 17 nm (**Figure 5-2**). The rHDL generated in this reaction are larger in size than discoidal particles formed with full-length apoA-V.

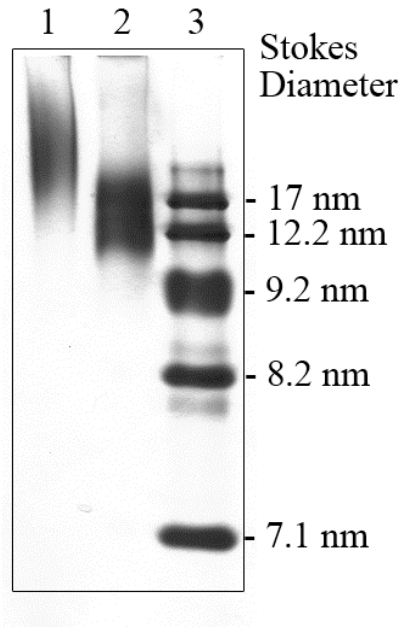

Figure 5-2. Native PAGE of apoA-V(296-343)•DMPC complexes. ApoA-V(296-343)•DMPC complexes were prepared as described under "Materials and Methods" and applied to a 4 – 20% acrylamide gradient gel. Following electrophoresis the gel was stained with Gel Code Blue. Lane 1, apoA-V(296-343)•DMPC complexes (5 µg of protein); lane 2, full-length apoA-V•DMPC complexes (5 µg of protein); lane 3, molecular size standards.

ApoA-V(296-343) lipoprotein binding properties

When isolated human LDL is incubated with PL-C, conversion of phophatidylcholine to diacylglycerol induces lipoprotein particle instability, aggregation and sample turbidity development (**Figure 5-3**). In control incubations lacking PL-C, no change in LDL sample turbidity was observed. When conducted in the presence of apoA-I, LDL was protected from PL-C induced aggregation and turbidity development as a result of apoA-I association with the modified particle surface (*7*). By contrast, corresponding incubations with apoA-V(296-343) failed to protect LDL from PL-C induced sample turbidity development.

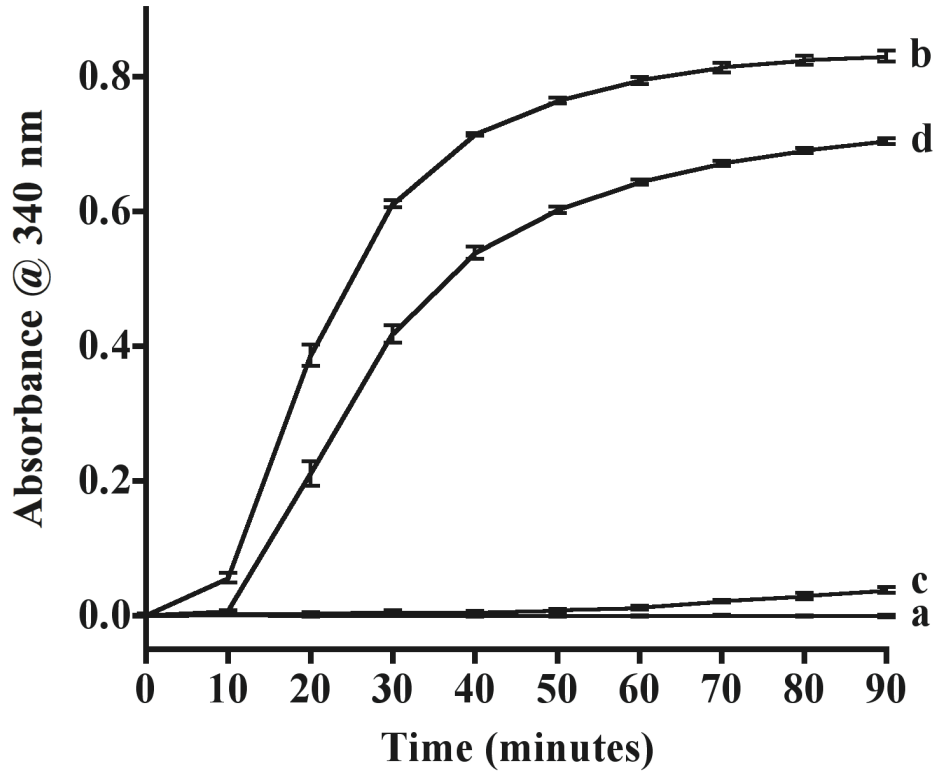

Figure 5-3. **Effect of apoA-V(296-343) on PL-C induced aggregation of human LDL.** Human LDL (50 µg protein) was incubated at 37 ºC in the absence (curve a) or presence (curve b) of PL-C (0.6 unit). Other incubations contained LDL, PL-C, and 50 µg apoA-V(296-343) peptide (curve d) or 50 µg apoA-I (curve c). Sample absorbance at 340 nm was measured as a function of time. The values represent the means ± standard deviation (n = 3).

Far UV CD spectroscopy

Far UV CD spectroscopy analysis suggests apoA-V(296-343) is largely unstructured in buffer (**Figure 5-4**). In the presence of the lipid mimetic cosolvent, TFE (50% v/v), however, major minima at 208 nm and 222 nm are present, indicative of α-helix secondary structure.

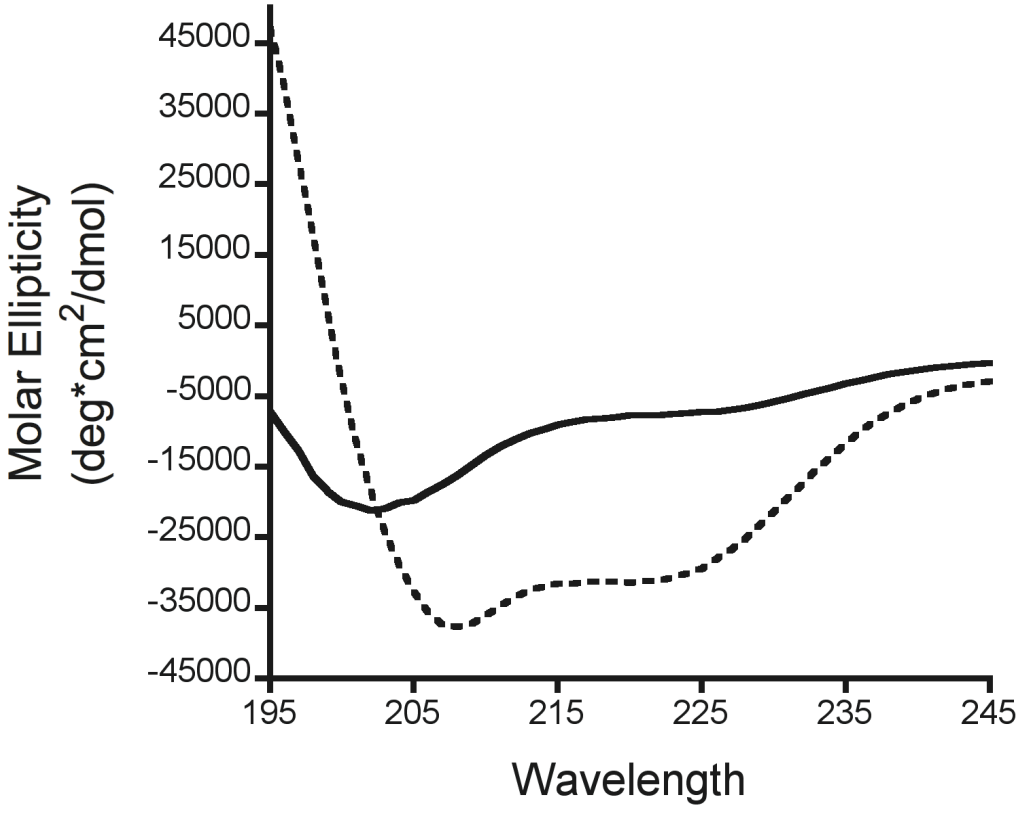

Figure 5-4. Far UV CD of 0.5 mg/mL apoA-V(296-343) in 10 mM sodium phosphate, pH 7.4 (solid line) and in 50% TFE (dashed line).

NMR of ^{15}N-labeled apoA-V(296-343)

[Data collected in collaboration with the laboratory of Dr. Brian D. Sykes of the University of Alberta]

When bacteria used to express the variant apoA-V(148-343) were cultured in M9 minimal media containing ^{15}N as the sole nitrogen source, uniformly ^{15}N-labeled apoA-V(296-343) was generated. Mass spectrometry analysis of the sample yielded a value of 5,388 Da, in good agreement with the expected theoretical calculated mass for a fully ^{15}N enriched peptide (5387.7 Da). Two dimensional ^{15}N- ^{1}H correlation NMR spectroscopy of ^{15}N-labelded apoA-V(296-343) in buffer (90% H_2O/10% D_2O, containing 90 mM KCl, 9 mM imidazole, and 0.5 mM DSS-d_6) gave rise to a spectrum that showed poor resonance dispersion, consistent with a general lack of secondary structure under these conditions (**Figure 5-5a**). By contrast, spectra recorded in 50% buffer/50% TFE, displayed significantly increased chemical shift dispersion, consistent with adoption of secondary structure (**Figure 5-5b**). Given the prospect of assigning these resonances and ultimate structure determination, a second apoA-V(296-343) peptide, enriched in both ^{15}N and ^{13}C, was generated. Using a panel of heteronuclear multi-dimensional NMR experiments, the backbone and side-chain atoms of apoA-V were assigned. As seen in Figure 5-5b, all resonances, except for G297, H298, S338, H339, which were not visible in the ^{15}N-^{1}H HSQC, have been assigned. Secondary chemical shifts values (defined as the difference between the measured chemical shift of given atom and value corresponding with chemical shift for the same atom in random coil conformation) for ^{13}C', ^{13}Ca, ^{13}Cb, Ha, HN and/or ^{15}N atoms characterize probability of helical or b-sheet conformation occurrence. Program TALOS+ (*8*) uses available secondary chemical shifts to calculate Random Coil Index (RCI) and predict secondary structure (*9*). Positive values of RCI show possibility of b-sheet occurrence while negative values indicate helical conformation.

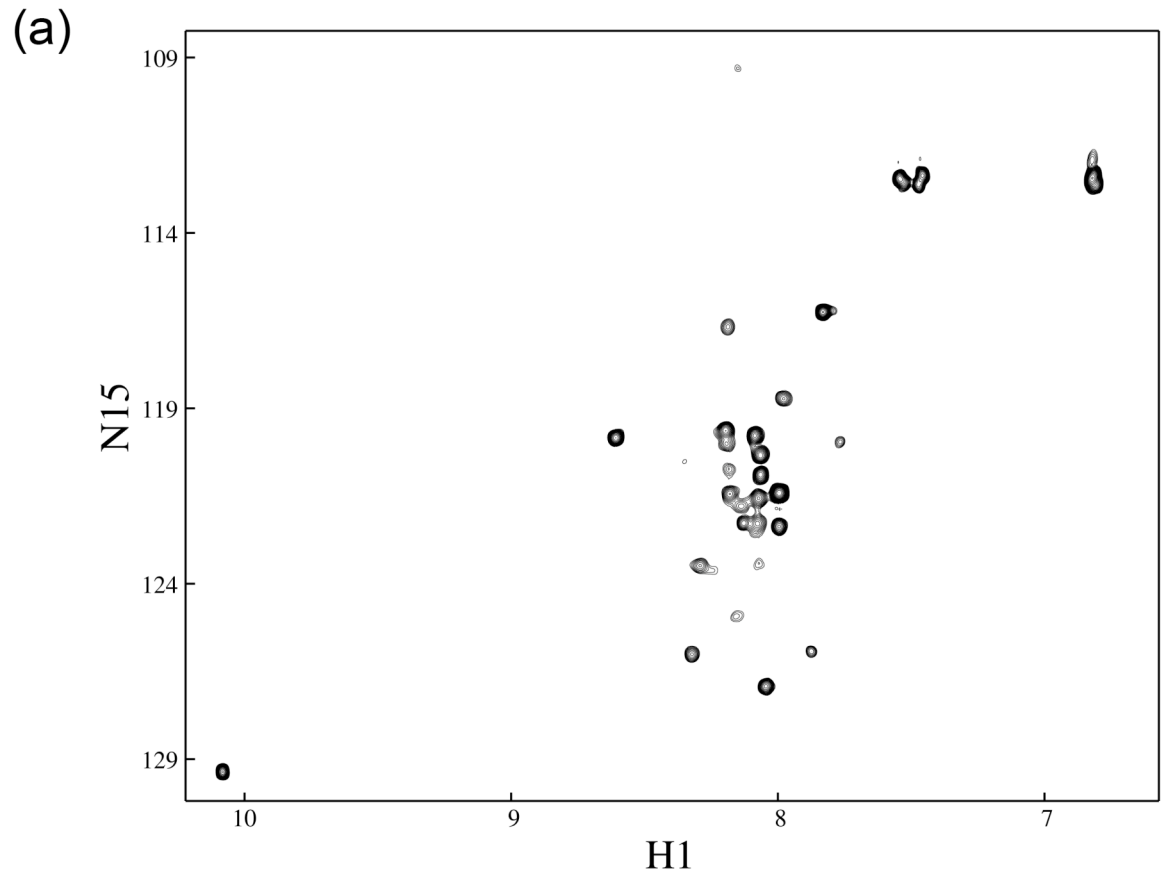

Figure 5-5. (a) 2D ^{1}H-^{15}N HSQC of ^{15}N-labeled apoA-V(296-343) in buffer alone (90% H_2O/10% D_2O, containing 50 mM KCl, 5 mM imidazole, and 0.5 mM DSS-d_6) acquired at 500 MHz.

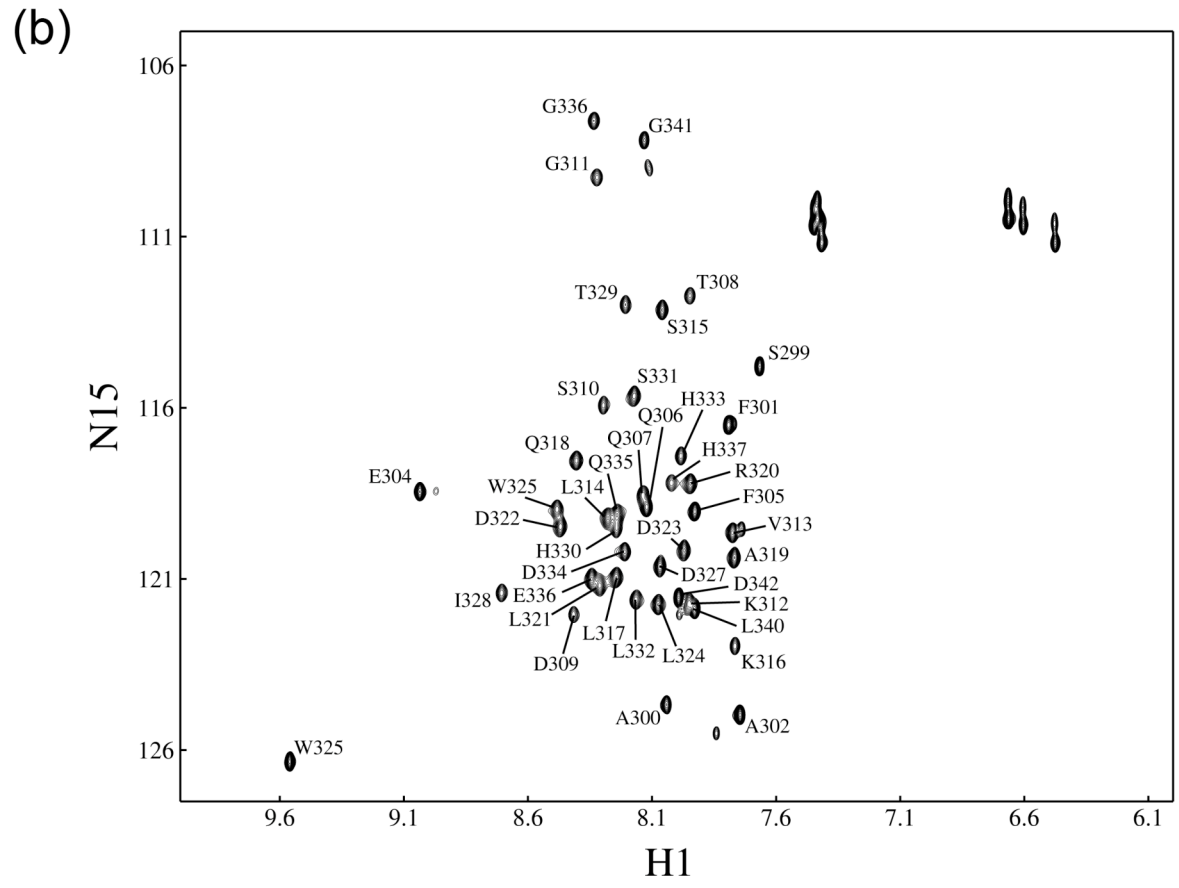

Figure 5-5. (b) 2D ^{1}H-^{15}N HSQC of ^{15}N-labeled apoA-V(296-343) in 50% TFE/50% buffer acquired at 800 MHz. Peak assignments are indicated.

Prediction of the secondary structure using TALOS+ indicated peptide residues 309 – 334 adopt an α-helix under these experimental conditions (**Figure 5-6**).

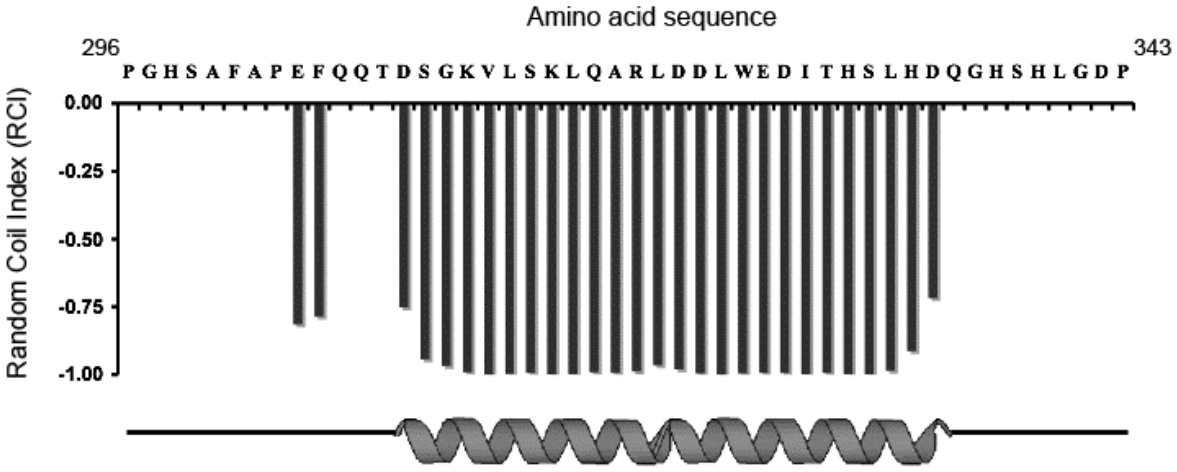

Figure 5-6. Secondary structure prediction using the program TALOS+ showing helical structure between residues 309 – 334. Residues G297, H298, S338, H339 could not be assigned and are not predicted.

5.5 DISCUSSION

The mechanism whereby apoA-V influences plasma TG homeostasis has been the subject of intensive investigation (*10, 11*). Studies have revealed that this protein associates with plasma lipoproteins and possesses the capacity to bind cell surface molecules including heparan sulfate proteoglycans (HSPG), members of the LDL receptor family and glycosylphosphatidylinositol high-density lipoprotein binding protein 1 (*10*). Considering evidence from genetically engineered mouse models and population studies investigating correlations between common single nucleotide polymorphisms in *APOAV* and elevated plasma TG, better understanding of apoA-V structure and function relations may lead to new strategies to treat HTG. The fact that apoA-V concentration in plasma is extremely low (~100 ng/ml) suggests it possesses potent biological activity (*12*).

Limited proteolysis and denaturation studies revealed that apoA-V is comprised of two independently folded structural domains (*13*). The N-terminal domain, comprising residues 1 – 146, adopts a helix bundle molecular architecture in the absence of lipid (*13*). The C-terminal domain, comprising residues 147 – 343, is less well understood but is known to contain a sequence element (residues 186 – 227) that is rich in positively charged amino acids and lacks negatively charged residues. It has been postulated that this region of the protein is responsible for apoA-V interactions with cell surface proteins and HSPG (*14-16*).

In lipid binding studies, while the peptide corresponding to apoA-V(296-343) displays high phospholipid vesicle solubilization activity and undergoes a 16 nm blue shift in wavelength of maximum tryptophan fluorescence emission (arising from the single Trp at sequence position 325) in the presence of phospholipid (*3*), it fails to associate with the surface of a spherical lipoprotein substrate. This result illustrates important differences between lipoprotein binding and vesicle solubilization activity. The ability of apolipoproteins to bind PL-C treated LDL is dependent on creation of binding sites, via PL-C mediated conversion of phosphatidylcholine to diacylglycerol, whereas interaction with phospholipid bilayer vesicles proceeds optimally at the phospholipid gel to liquid-crystal phase transition temperature (*17*). It appears that the lack of secondary structure in buffer precludes recognition / binding to the surface of a lipoprotein yet its intrinsic capacity to associate with lipid is retained in the phospholipid vesicle solubilization assay, perhaps owing to the induction of secondary structure as part of the solubilization reaction.

A concept that has emerged from structural studies conducted to date is that the C-terminal segment beyond the four consecutive Pro may be responsible for initiation of apoA-V lipid binding activity. This interpretation is consistent with the lipid binding properties of other apolipoproteins, such as apoE and apoA-I (*18*), and is supported by data showing that removal of this C-terminal region results in an impaired ability of apoA-V to bind lipid (*3*). It may be postulated that initiation of lipid binding is mediated by hydrophobic interactions between nonpolar residues in the C-terminal peptide and the hydrophobic lipid surface and/or ionic interactions between charged residues and phospholipid head groups. In both types of interactions, the C-terminal peptide may be envisioned to mediate initial recognition of the lipoprotein particle, followed by stable binding of the entire protein.

The experiments described in this study indicate that in order to initiate lipid binding, apoA-V(296-343) may need to exist within the context of the intact protein. Far UV CD and NMR spectroscopy experiments show that apoA-V(296-343) is unstructured in buffer alone. In the case of other apolipoproteins, a more loosely folded structure has been associated with enhanced lipid binding activity (*19*). It is conceivable the C-terminal region of apoA-V initiates lipid binding and that this process induces stable secondary structure formation in this segment of the protein. In this case, it seems plausible that lipid binding elicits a subsequent conformational change in the N-terminal helix bundle that results in opening of the bundle and exposure of its hydrophobic interior to potential lipid interaction sites. A consequence of this may also include exposure of the positively charged sequence motif (residues 186 – 227) that underlies the biological effects of ApoA-V.

In an effort to test hypothesis related to this model, we sought to characterize the structural properties of the C-terminal peptide. In order to study the peptide in isolation, methods were developed to produce recombinant peptide. Using this system, efficient stable isotope enrichment of the peptide was readily achieved. A panel of heteronuclear multidimensional NMR experiments was employed to assign the apoA-V spectrum and define its structure in a lipid mimetic environment. Results obtained suggest apoA-V(296-343) undergoes a lipid-induced conformational change, transitioning from an unstructured or molten globule-like state in the lipid-free environment to α-helix in a lipid mimetic environment. NMR analysis reveals the region between residues 309 – 334 adopts a α-helix secondary structure in a lipid mimetic environment. This data confirms predictions from the Coils program (*20*) that the region between Gly311 – Leu332 in apoA-V(296-343) adopts α-helical secondary structure. Edmundson helical wheel projection (*21*) of Gly311 – Ile328 reveals this region forms an amphipathic α-helix (**Figure 5-7)**. Primary sequence analysis reveals almost all of the hydrophobic and charged residues within apoA-V(296-343) reside within the α-helical segment. In the presence of lipid, the extreme carboxyl terminus of apoA-V adopts an amphipathic α-helix enriched in hydrophobic residues on one face and charged residues on the other face of the helix. This dramatic induction of structure supports the concept that the C-terminal region of apoA-V may serve as a lipid-sensor that functions in initiation of apoA-V lipid binding and subsequent structure conformation changes in the entire protein.

Since our data shows apoA-V C-terminal peptide can adopt structure, it must be considered that, when present in the context of the intact protein, this C-terminal region possesses a more defined structure. Indeed, an important question arising from this study relates to whether the C-terminal peptide structure determined here resembles that of the peptide when present in the context of the intact protein, especially when bound to lipid. To determine this, we are pursuing an expressed protein ligation strategy to generate a segmentally isotope labeled full-length apoA-V wherein only residues 296-343 are enriched with stable isotope (*22*). This approach will allow detailed analysis of the solution properties and lipid binding induced conformational changes in this region of the protein within the context of the intact apoA-V protein.

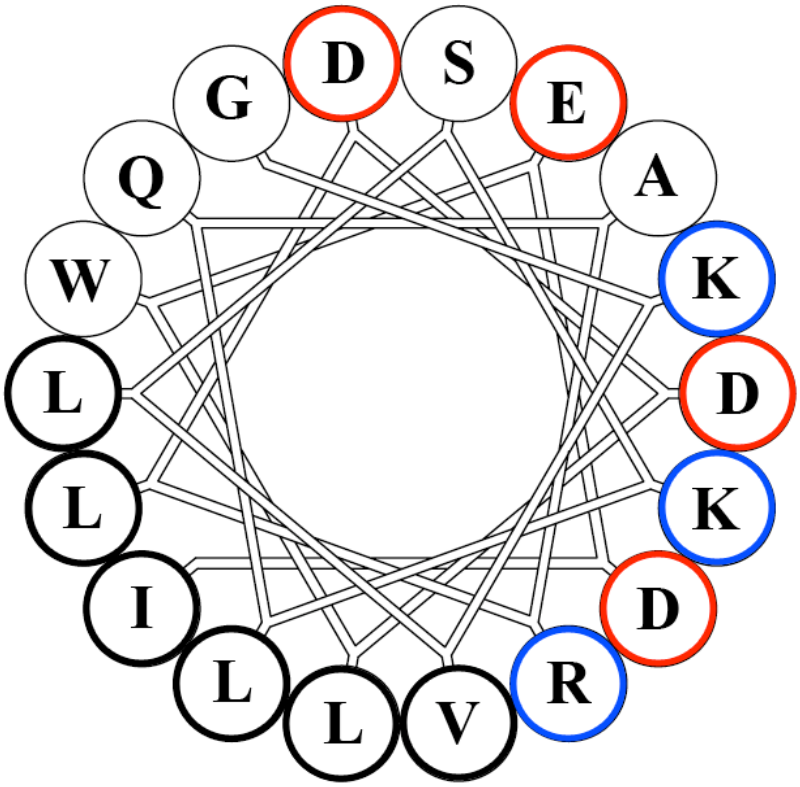

Figure 5-7. Helical wheel projection of Gly311 – Ile328 within apoA-V(296-343). Hydrophobic residues are circled in bold, positively-charged residues are circled in blue, and negatively-charged residues are circled in red.

5.6 ACKNOWLEDGMENTS

Thank you to Clayton Mauldin of the University of California, Berkeley for mass spectrometry data and Dr. Susan Marqusee of the University of California, Berkeley for use of the circular dichroism spectroscopy instrument.

5.7 MATERIALS AND METHODS

Preparation of apoA-V(296-343)

Site-directed mutagenesis was performed with the QuikChange II XL site-directed mutagenesis kit (Strategene) on an N-terminal His-tag containing a human apoA-V construct encoding residues 148 – 343. Primers were designed to mutate the sole naturally occurring Met at position 253 (numbering corresponds to sequence position in mature, full-length apoA-V) to Ile and Pro295 to Met. Introduction of the desired mutations was verified by DNA sequencing. The variant apoA-V(148-343) was cloned into pET20b+ vector, and unlabeled, uniformly ^{15}N-labeled or double $^{15}N/^{13}C$-labeled variant apoA-V(148-343), were expressed in *Escherichia coli* BL21 cells cultured in NCZYM (unlabeled protein) or M9 minimal media (isotopically labeled protein) and purified as described previously for full-length recombinant apoA-V (*23*). Purified variant apoA-V(148-343) was then solubilized in 80% formic acid at a concentration of 5 mg/ml. CNBr was added at a CNBr : Met ratio > 100 and incubated under N_2 atmosphere for 24 h in the dark. The reaction was quenched by addition of >10 fold excess deionized water and the sample lyophilized to remove residual CNBr. The freeze-dried product was resuspended and subjected to affinity chromatography on a Hi-Trap Ni^{2+} chelation column. Since only the unreacted variant apoA-V(148-343) substrate and the N-terminal CNBr cleavage product, apoA-V(148-295) possess a His-tag, the desired peptide, apoA-V(296-343), elutes in the unbound fraction free of contamination.

Analytical procedures

Protein concentration in samples were determined with the bicinchoninic acid assay (Pierce) using bovine serum albumin as standard. SDS-PAGE was performed on 4 – 12% acrylamide slab gels, NuPAGE MES buffer system (Invitrogen), at a constant 200 V for 35 min. Gels were stained with Gel Code Blue (Pierce). Mass spectrometry was performed on an Applied Biosystems Voyager System 6322. The matrix used was α-cyano-4-hydroxycinnarnic acid, and the matrix and sample were dissolved in 1:1 water:acetonitrile (0.1% TFA) and drop cast.

Preparation of apoA-V(296-343) reconstituted high density lipoprotein (rHDL)

Bilayer vesicles of dimyristoylphosphatidylcholine (DMPC) were prepared as described (*23*) and incubated in the presence of apoA-V(296-343) at a DMPC:peptide weight ratio of 3:1. Following bath sonication at 24 °C, the complexes generated were characterized by non-denaturing gradient PAGE as described by Nichols *et al*. (*24*).

Low density lipoprotein (LDL) binding assay

Human LDL (Intracel) was incubated for 90 min at 37 °C in the presence or absence of *Bacillus cereus* phospholipase C (PL-C) (0.6 U per 50 μg LDL protein). Where indicated, apoA-

V(296-343) or recombinant human apoA-I (*25*) was included in the reaction mixture (50 µg per 50 µg LDL protein). Incubations were conducted in 50 mM Tris-HCl, pH 7.5, 150 mM NaCl and 2 mM $CaCl_2$ in a total sample volume of 200 µL. Sample turbidity was measured at 340 nm on a Spectramax 340 microtiter plate reader (Sunnyvale, CA, USA) (*7*).

Far UV circular dichroism (CD) spectroscopy

Far UV CD spectroscopy measurements were performed on an AVIV 410 spectrophotometer. Scans were obtained between 195 and 245 nm in 10 mM sodium phosphate, pH 7.4, using a protein concentration of 0.5 mg/ml.

Nuclear magnetic resonance (NMR) spectroscopy

NMR experiments were performed on 1.5 mM samples of uniformly ^{15}N- or $^{15}N/^{13}C$-labeled apoA-V(296-343) in 500 µl of 50% trifluoroethanol, TFE-d_3/40% H_2O/10% D_2O, containing 40 mM KCl, 4 mM imidazole. 0.5 mM 2,2-dimethyl-2-silapentane-5-sulfonate (DSS-d_6) was included as internal chemical shift reference. NMR experiments were carried out at 25°C on Varian INOVA 500, 600 and 800 MHz NMR spectrometers. Data were processed using the program NMRPipe (*26*) and analyzed using the program NMRView (*27*). Sequential assignment of the backbone atoms of apoA-V(296-343) were obtained using 2D ^{15}N-HSQC, 3D ^{15}N-edited NOESY (75 ms mix), HNHA, HNCACB, and CBCA(CO)NNH experiments. 2D ^{13}C-HSQC, 3D H(CCO)NH, C(CO)NNH, ^{13}C-edited NOESY (100 ms mix) experiments provided side-chain assignments. Secondary structure predictions were obtained using the program TALOS+ (*8*).

5.8 REFERENCES

1. Pennacchio, L. A., Olivier, M., Hubacek, J. A., Cohen, J. C., Cox, D. R., Fruchart, J. C., Krauss, R. M., and Rubin, E. M. (2001) An apolipoprotein influencing triglycerides in humans and mice revealed by comparative sequencing, *Science 294*, 169-173.
2. van der Vliet, H. N., Sammels, M. G., Leegwater, A. C., Levels, J. H., Reitsma, P. H., Boers, W., and Chamuleau, R. A. (2001) Apolipoprotein A-V: a novel apolipoprotein associated with an early phase of liver regeneration, *J Biol Chem 276*, 44512-44520.
3. Beckstead, J. A., Wong, K., Gupta, V., Wan, C. P., Cook, V. R., Weinberg, R. B., Weers, P. M., and Ryan, R. O. (2007) The C terminus of apolipoprotein A-V modulates lipid-binding activity, *J Biol Chem 282*, 15484-15489.
4. Wong-Mauldin, K., Raussens, V., Forte, T. M., and Ryan, R. O. (2009) Apolipoprotein A-V N-terminal domain lipid interaction properties in vitro explain the hypertriglyceridemic phenotype associated with natural truncation mutants, *J Biol Chem 284*, 33369-33376.
5. Marcais, C., Verges, B., Charriere, S., Pruneta, V., Merlin, M., Billon, S., Perrot, L., Drai, J., Sassolas, A., Pennacchio, L. A., Fruchart-Najib, J., Fruchart, J. C., Durlach, V., and Moulin, P. (2005) Apoa5 Q139X truncation predisposes to late-onset hyperchylomicronemia due to lipoprotein lipase impairment, *J Clin Invest 115*, 2862-2869.
6. Oliva, C. P., Pisciotta, L., Li Volti, G., Sambataro, M. P., Cantafora, A., Bellocchio, A., Catapano, A., Tarugi, P., Bertolini, S., and Calandra, S. (2005) Inherited apolipoprotein A-V deficiency in severe hypertriglyceridemia, *Arterioscler Thromb Vasc Biol 25*, 411-417.
7. Liu, H., Scraba, D. G., and Ryan, R. O. (1993) Prevention of phospholipase-C induced aggregation of low density lipoprotein by amphipathic apolipoproteins, *FEBS Lett 316*, 27-33.
8. Shen, Y., Delaglio, F., Cornilescu, G., and Bax, A. (2009) TALOS+: a hybrid method for predicting protein backbone torsion angles from NMR chemical shifts, *J Biomol NMR 44*, 213-223.
9. Berjanskii, M. V., and Wishart, D. S. (2008) Application of the random coil index to studying protein flexibility, *J Biomol NMR 40*, 31-48.
10. Forte, T. M., Shu, X., and Ryan, R. O. (2009) The ins (cell) and outs (plasma) of apolipoprotein A-V, *J Lipid Res 50 Suppl*, S150-155.
11. Wong, K., and Ryan, R. O. (2007) Characterization of apolipoprotein A-V structure and mode of plasma triacylglycerol regulation, *Curr Opin Lipidol 18*, 319-324.
12. O'Brien, P. J., Alborn, W. E., Sloan, J. H., Ulmer, M., Boodhoo, A., Knierman, M. D., Schultze, A. E., and Konrad, R. J. (2005) The novel apolipoprotein A5 is present in human serum, is associated with VLDL, HDL, and chylomicrons, and circulates at very low concentrations compared with other apolipoproteins, *Clin Chem 51*, 351-359.
13. Wong, K., Beckstead, J. A., Lee, D., Weers, P. M., Guigard, E., Kay, C. M., and Ryan, R. O. (2008) The N-terminus of apolipoprotein A-V adopts a helix bundle molecular architecture, *Biochemistry 47*, 8768-8774.

14. Lookene, A., Beckstead, J. A., Nilsson, S., Olivecrona, G., and Ryan, R. O. (2005) Apolipoprotein A-V-heparin interactions: implications for plasma lipoprotein metabolism, *J Biol Chem 280*, 25383-25387.
15. Merkel, M., Loeffler, B., Kluger, M., Fabig, N., Geppert, G., Pennacchio, L. A., Laatsch, A., and Heeren, J. (2005) Apolipoprotein AV accelerates plasma hydrolysis of triglyceride-rich lipoproteins by interaction with proteoglycan-bound lipoprotein lipase, *J Biol Chem 280*, 21553-21560.
16. Nilsson, S. K., Lookene, A., Beckstead, J. A., Gliemann, J., Ryan, R. O., and Olivecrona, G. (2007) Apolipoprotein A-V interaction with members of the low density lipoprotein receptor gene family, *Biochemistry 46*, 3896-3904.
17. Narayanaswami, V., Wang, J., Kay, C. M., Scraba, D. G., and Ryan, R. O. (1996) Disulfide bond engineering to monitor conformational opening of apolipophorin III during lipid binding, *J Biol Chem 271*, 26855-26862.
18. Saito, H., Lund-Katz, S., and Phillips, M. C. (2004) Contributions of domain structure and lipid interaction to the functionality of exchangeable human apolipoproteins, *Prog Lipid Res 43*, 350-380.
19. Soulages, J. L., and Bendavid, O. J. (1998) The lipid binding activity of the exchangeable apolipoprotein apolipophorin-III correlates with the formation of a partially folded conformation, *Biochemistry 37*, 10203-10210.
20. Lupas, A., Van Dyke, M., and Stock, J. (1991) Predicting coiled coils from protein sequences, *Science 252*, 1162-1164.
21. Schiffer, M., and Edmundson, A. B. (1967) Use of helical wheels to represent the structures of proteins and to identify segments with helical potential, *Biophys J 7*, 121-135.
22. Hauser, P. S., Raussens, V., Yamamoto, T., Abdullahi, G. E., Weers, P. M., Sykes, B. D., and Ryan, R. O. (2009) Semisynthesis and segmental isotope labeling of the apoE3 N-terminal domain using expressed protein ligation, *J Lipid Res 50*, 1548-1555.
23. Beckstead, J. A., Oda, M. N., Martin, D. D., Forte, T. M., Bielicki, J. K., Berger, T., Luty, R., Kay, C. M., and Ryan, R. O. (2003) Structure-function studies of human apolipoprotein A-V: a regulator of plasma lipid homeostasis, *Biochemistry 42*, 9416-9423.
24. Nichols, A. V., Krauss, R. M., and Musliner, T. A. (1986) Nondenaturing polyacrylamide gradient gel electrophoresis, *Methods Enzymol 128*, 417-431.
25. Ryan, R. O., Forte, T. M., and Oda, M. N. (2003) Optimized bacterial expression of human apolipoprotein A-I, *Protein Expr Purif 27*, 98-103.
26. Delaglio, F., Grzesiek, S., Vuister, G. W., Zhu, G., Pfeifer, J., and Bax, A. (1995) NMRPipe: a multidimensional spectral processing system based on UNIX pipes, *J Biomol NMR 6*, 277-293.
27. Johnson, B. A., and Blevins, R. A. (1994) NMRView: A computer porgram for the visualization and analysis of NMR data, *J of Biomol NMR 4*, 603-614.